Mathematical Challenges of the Euclid Spatial Project

J.-L. Starck
CEA, IRFU, Service d'Astrophysique, France
jstarck@cea.fr
http://jstarck.free.fr
http://www.cosmostat.org

Collaborators: F. Ngole, A. Leonard, S. Pires, F. Lanusse
on behalf of the *Euclid Consortium*

Euclid & Weak Lensing

- **Part 1: Introduction to Euclid & Weak Lensing**
- Part 2: Shear WL Measurements
- Part 3: From Shear to 2D and 3D Maps
- Part 4: Challenges in the WL Community
- Part 5: WL Inverse Problems and Sparse Solutions
  - Point Spread Function superresolution
  - 2D mass mapping
  - 3D mass mapping

From Observations to Cosmological Model

$$\mathcal{M}(\Omega_M, \Omega_\Lambda, \Omega_b, \sigma_8, \ldots)$$

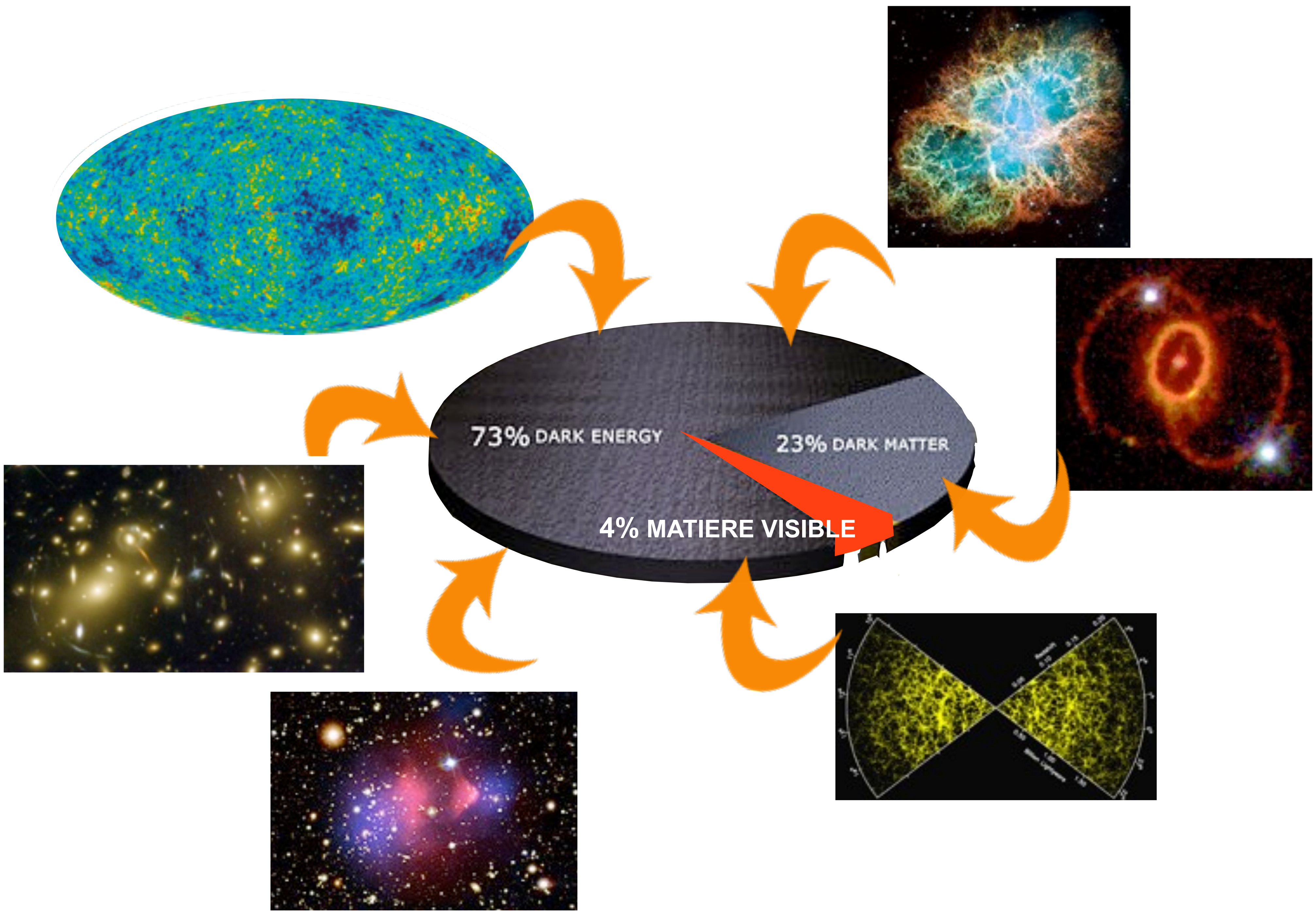

Euclid

Understand the origin of the Universe's accelerating expansion:

→probe the properties and nature of *dark energy, dark matter, gravity* and distinguish their effects decisively

→by tracking their observational signatures on the

- geometry of the universe:
  Weak Lensing + Galaxy Cluster

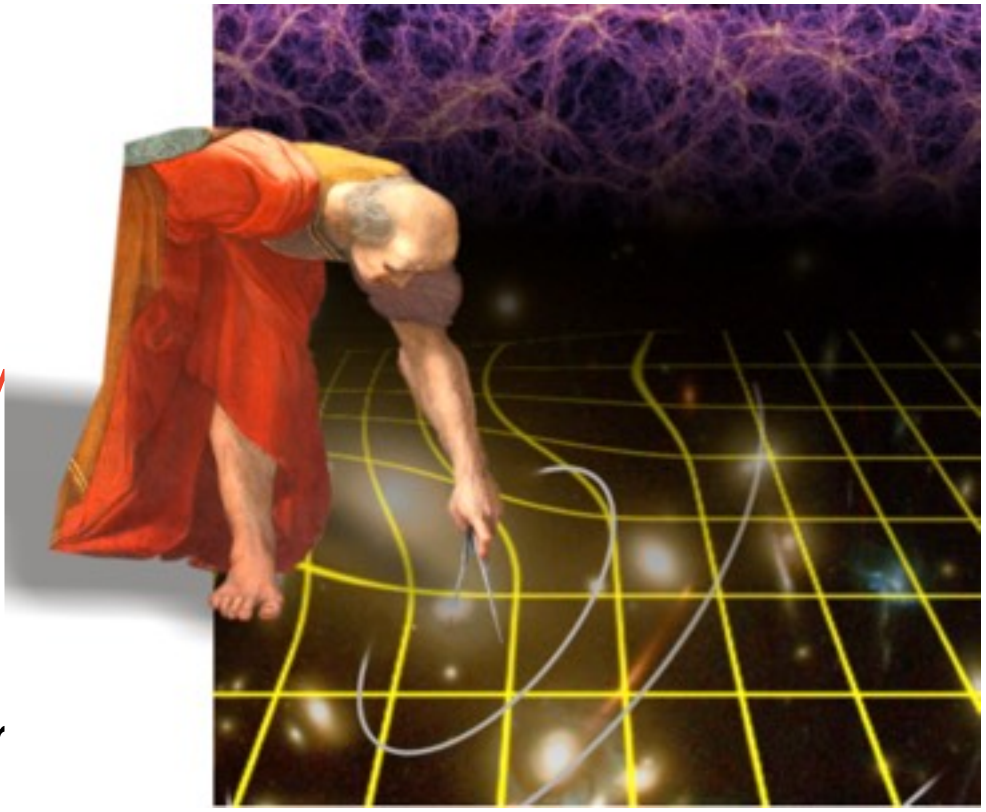

- cosmic history of structure formation: WL, z-space distortion, clusters of galaxies

→ **Controling systematic residuals to an unprecedented level of accuracy, that cannot be reached by any other competing missions/telescopes**

Gains in space:

Stable data: homogeneous data set over the whole sky

→**Systematics** are small, understood and controlled

→Homogeneity : Selection function perfectly controlled

Euclid mission element

Euclid Consortium

- Launch Soyuz, in 2020, L2 Orbit
- 6 years mission
- Telescope: 1.2 m
- Instruments:
- **VIS**: Visible imaging channel:
  - 0.54 deg^2, 0.10'' pixels, 0.16'' PSF FWHM,
  - 1 broad band R+I+Z (0.55-0.92mu),
  - 36 CCD detectors, galaxy shapes
- **NISP**: NIR photometry channel:
  - 0.54 deg^2, 0.3'' pixels,
  - 3 bands Y,J,H (1.0-1.7mu),
  - 16 HgCdTe detectors, photo-z's
- **NISP**: NIR Spectroscopic channel:
  - 0.54 deg^2,
  - R(mean)=250,
  - 0.9-1.7mu, slitless, spectro redshifts

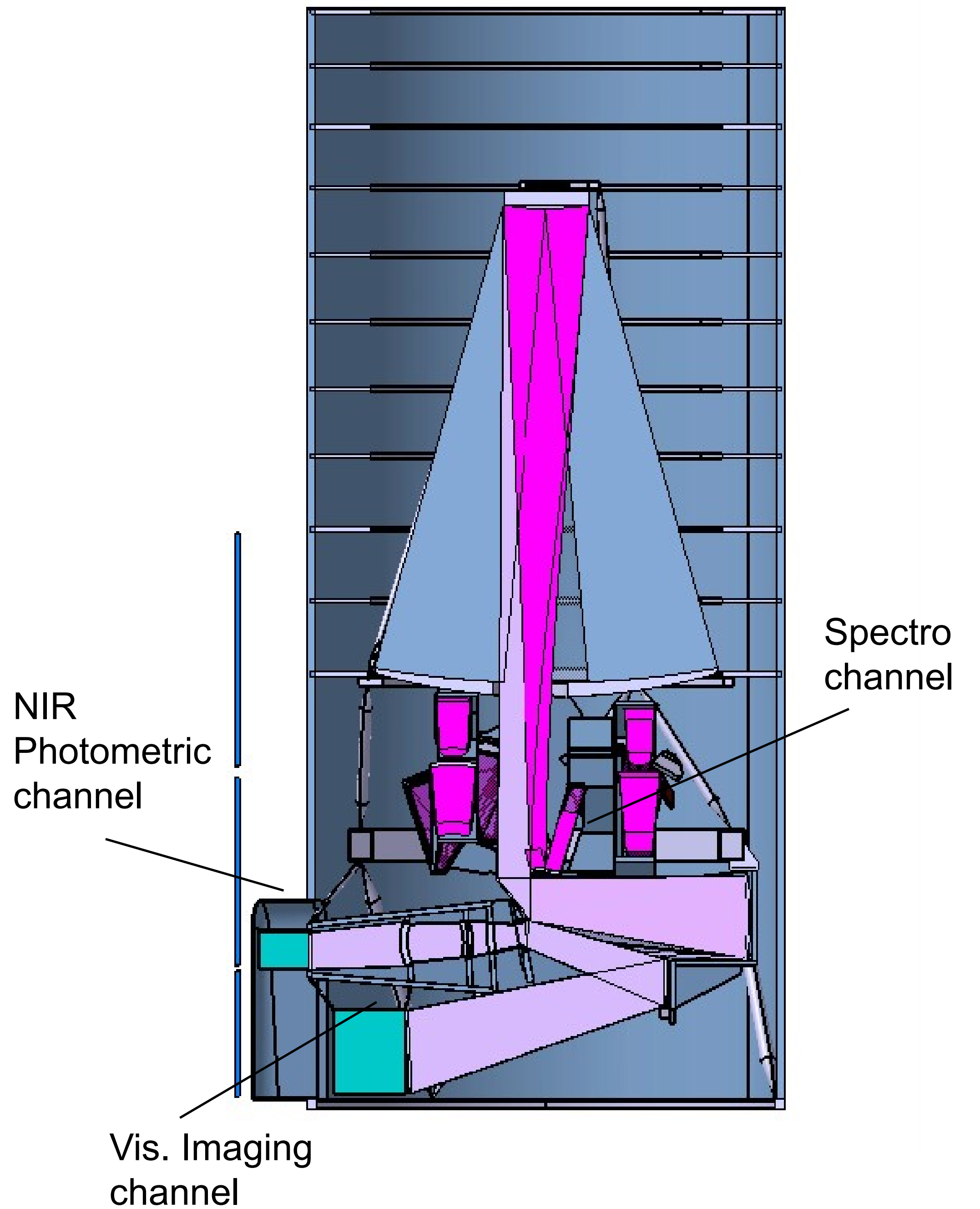

Euclid mission baseline: surveys

Euclid Consortium

I. Wide Survey: 15,000 deg^2: Extragalactic sky - 5.2 years

- **Visible:**
  - Diffraction limited images (0.16 " FWHM PSF)
  - Galaxy shapes for 1.5.10^9 galaxies to $RIZ_{AB} \leq 24.5$ (AB, 10σ Extended source)
  - 30-40 gal/amin^2, $<z>\sim 0.9$
- **NIR photometry**:
  - Y, J, $H \leq$ 24 (AB, 5σ Point source), 0.33''/pixel
  - photo-z's errors <0.05(1+z) with ground based PS, DES, LSST, HSC, etc…
- **NIR slitless Spectro:**
  - R=250 at 1.2 micron:
  - Redshifts for 50.10^6 gal with em. line fluxes >4.10^{-16} ergs/cm^2/s at 0<z<2 and
  - spectro-z errors < 0.001

II. Deep Survey: 40 deg^2 (at ecliptic poles?) 1 visit/month - 6 months

- Science: +2 magnitudes in depth for both visible and NIR imaging data.
- Spectroscopy of ~10,000 galaxies
- Calibrations: monitoring of PSF (>40 visits over 6 years), calib. of NIR data

Euclid Figure of Merit

Euclid Consortium

	Modified Gravity	Dark Matter	Initial Conditions	Dark Energy		
Parameter	γ	m_ν/eV	f_{NL}	w_p	w_a	FoM
Euclid Primary (WL+GC)	0.010	0.027	5.5	0.015	0.150	430
Euclid All (WL+GC)+ CL+ISW	0.009	0.020	2.0	0.013	0.048	1540
Euclid+Planck (Euclid All)	0.007	0.019	2.0	0.007	0.035	4020
Current	0.200	0.580	100	0.100	1.500	~10
Improvement Factor	**30**	**30**	**50**	**>10**	**>50**	**>300**

Euclid Consortium

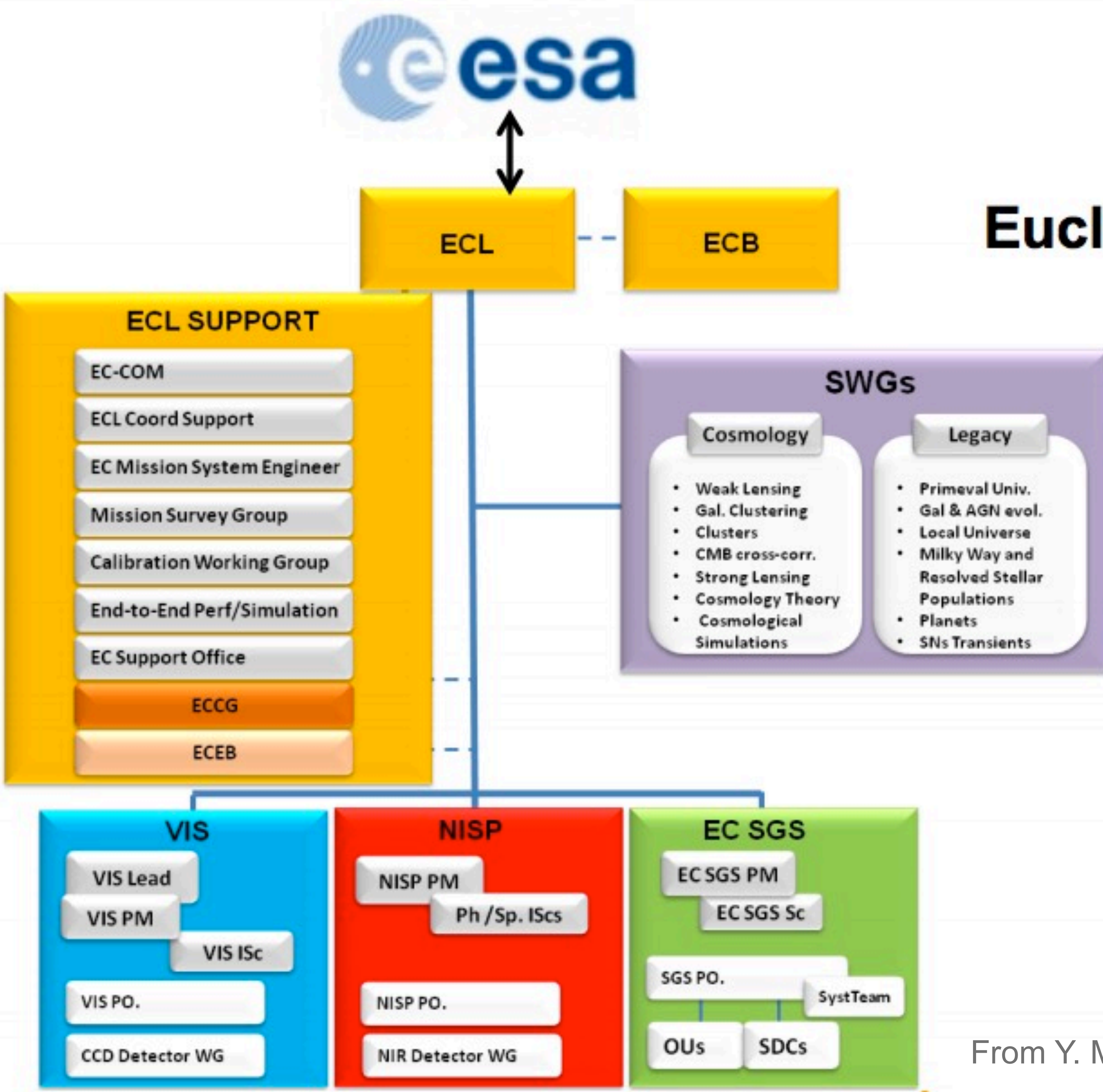

Euclid Consortium

- ~1200 members,
- 130 Labs
- 13 European countries:

Austria, Denmark, France, Finland,, Germany, Italy, The Netherlands, Norway, Portugal, Romania, Spain, Switzerland, UK

\+ US/NASA and Berkeley labs.

From Y. Mellier presentation, Marseille, 2014

Weak Lensing

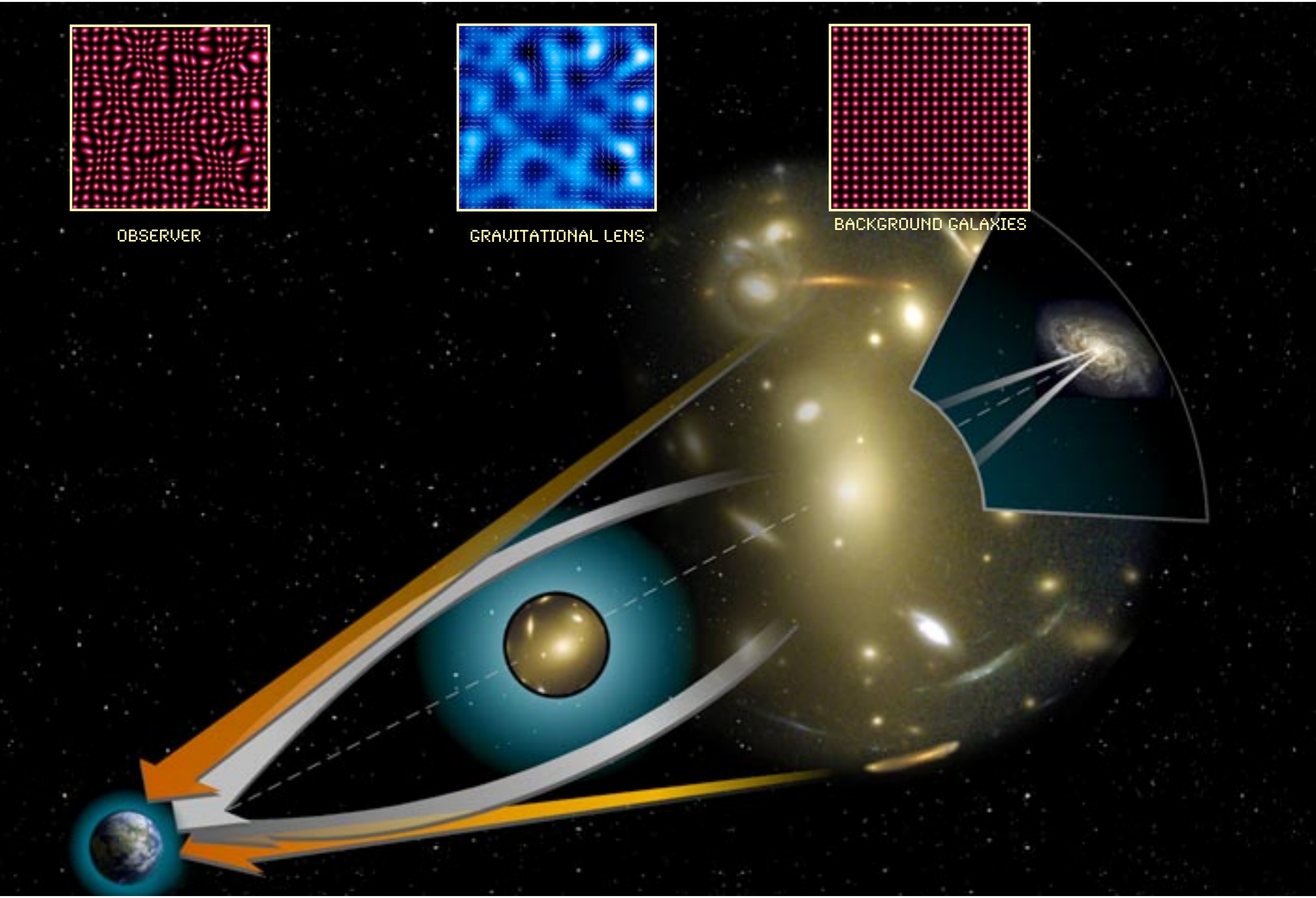

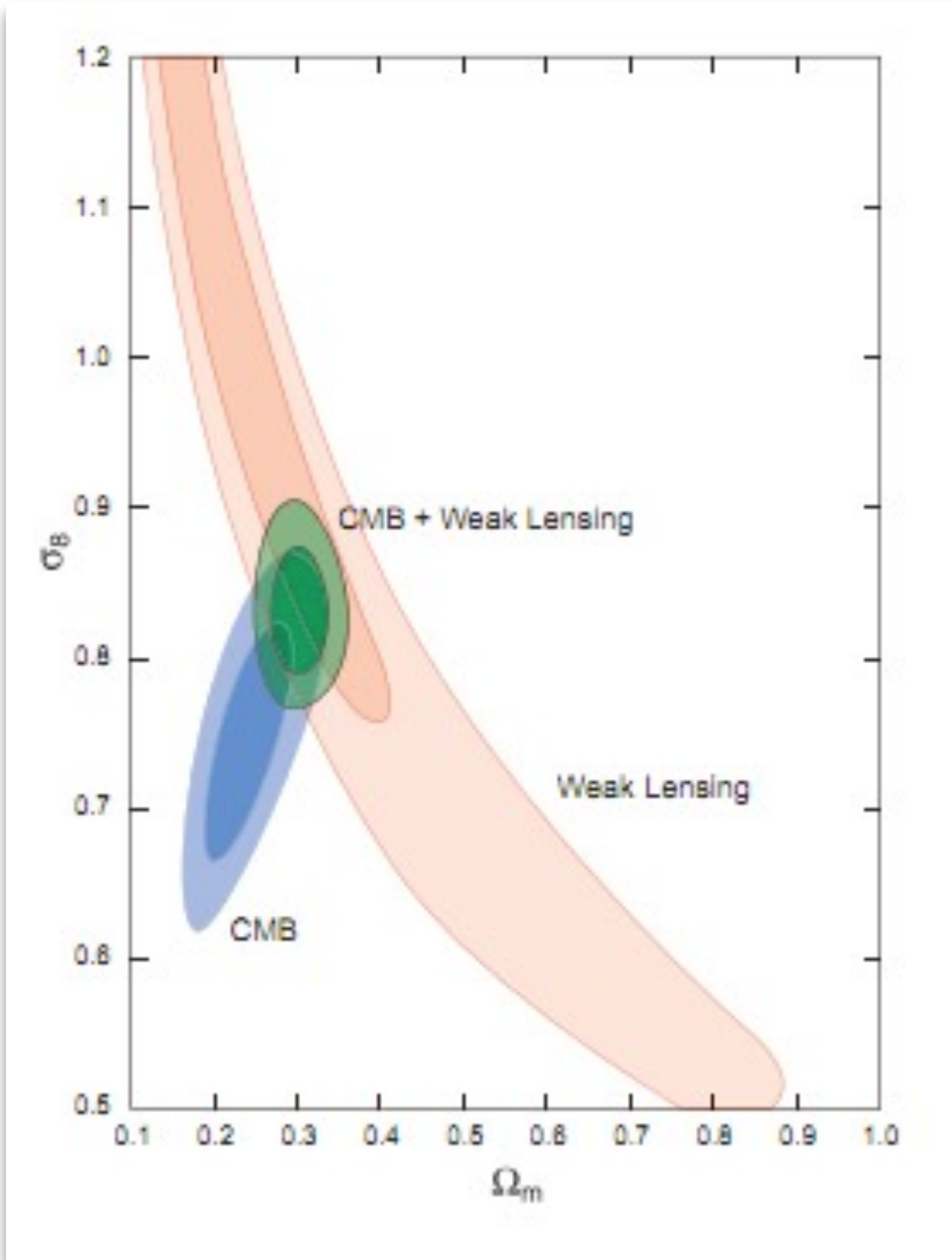

Massey et al, “The dark matter of gravitational lensing”,Reports on Progress in Physics, 73, 8, 2010.

Euclid Red Book

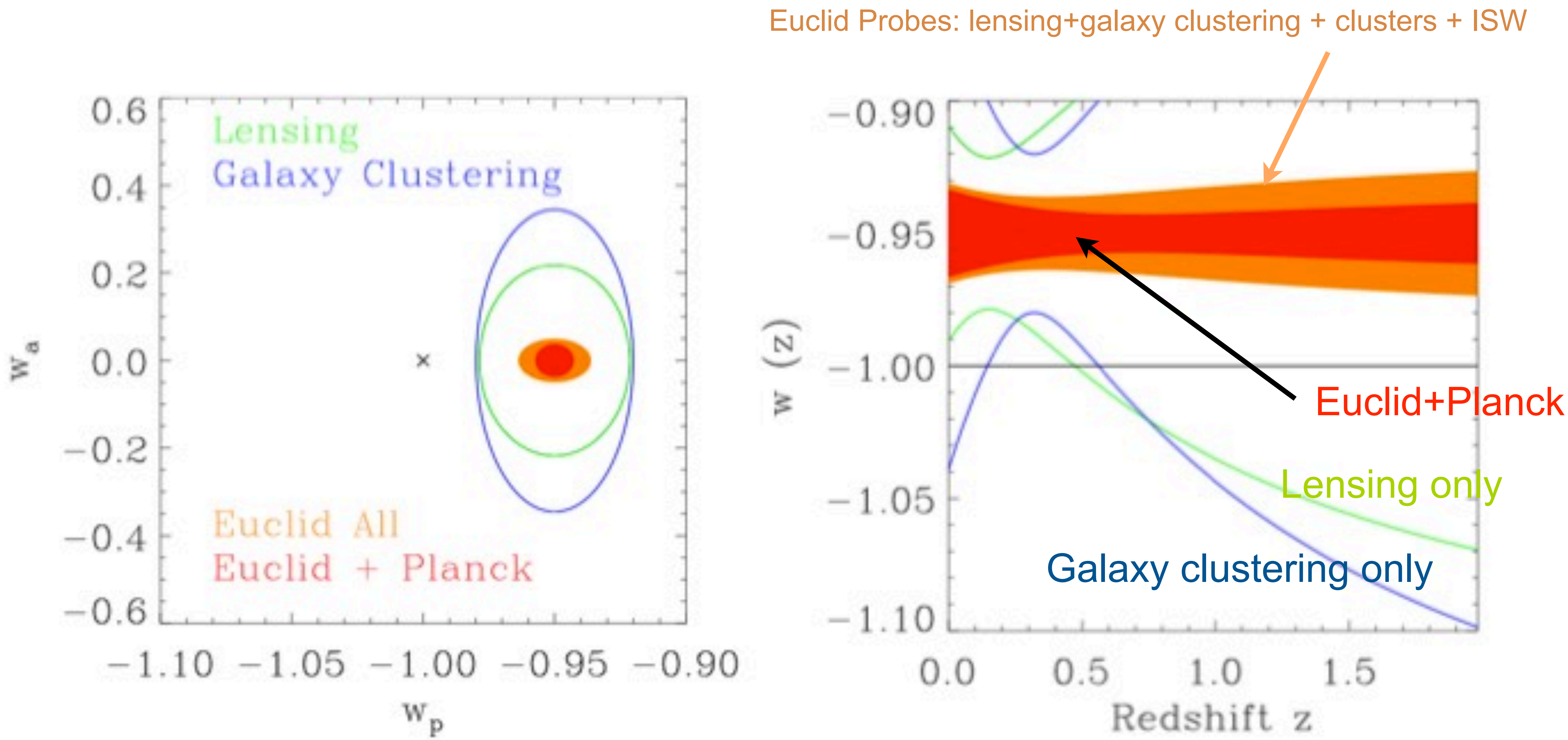

Figure 2.4: The expected constraints from Euclid in the dynamical dark energy parameter space. We show lensing only (green), galaxy clustering only (blue), all the Euclid probes (lensing+galaxy clustering+clusters+ISW; orange) and all Euclid with Planck CMB constraints (red). The cross shows a cosmological constant model. Left panel: the expected 68% confidence contours in the (w_p, w_a). Right panel: the 1σ constraints on the function w(z) parameterised by (w_p, w_a) as a function of redshift (green-lensing alone, blue-galaxy clustering alone, orange-all of the Euclid probes, red-Euclid combined with Planck).

Euclid & Weak Lensing

- Part 1: Introduction to Euclid & Weak Lensing
- **Part 2: Shear WL Measurements**
- Part 3: From Shear to 2D and 3D Maps
- Part 4: Challenges in the WL Community
- Part 5: WL Inverse Problems and Sparse Solutions
  - Point Spread Function superresolution
  - 2D mass mapping
  - 3D mass mapping

Shape Parameters

γ_1 = deformation along the x-axis,

and γ_2 at 45 degrees from it.

$$\gamma = \gamma_1 + i\gamma_2 = |\gamma| e^{2i\theta}$$

Where the modulus represents the amount of shear and the phase represents its direction.

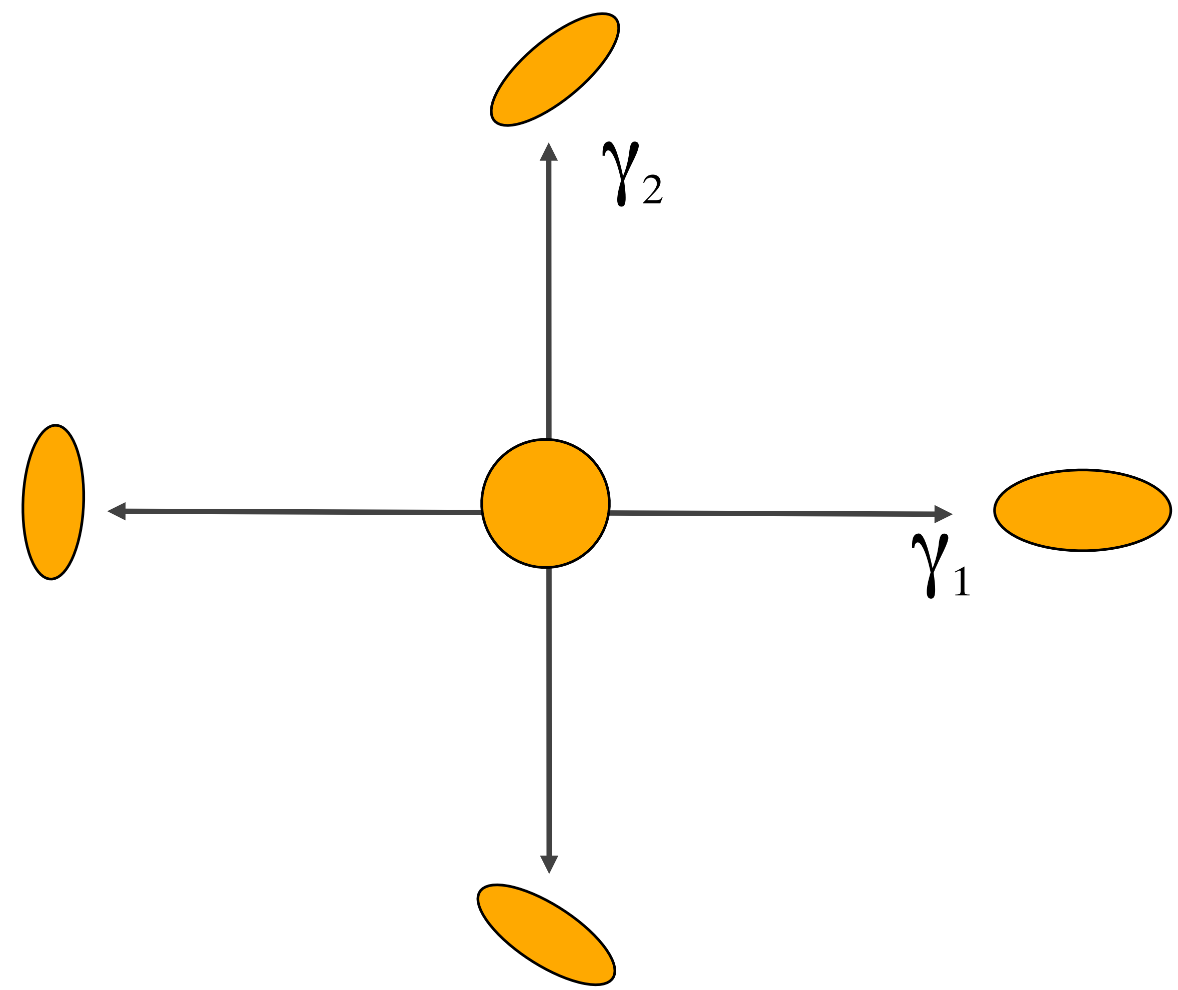

$$\gamma_1 = \frac{M_{1,1} - M_{2,2}}{M_{1,1} + M_{2,2}}, \gamma_2 = \frac{2M_{1,2}}{M_{1,1} + M_{2,2}}, \qquad M_{i,j} = \int \theta_i \theta_j S(\theta) w(\theta) d\theta^2$$

$M_{1,1} - M_{2,2}$ and $2M_{1,2}$ correspond respectively to the flattening along the x axis and the 45° axis. $M_{1,1} + M_{2,2}$ is related to the size.

PB 1: We need accurate measurements from noisy data

Detection + Classification stars/galaxies

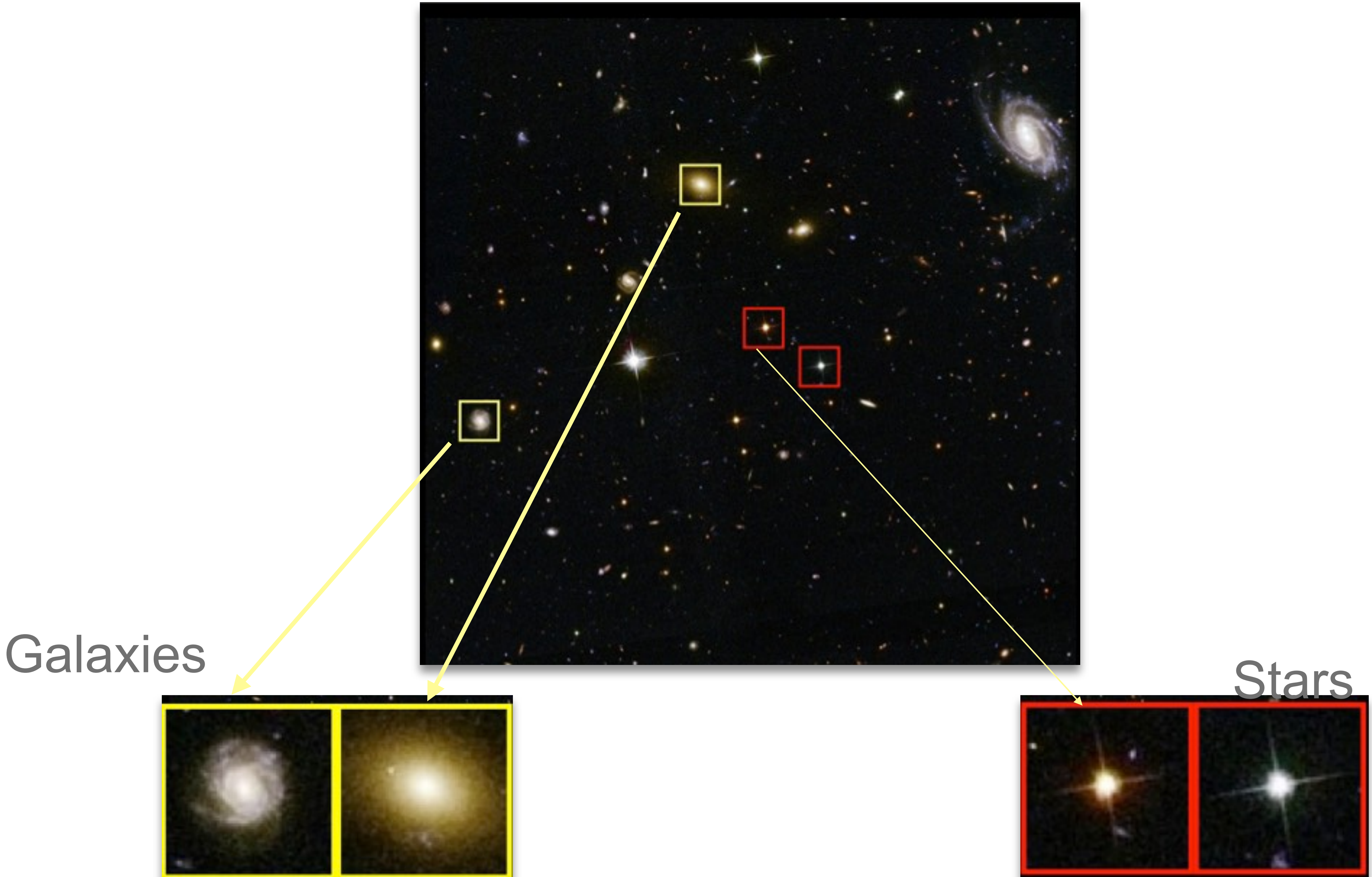

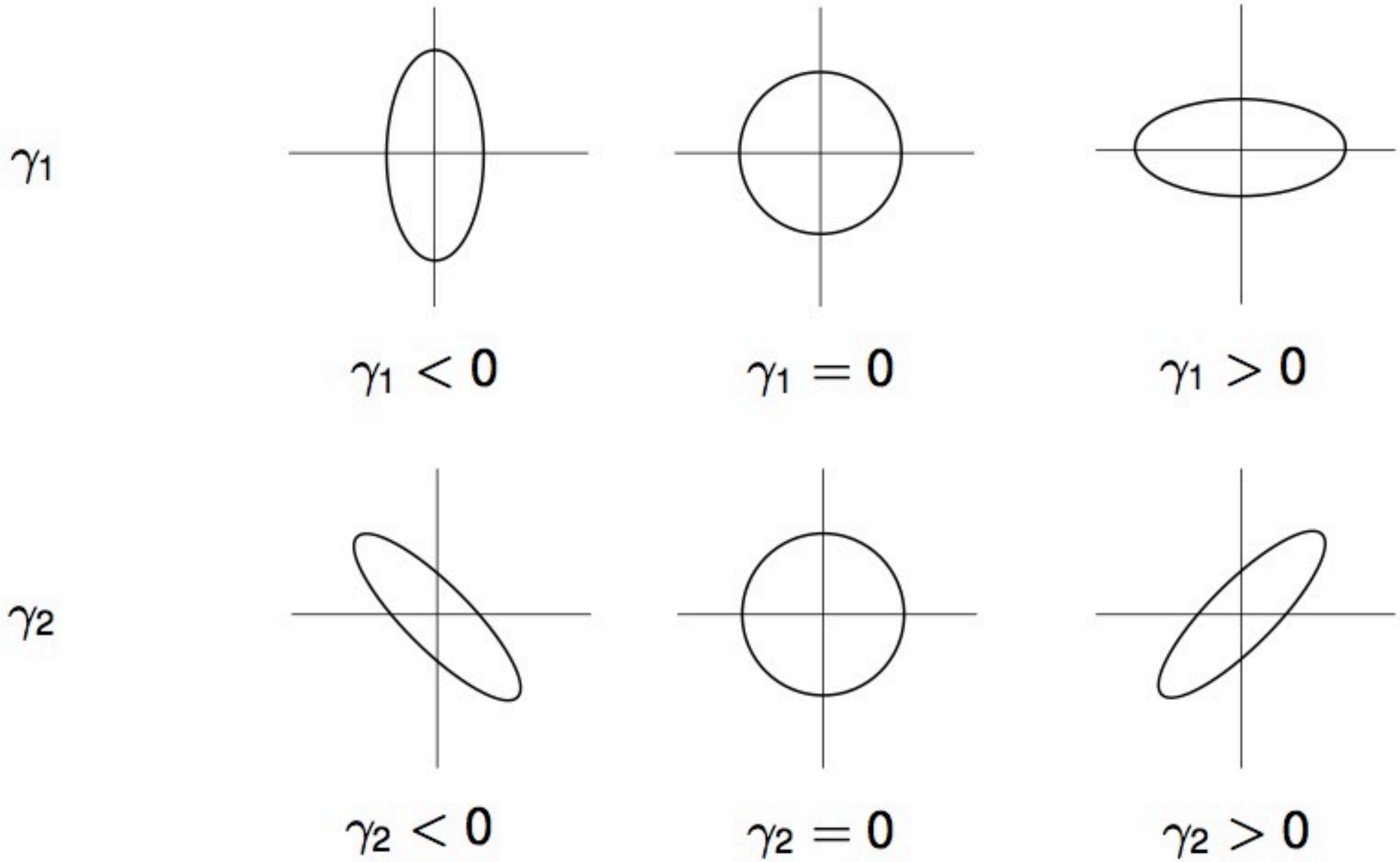
γ_1
$\gamma_1 < 0$
$\gamma_1 = 0$
$\gamma_1 > 0$
γ_2
$\gamma_2 < 0$
$\gamma_2 = 0$
$\gamma_2 > 0$

Motivation for spatial observations

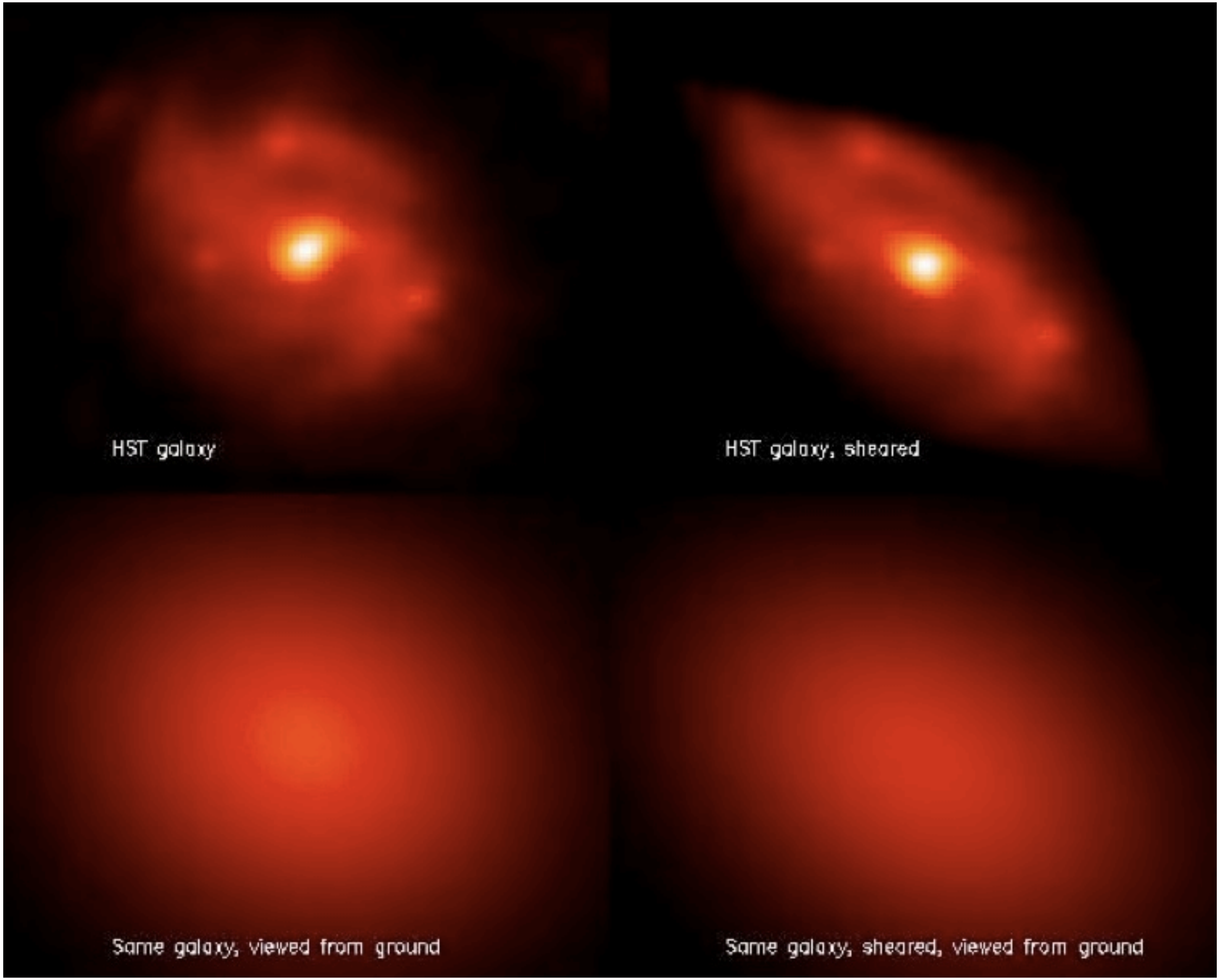

Weakly Lensed Galaxies

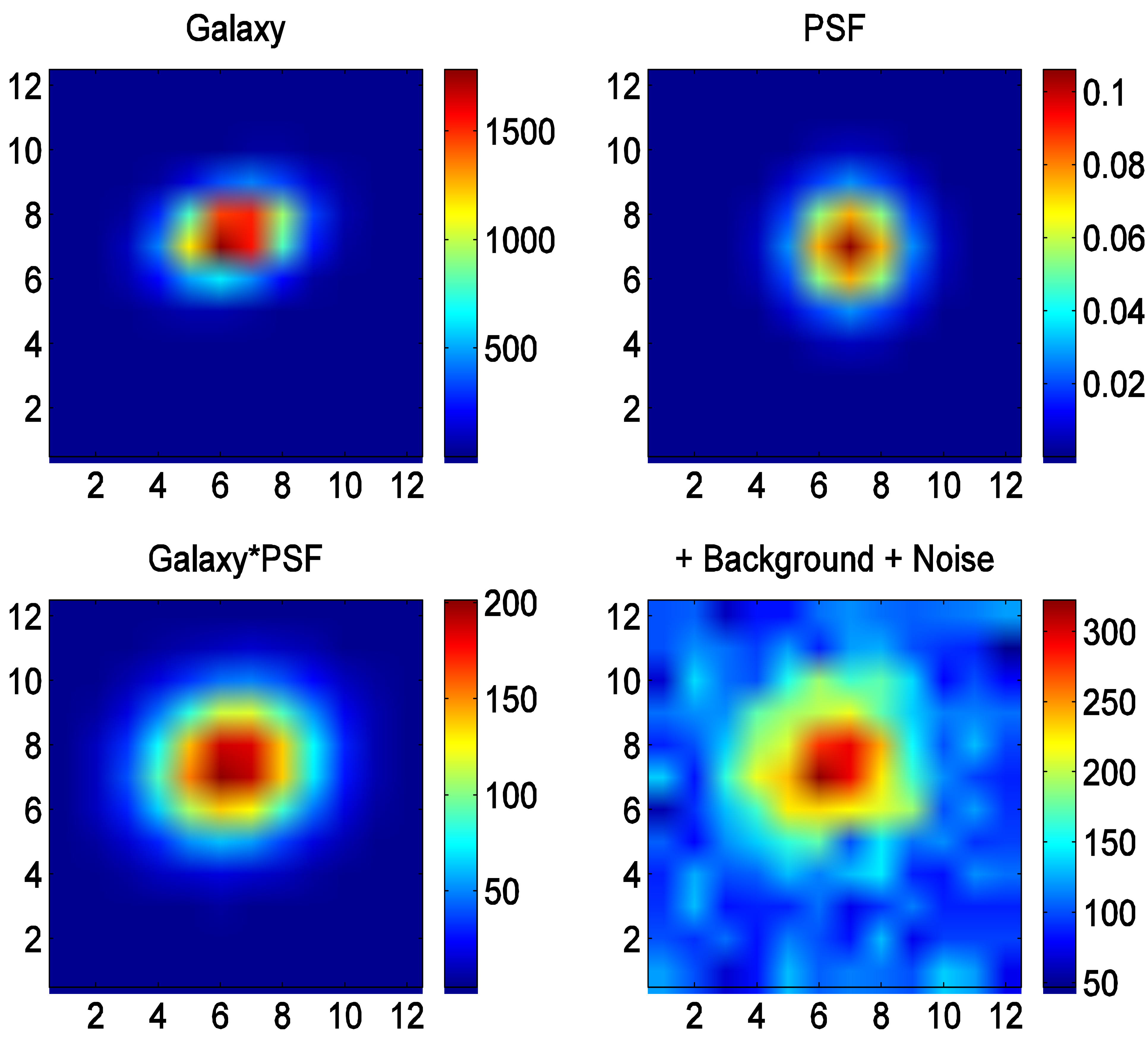

Point Spead Function

Galaxies are convolved by an asymetric PSF
+ Images are undersampled

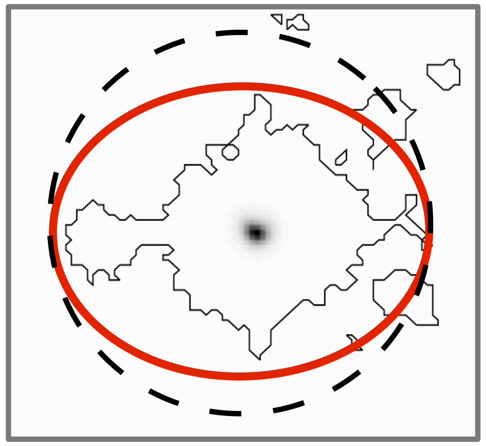

PB 2: Shape measurements must be deconvolved

Methods: Moments (KSB), Shapelets, Forward-Fitting, Bayesian estimation, etc

Space Variant PSF

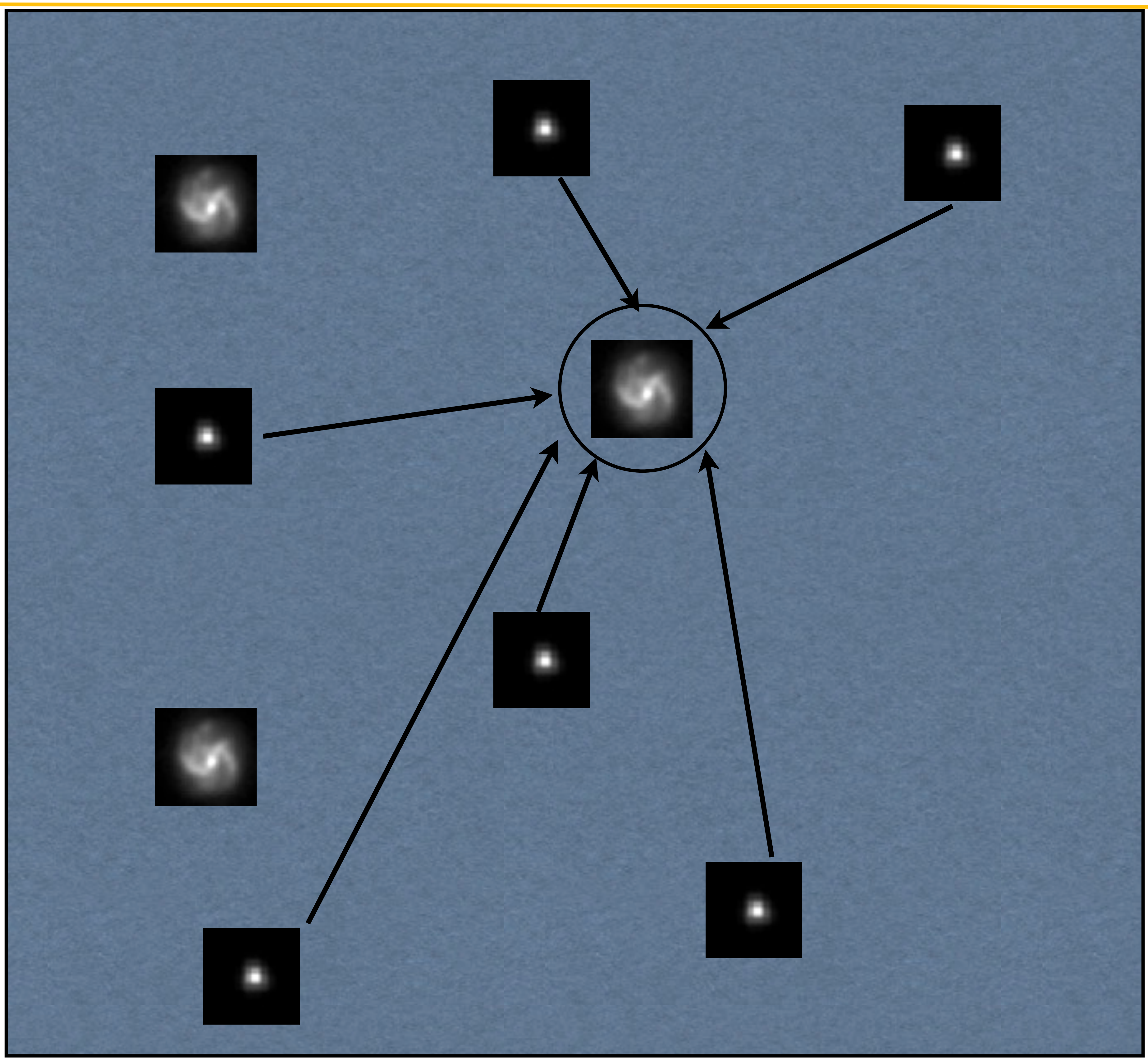

PB 3: We need to interpolate the PSF shape !

Intrinsic Ellipticities

✓ Galaxies have an intrinsic ellipticipty



PB 4: We need to correct the measurements from the intrinsic ellipticity

Shear Catalog & Map

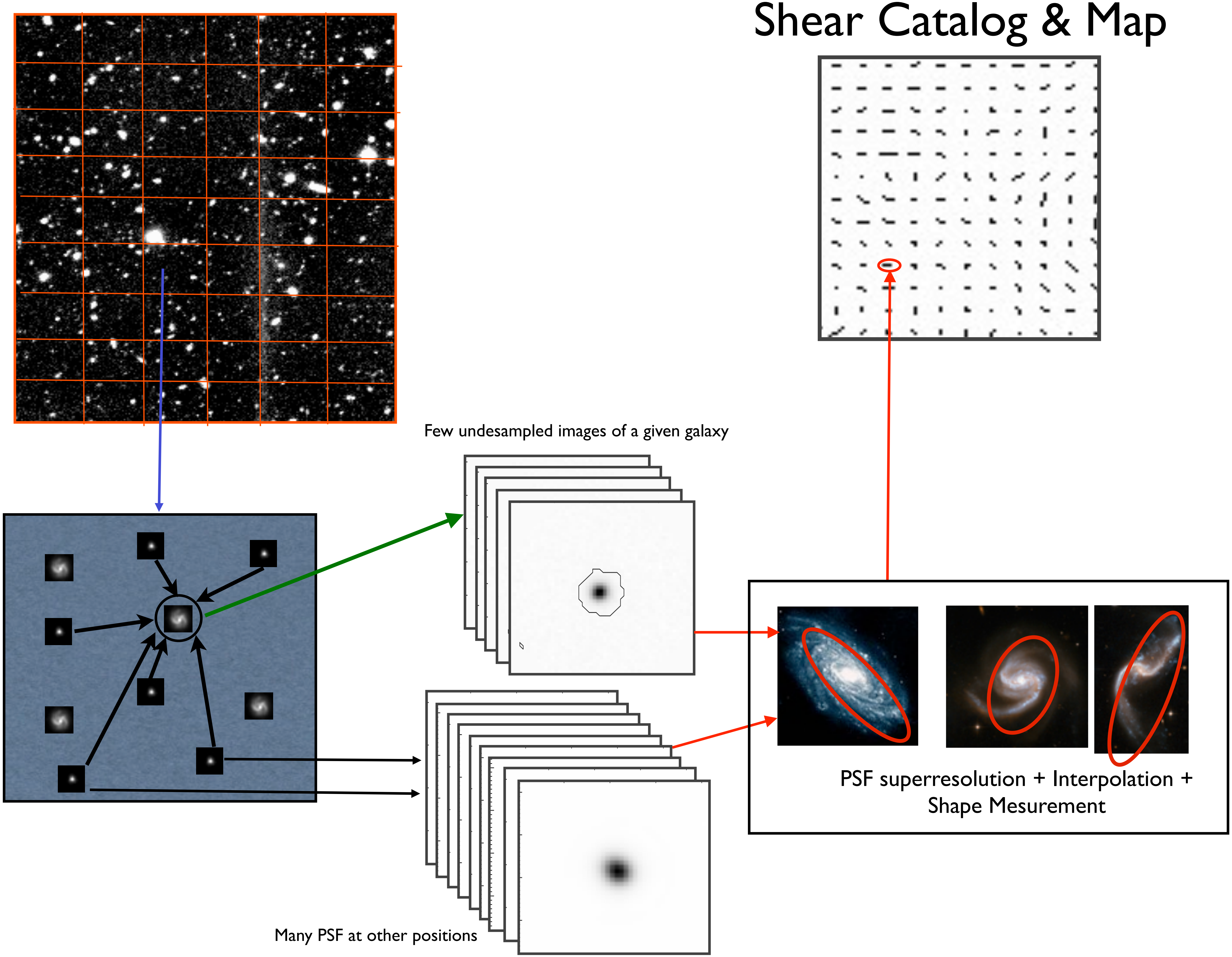

We need to solve a triple inverse problem !!!

1) Determine the PSF at any position from the measured PSF.

2) Measure the galaxy shear and correct it from the PSF.

3) Correct the shear from intrinsic ellipticities

+ noise and **missing data**!!!

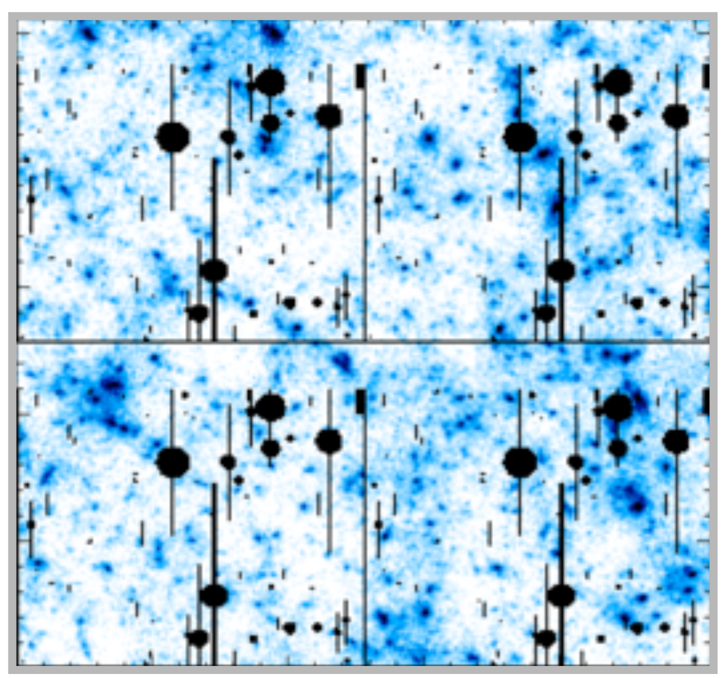

Missing data

Tomographic Weak Lensing

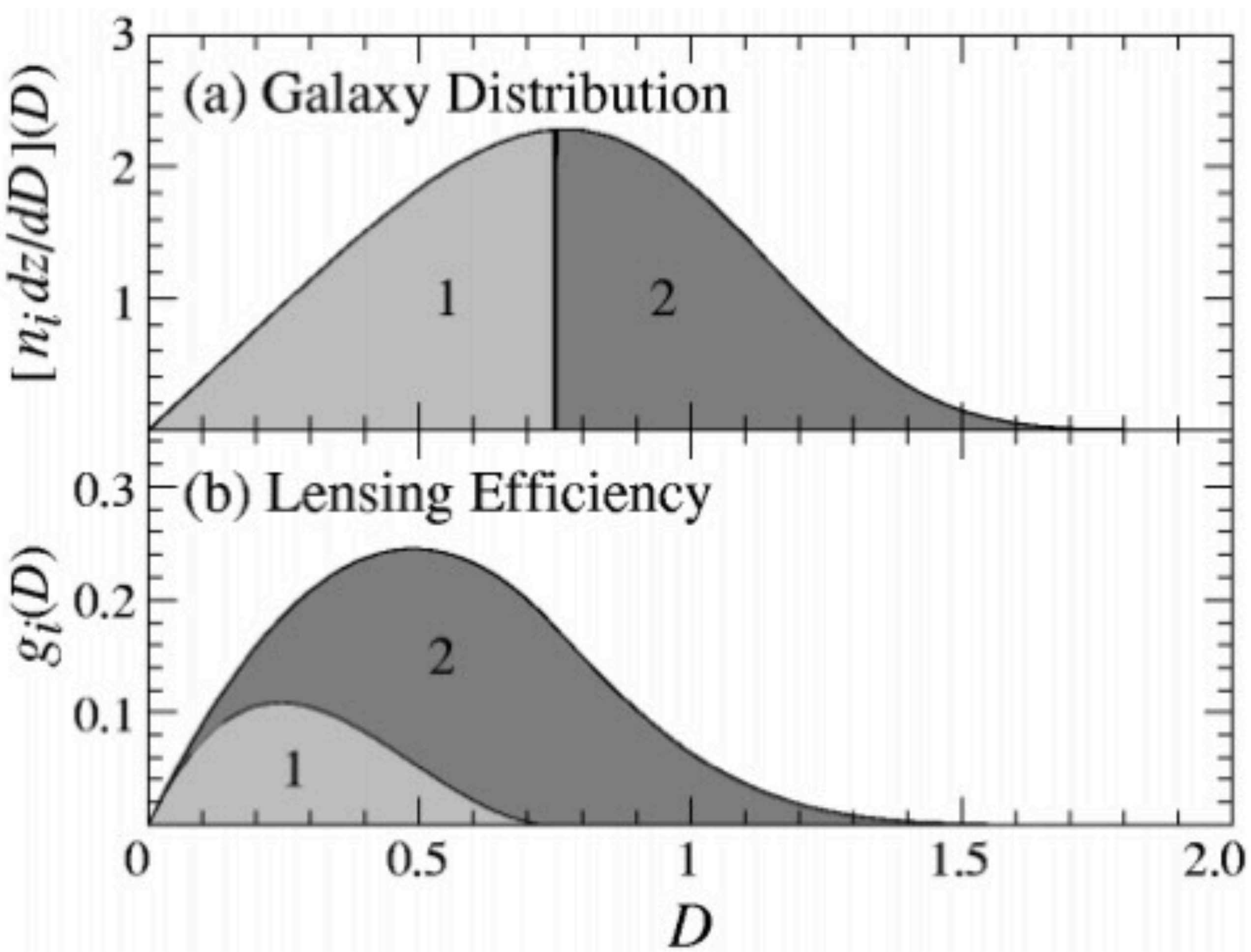

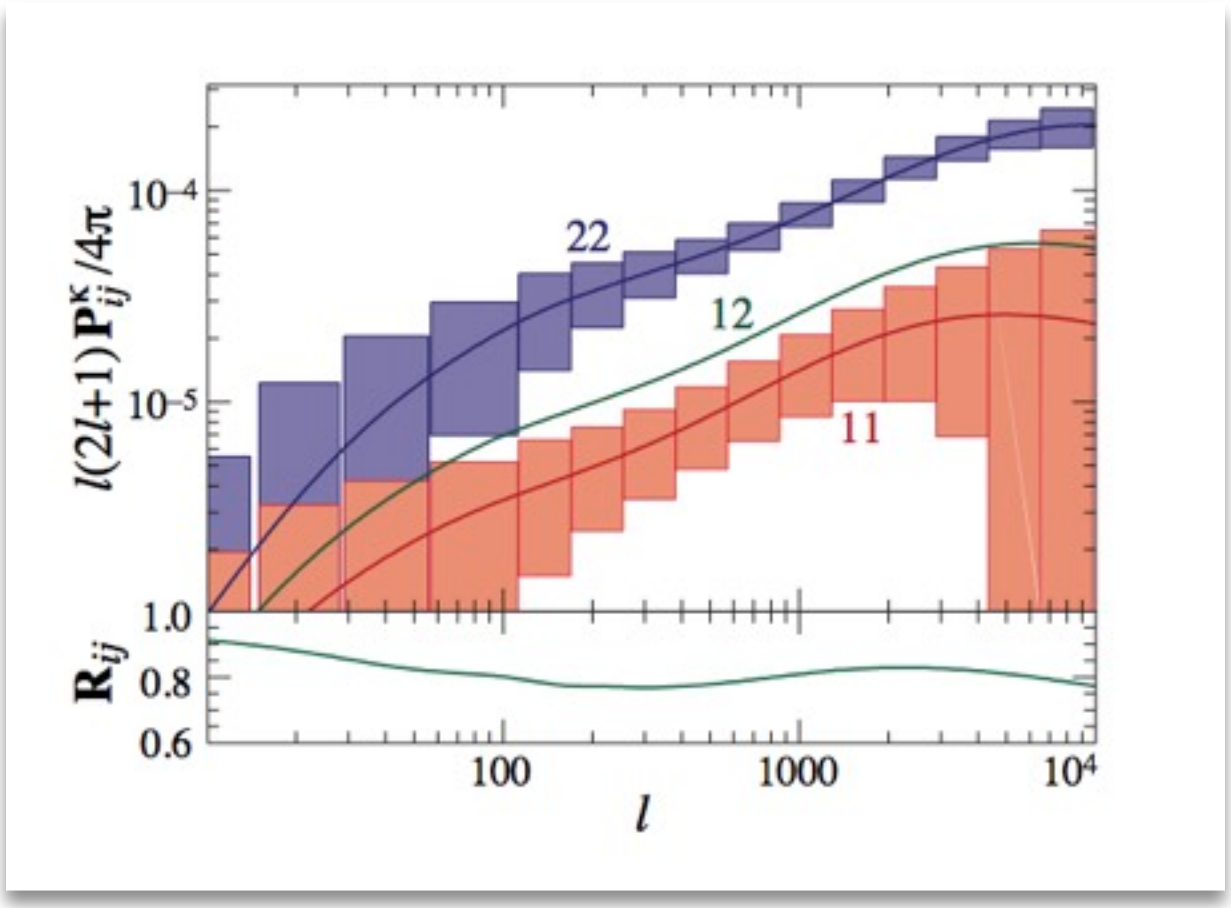

The power spectra of two slices, their cross power spectrum, and their correlation coefficient (Hu, ApJ, 1999).

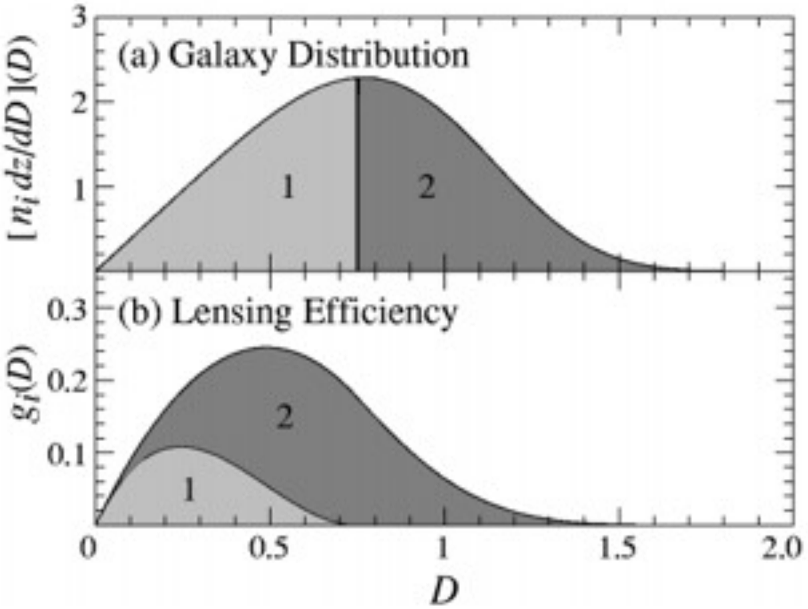

Degeneracy

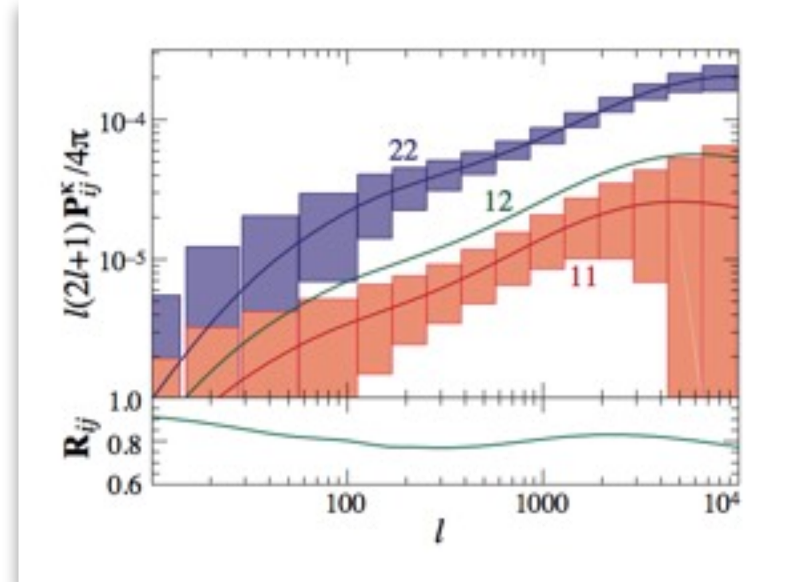

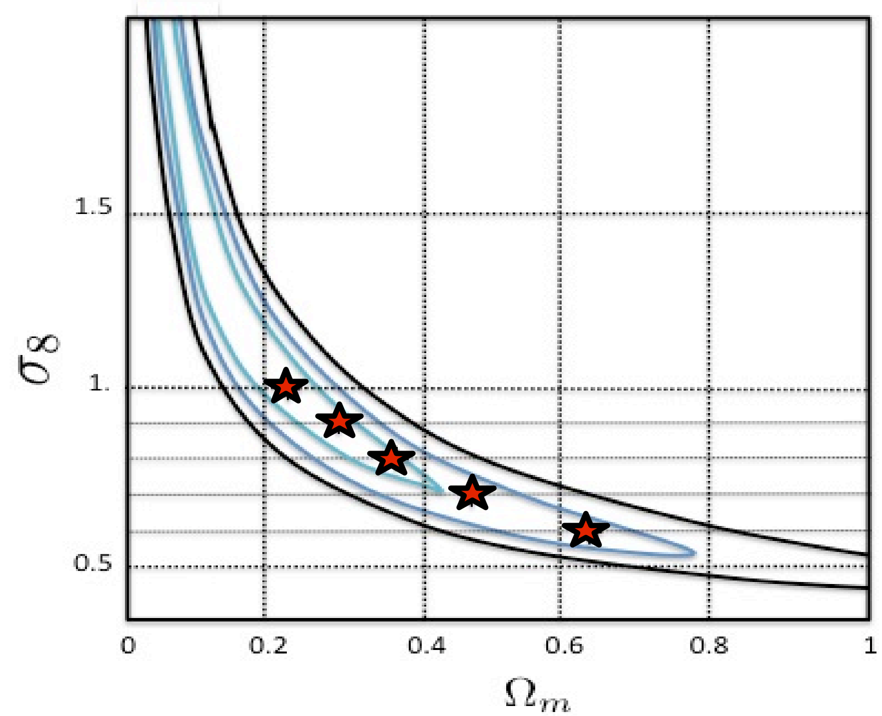

Model1 (σ_8=1, Ω_m=0.23)

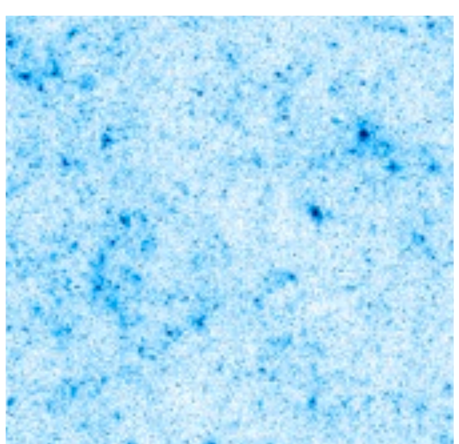

Model2 (σ_8=0.9, Ω_m=0.3)

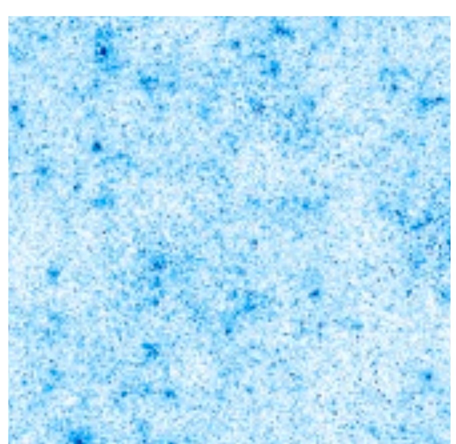

Model3 (σ_8=0.8, Ω_m=0.36)

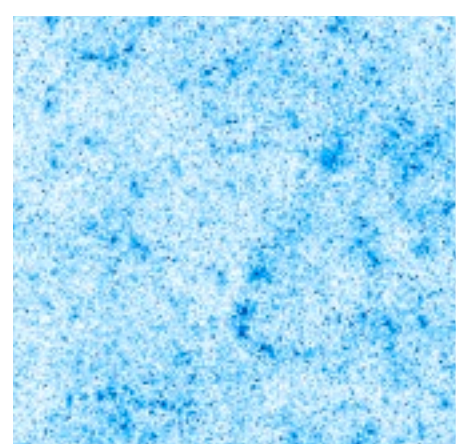

Model4 (σ_8=0.7, Ω_m=0.47)

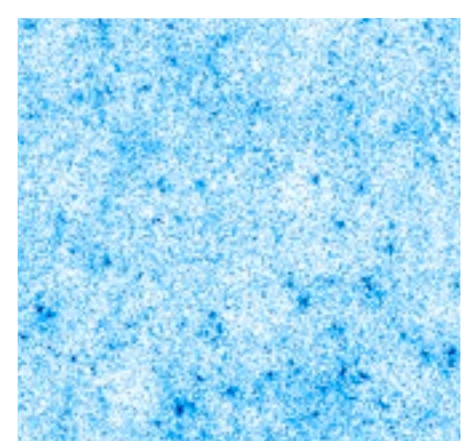

Model5 (σ_8=0.6, Ω_m=0.64)

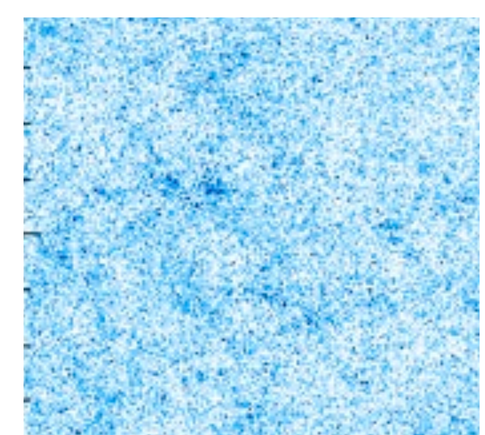

Euclid & Weak Lensing

- Part 1: Introduction to Euclid & Weak Lensing
- Part 2: Shear WL Measurements
- **Part 3: From Shear to 2D and 3D Maps**
- Part 4: Challenges in the WL Community
- Part 5: WL Inverse Problems and Sparse Solutions
  - Point Spread Function superresolution
  - 2D mass mapping
  - 3D mass mapping

Shear Field and Mass Map & Related Shear Mass Map

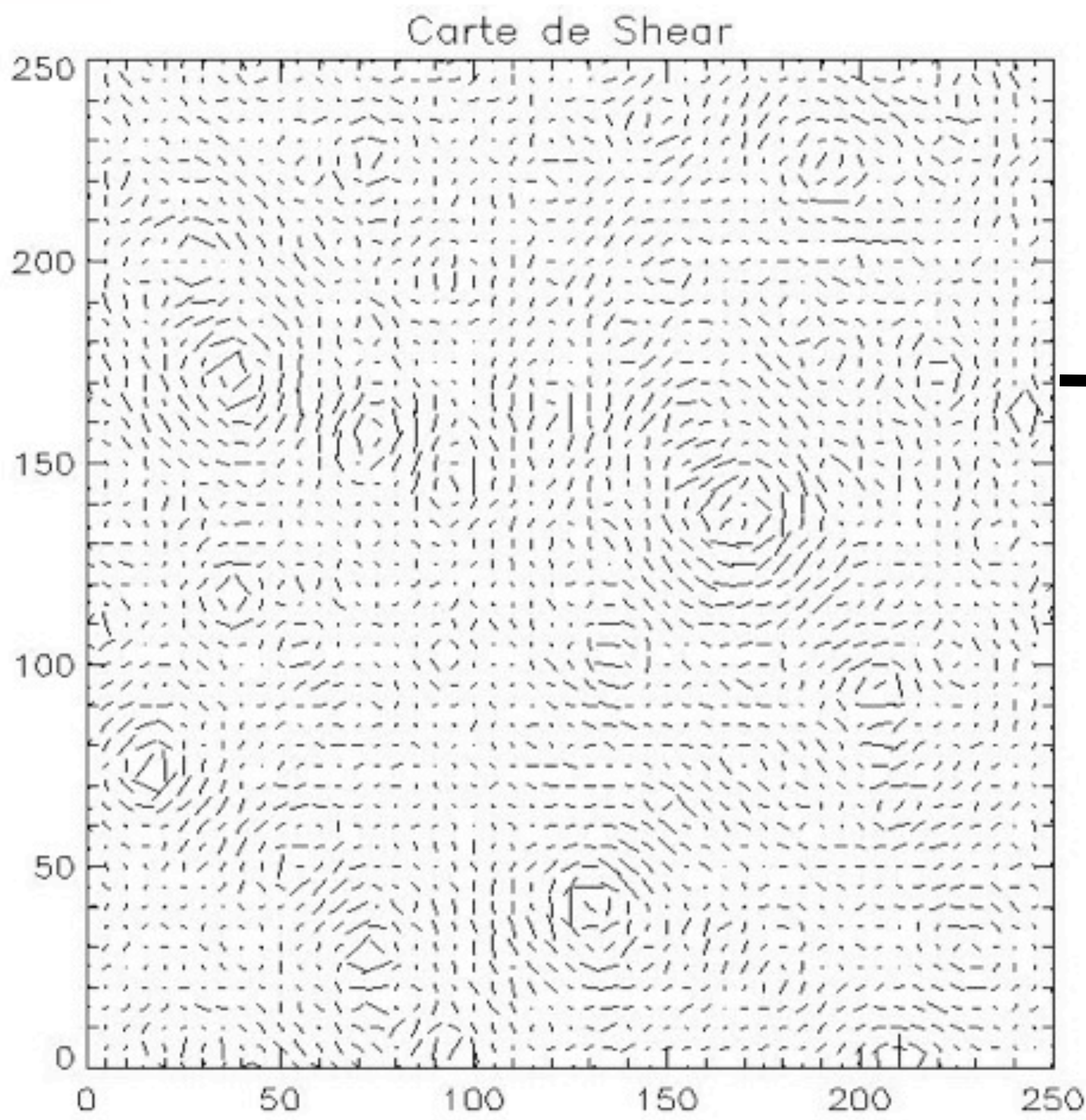

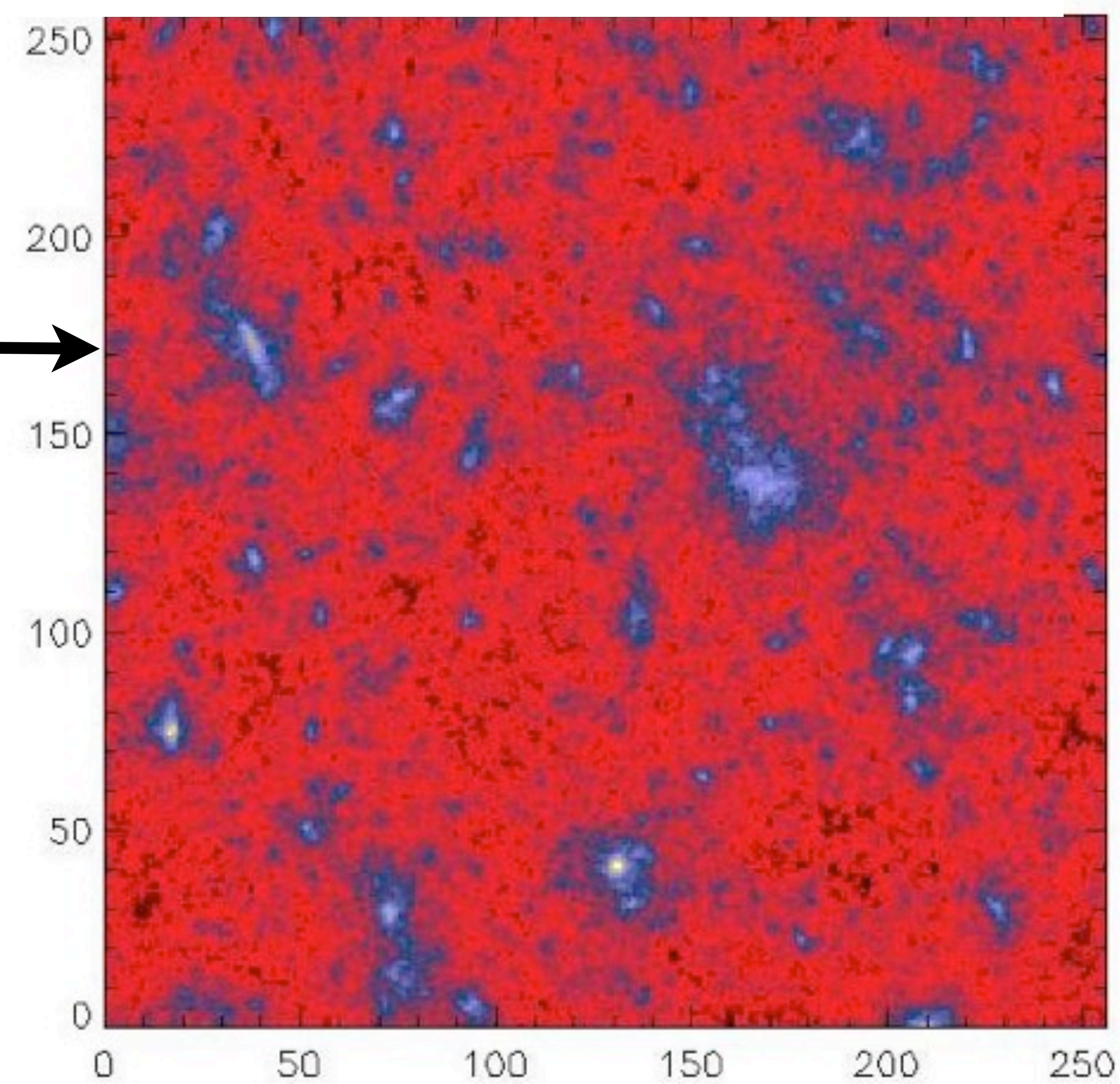

Inversion Equations

★ J.L. Starck, S. Pires and A. Réfrégier, A&A, Vol. 451, pp 1139-1150, 2006.
★ S. Pires, J.-L. Starck and A. Refregier, "Light on Dark Matter with Weak Gravitational Lensing", IEEE Signal Processing Magazine, 27, 1, pp 76--85, 2010.

SIMULATED SHEAR MAP

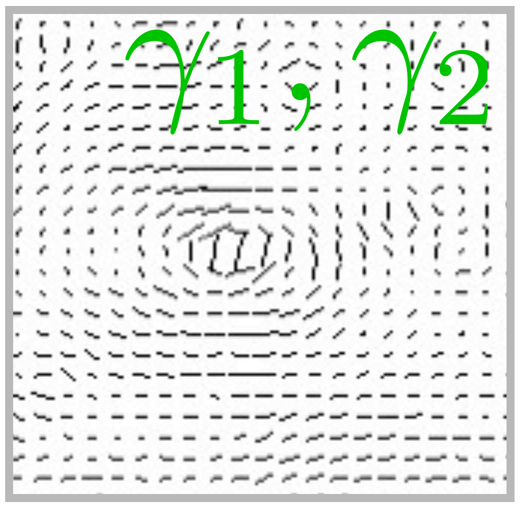

$$\gamma_1 = \frac{1}{2}(\partial_1^2 - \partial_2^2)\psi$$
$$\gamma_2 = \partial_1 \partial_2 \psi$$

LENSING POTENTIAL

ψ

$$\frac{1}{2}(\partial_1^2 + \partial_2^2)\,\psi = \kappa$$

SIMULATED MASS MAP
(Vale & White, 2003)

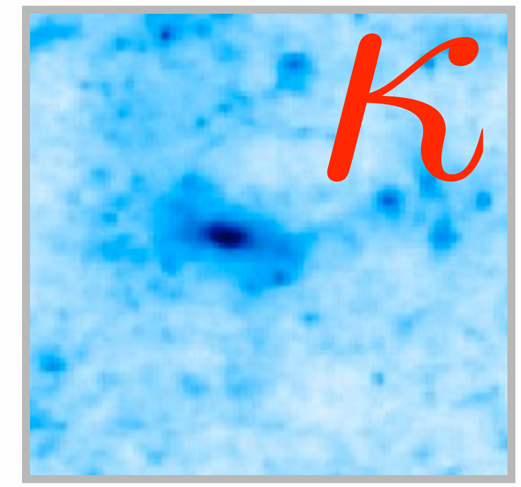

From mass to shear: $\gamma_i = \hat{P}_i \kappa$

From shear to mass: $\kappa = \hat{P}_1 \gamma_1 + \hat{P}_2 \gamma_2$

$$\hat{P}_1(k) = \frac{k_1^2 - k_2^2}{k^2}$$

$$\hat{P}_2(k) = \frac{2 k_1 k_2}{k^2}$$

$$\begin{pmatrix} \hat{E}(\boldsymbol{k}) = \hat{\kappa}(\boldsymbol{k}) \\ \hat{B}(\boldsymbol{k}) \end{pmatrix} = \underbrace{\frac{1}{|\boldsymbol{k}|^2} \begin{pmatrix} k_1^2 - k_2^2 & 2 k_1 k_2 \\ 2 k_1 k_2 & -k_1^2 + k_2^2 \end{pmatrix}}_{A_{\boldsymbol{\kappa}}} \begin{pmatrix} \hat{\gamma}_1(\boldsymbol{k}) \\ \hat{\gamma}_2(\boldsymbol{k}) \end{pmatrix}$$

A Simple Reconstruction is Very Noisy

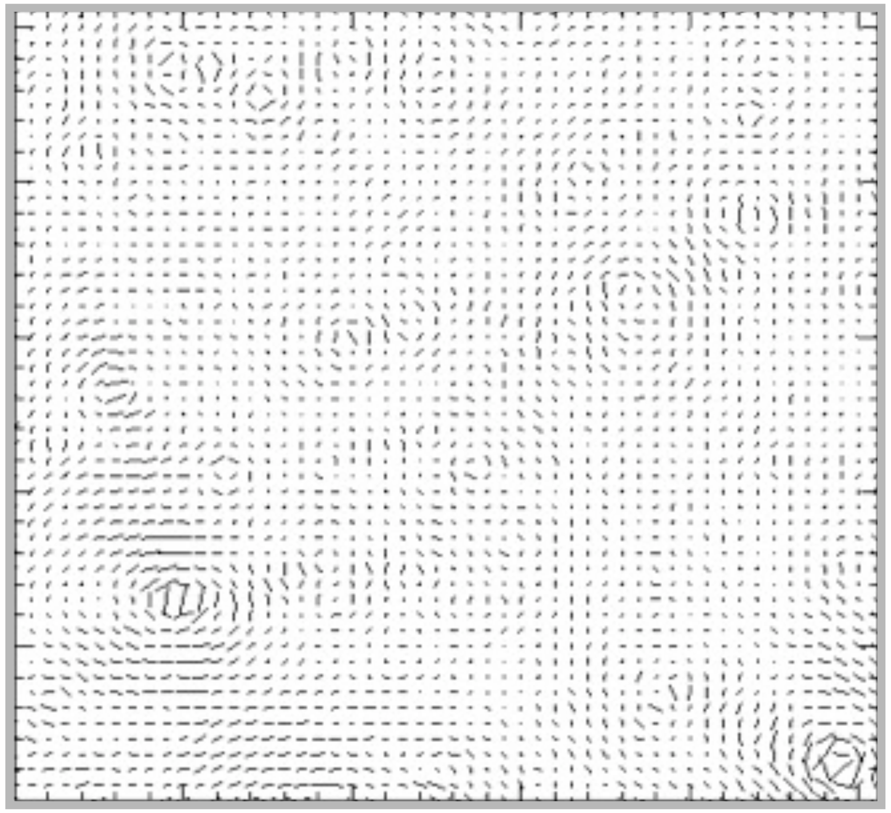

Shear map

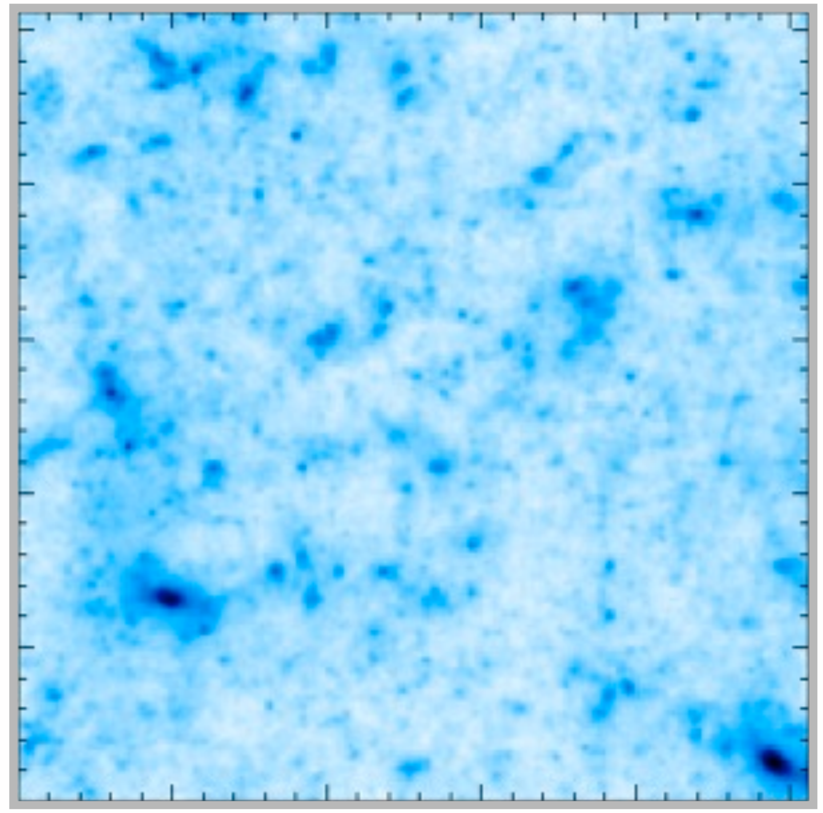

Original mass map

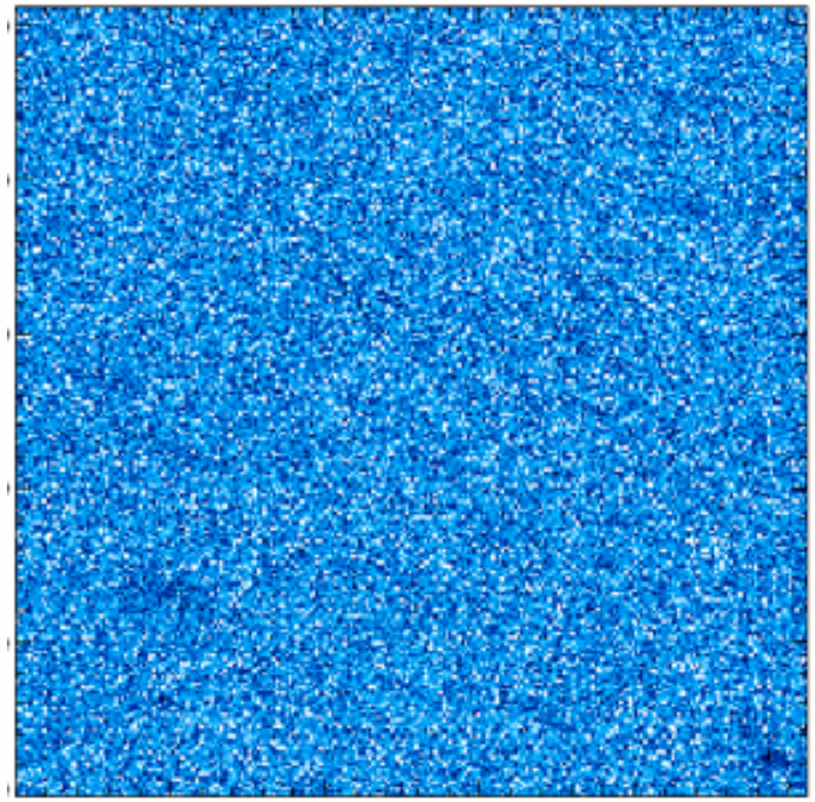

Mass map (space observations)

A Simple Reconstruction is Very Noisy

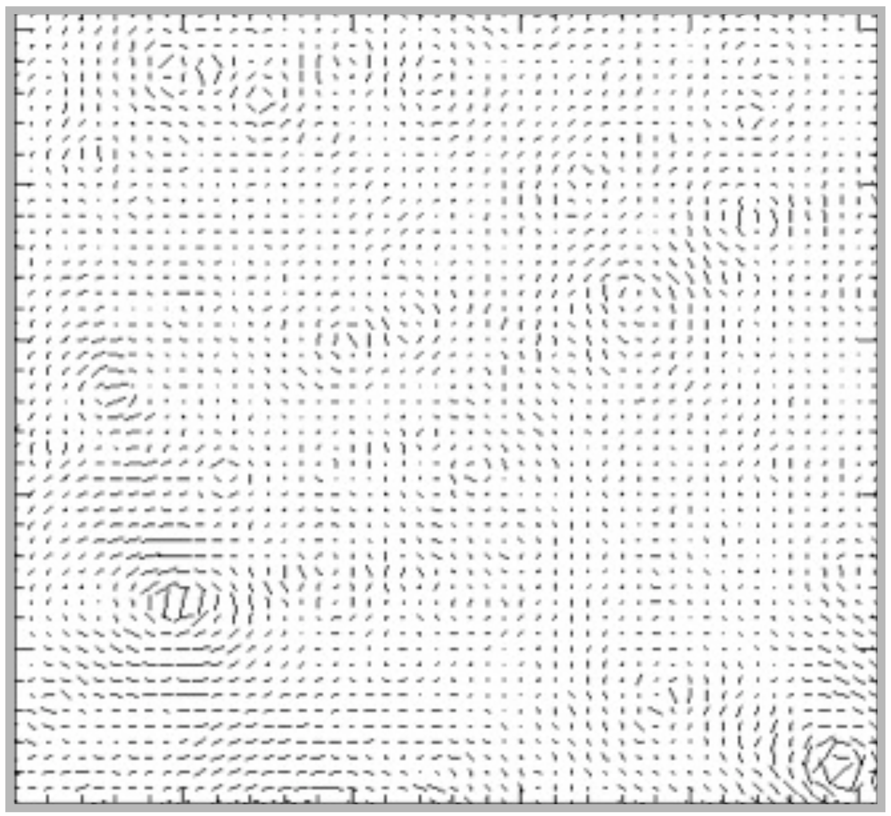

Shear map

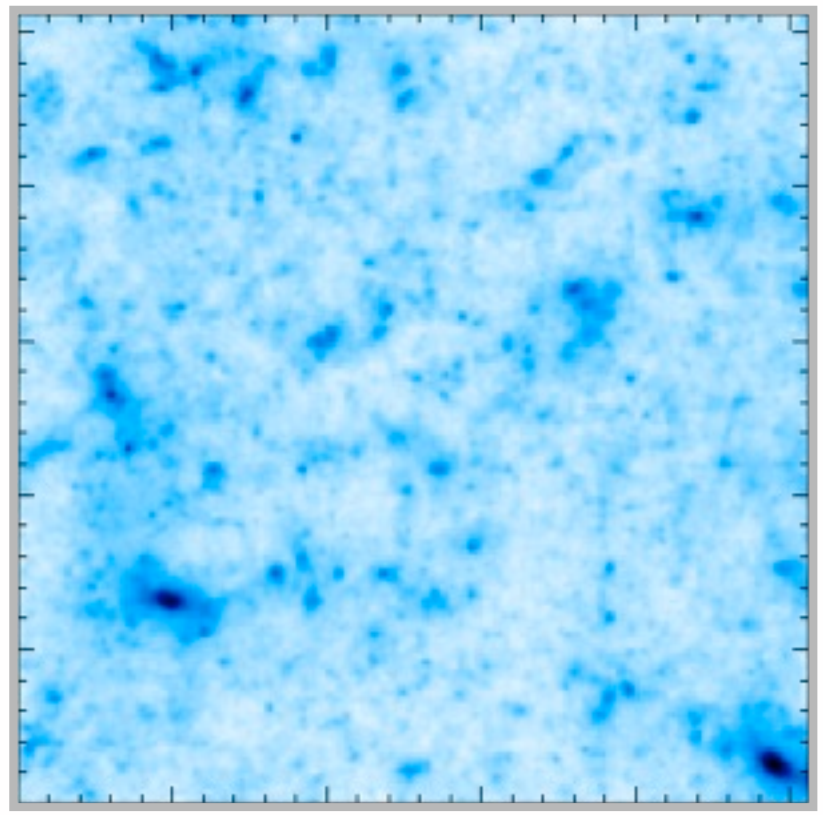

Original mass map

Mass map (space observations)

Density mass reconstruction

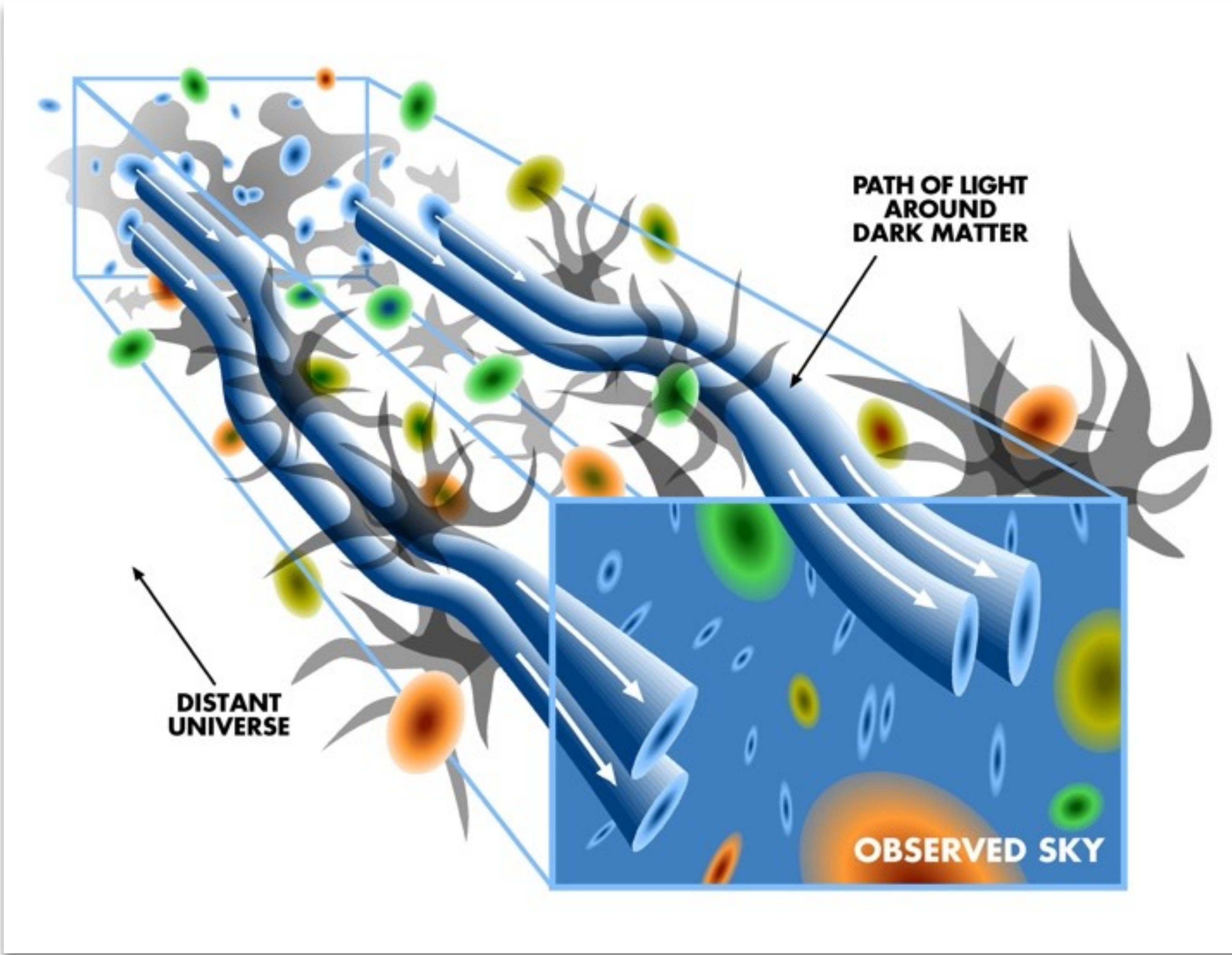

Pseudo-3D Weak Lensing

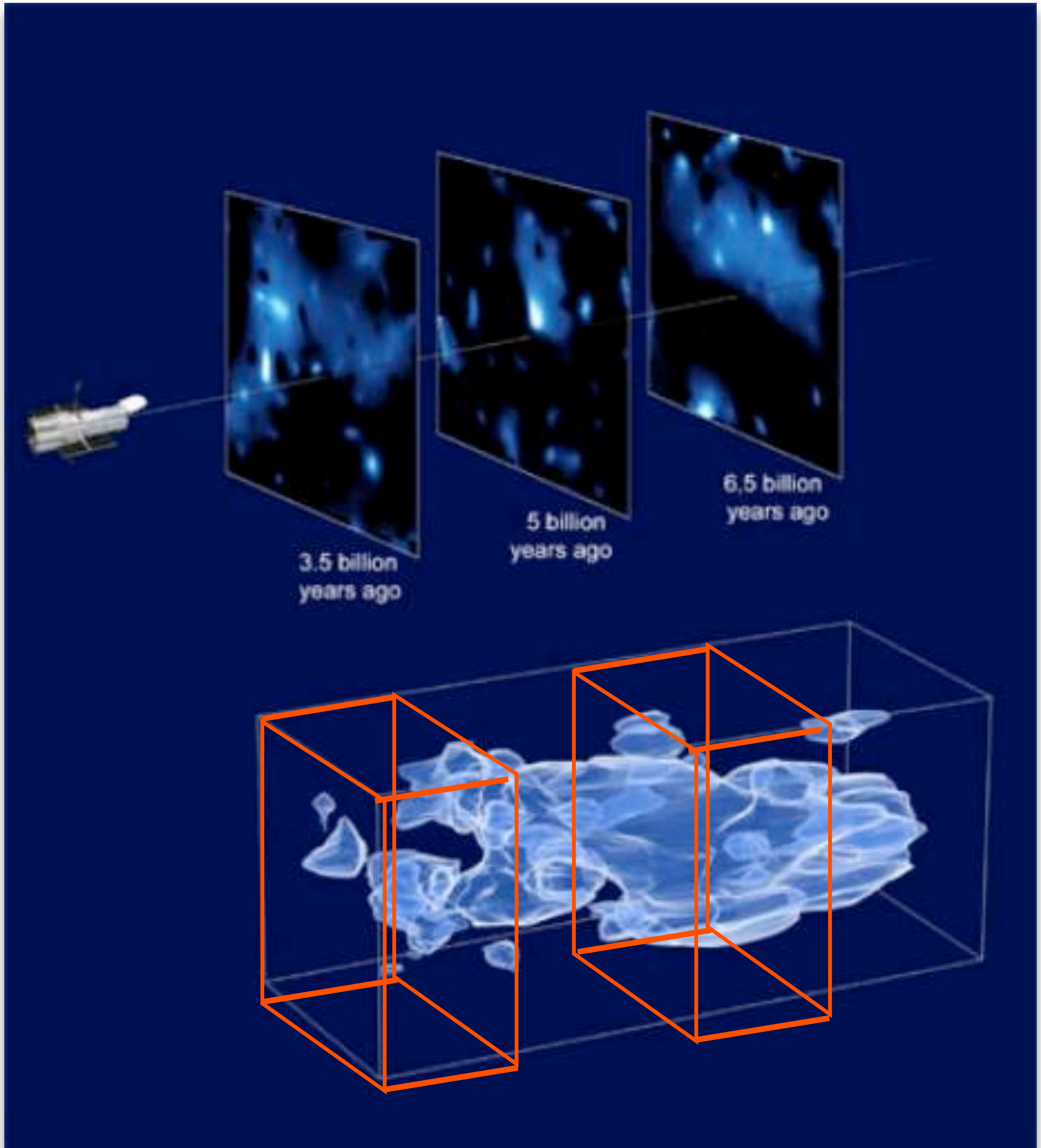

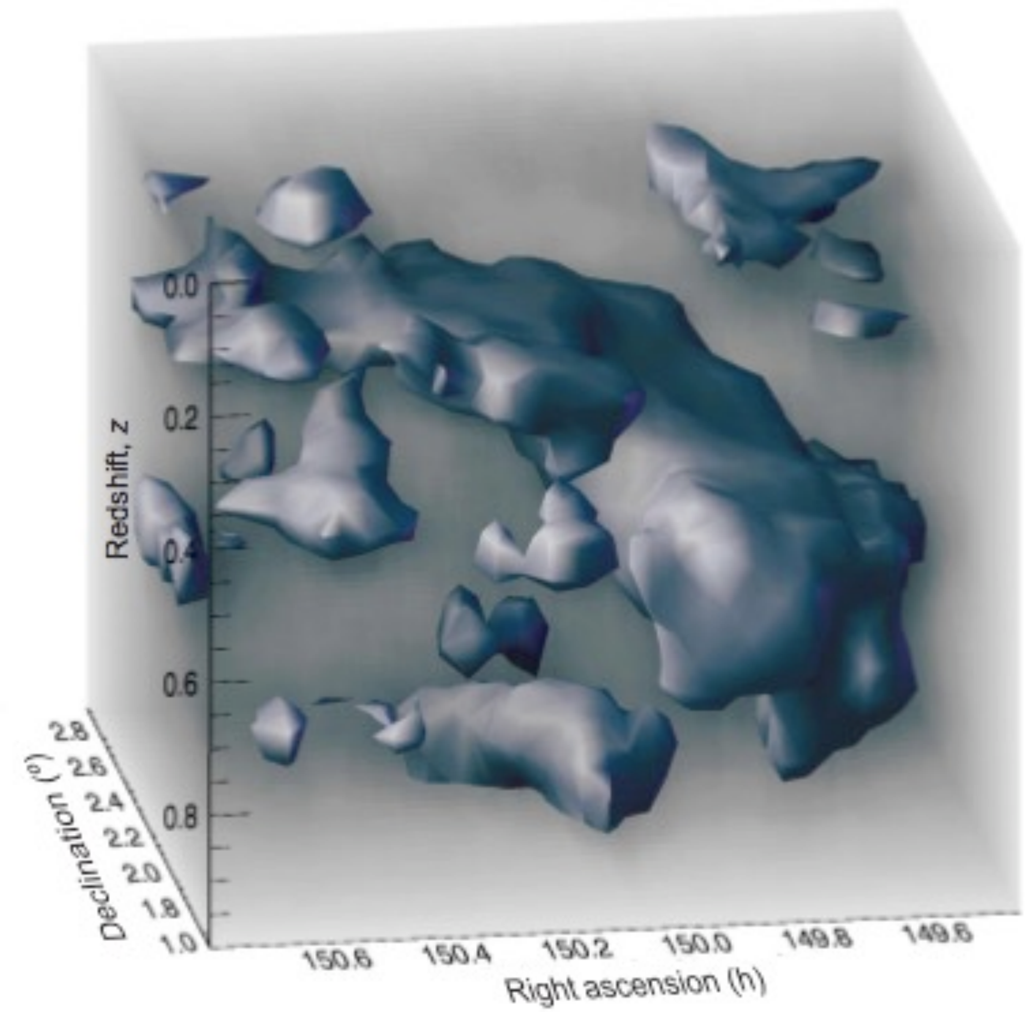

R. Massey et al, Maps of the Universe's Dark matter scaffolding, Nature, Vol. 445, pp. 286-290, 2007

3D Weak Lensing

The convergence κ, as seen in sources of a given redshift bin, is the linear transformation of the matter density contrast, δ, along the line-of-sight (Simon et al 2009):

$$\kappa = Q\delta + N$$ with $\delta(r) \equiv \rho(r)/\overline{\rho} - 1$

$$Q_{i\ell} = \frac{3H_0^2\Omega_M}{2c^2}\int_{w_\ell}^{w_{\ell+1}} dw \frac{\overline{W}^{(i)}(w) f_K(w)}{a(w)}, \quad \overline{W}^{(i)}(w) = \int_0^{w^{(i)}} dw' \frac{f_K(w-w')}{f_K(w')}\left(p(z)\frac{dz}{dw}\right)_{z=z(w')}$$

where H_0 is the hubble parameter, Ω_M is the matter density parameter, c is the speed of light, $a(w)$ is the scale parameter evaluated at comoving distance w, and

$$f_K(w) = \begin{cases} K^{-1/2}\sin(K^{1/2}w), & K > 0 \\ w, & K = 0 \\ (-K)^{-1/2}\sinh([-K]^{1/2}w) & K < 0 \end{cases},$$

gives the comoving angular diameter distance as a function of the comoving distance and the curvature, K, of the Universe.

3D Weak Lensing

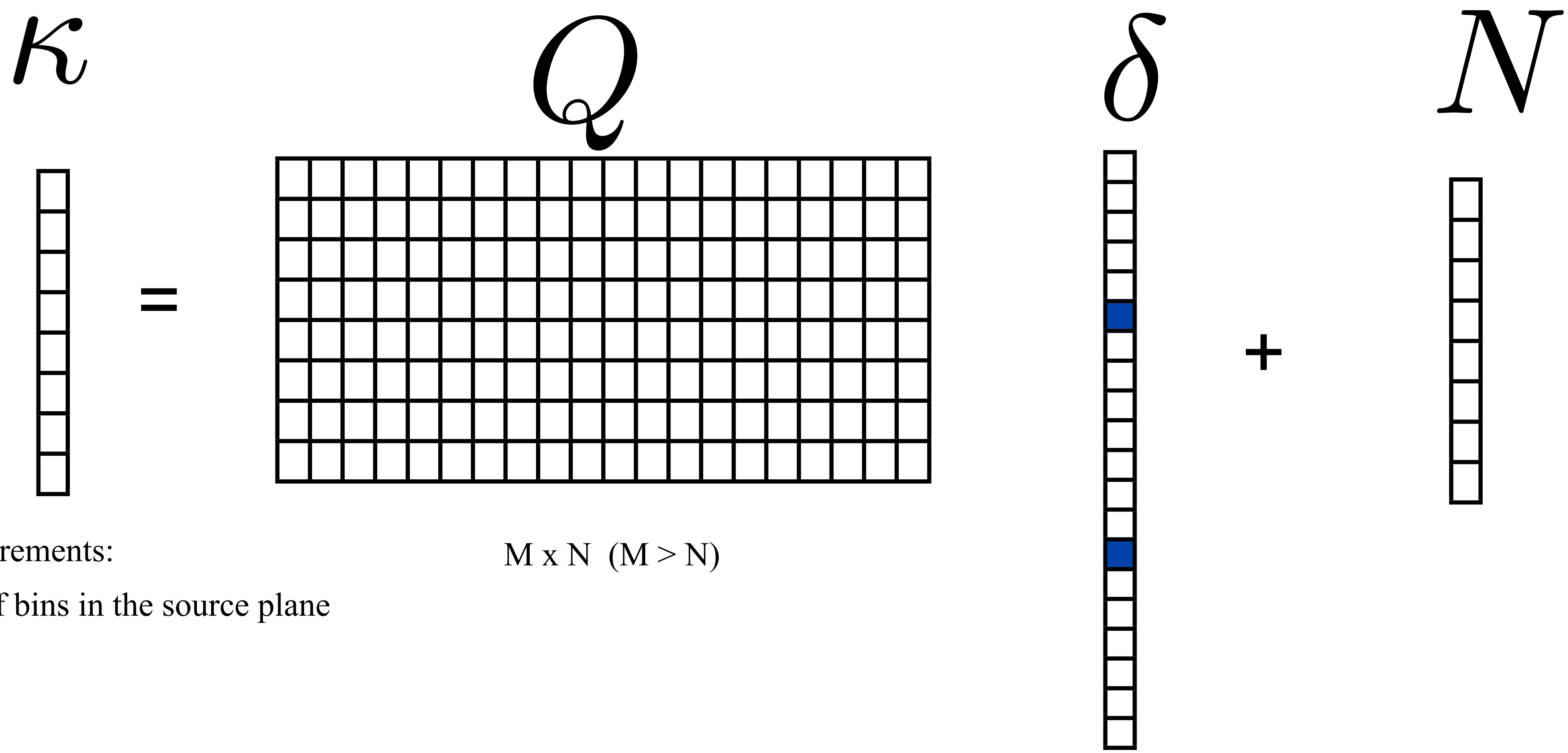

M measurements:
number of bins in the source plane

M x N (M > N)

N redshift bin for the density contrast

δ is sparse.

Q spreads out the information in δ along κ bins.

More unkown than measurements

Statistics of the Shear Field

Raw lensing measurement

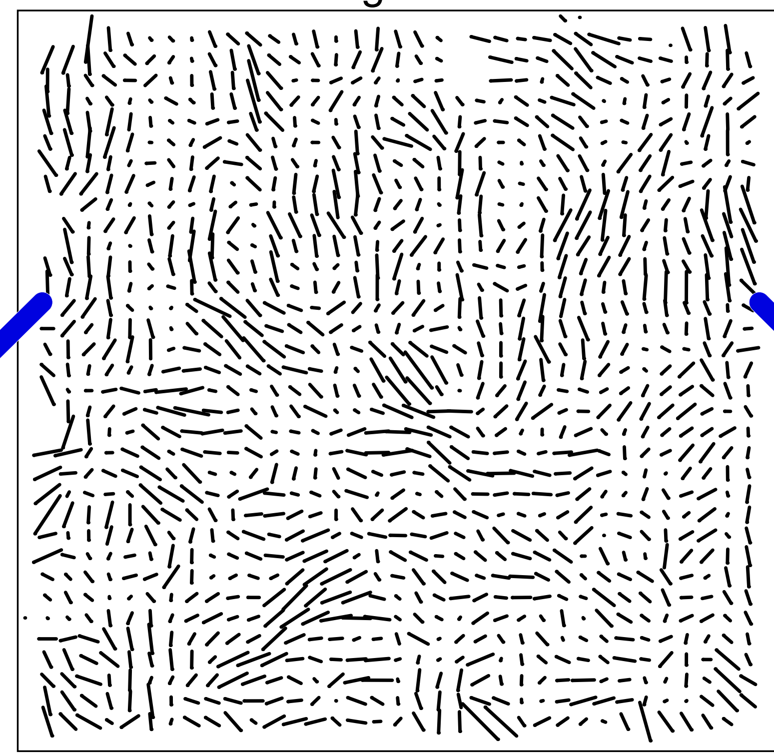

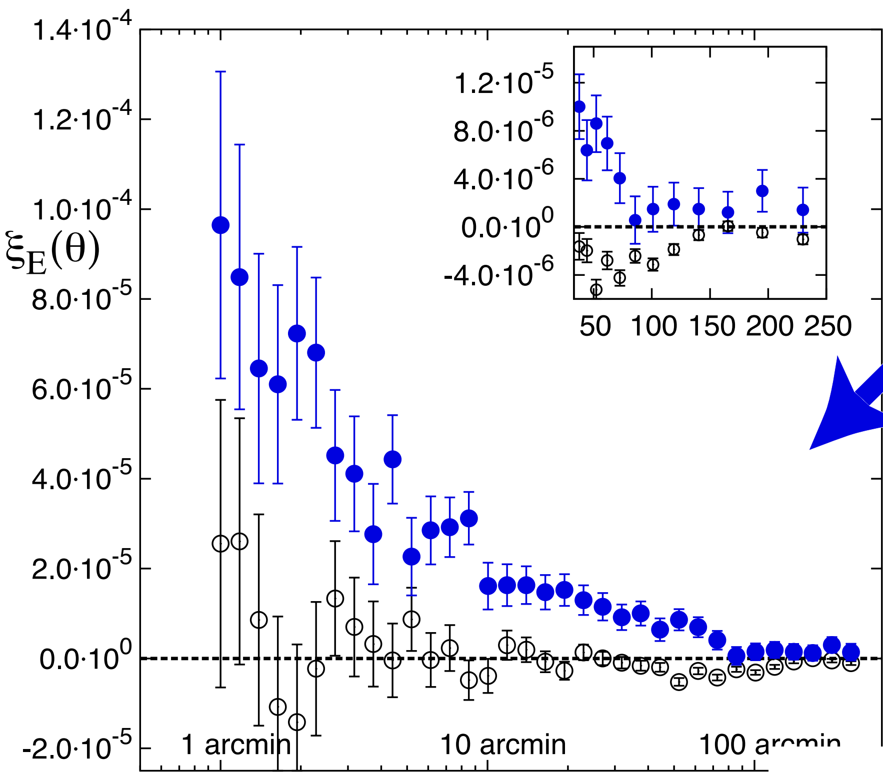

Correlation function

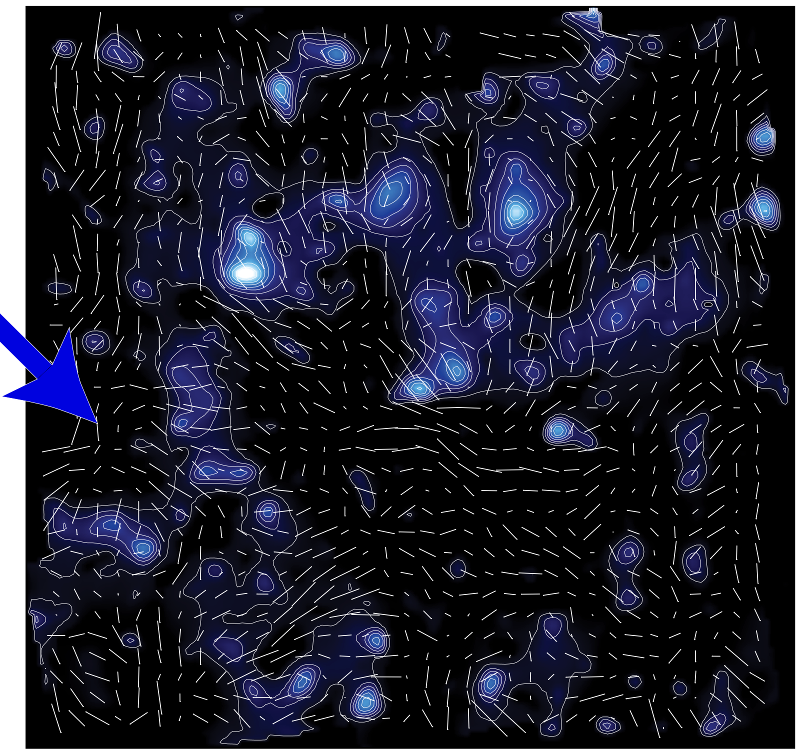

Dark matter distribution

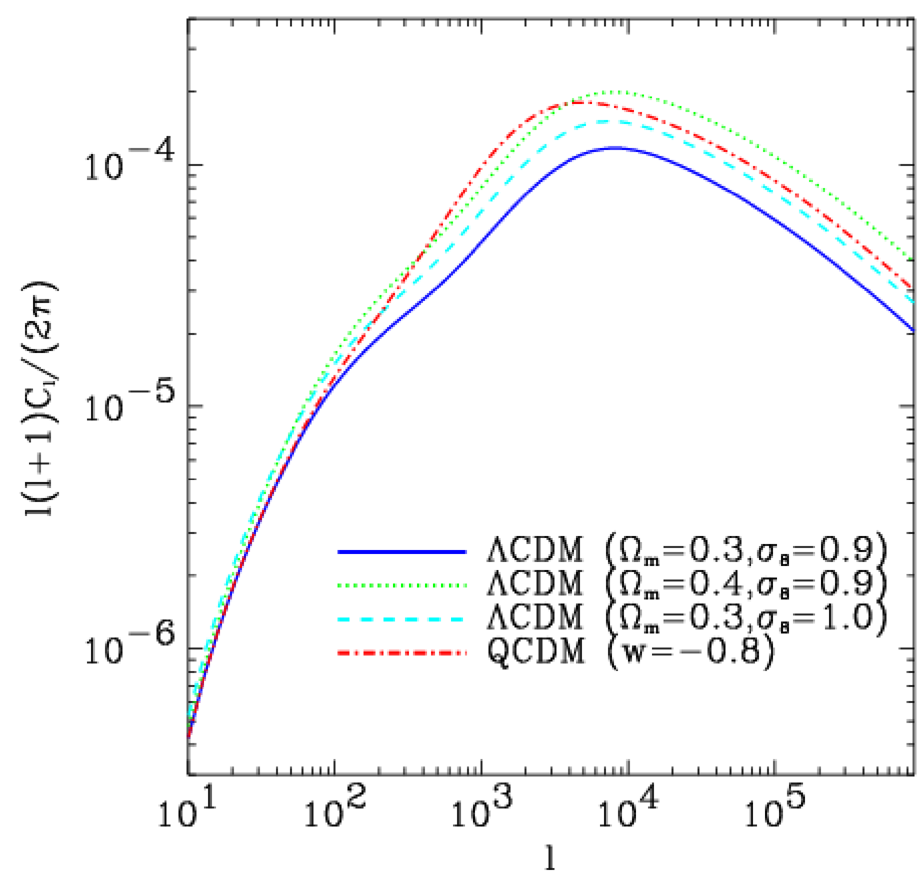

Courtesy of Adam Amara

Weak-lensing pipeline

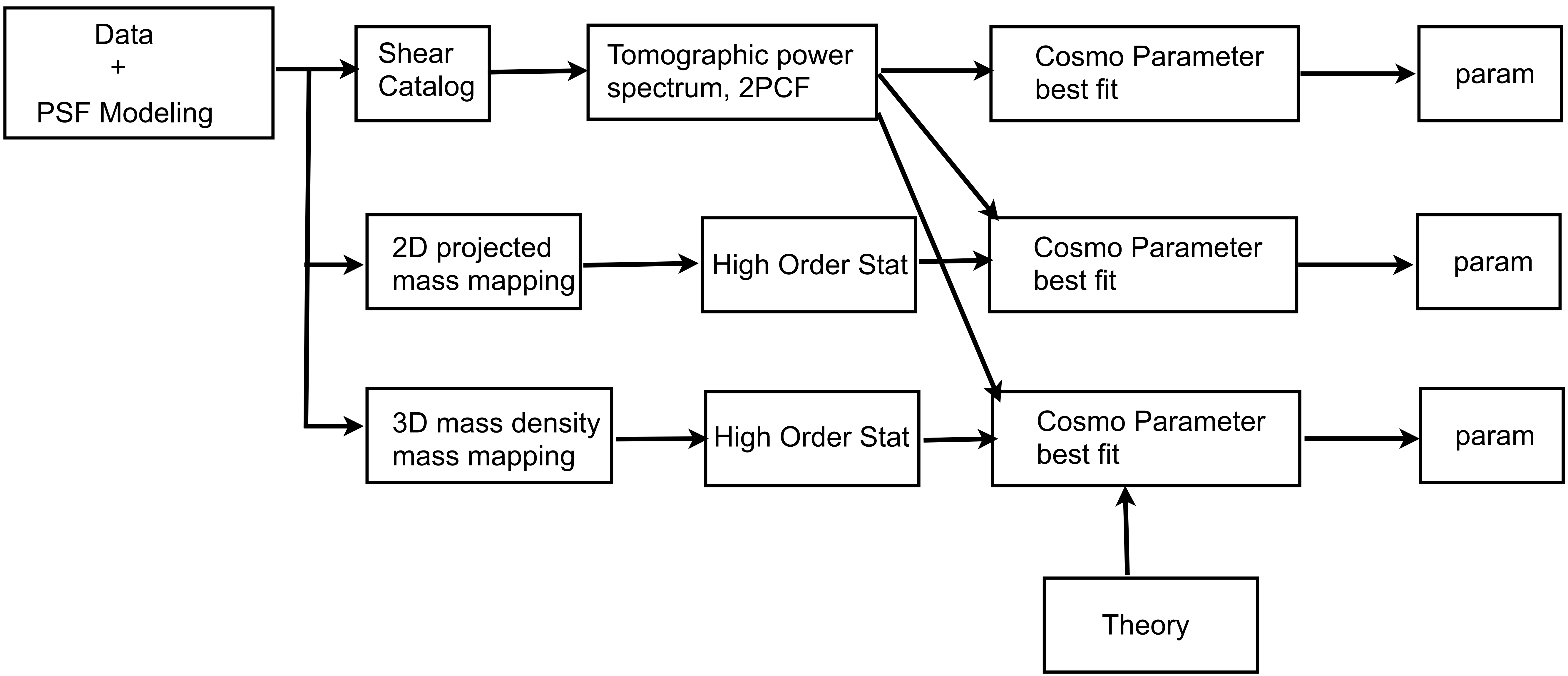

Euclid & Weak Lensing

- Part 1: Introduction to Euclid & Weak Lensing
- Part 2: Shear WL Measurements
- Part 3: From Shear to 2D and 3D Maps
- **Part 4: Challenges in the WL Community**
- Part 5: WL Inverse Problems and Sparse Solutions
  - Point Spread Function superresolution
  - 2D mass mapping
  - 3D mass mapping

Shape measurement techniques:

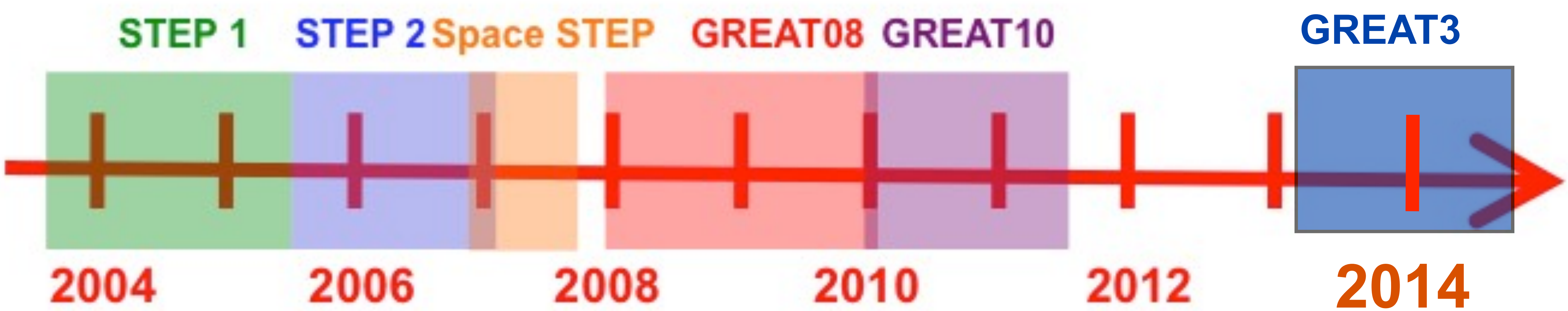

http://great3challenge.info

Barney Rowe, University College London

With Rachel Mandelbaum, Carnegie Mellon University,

and the GREAT3 Collaboration

GREAT3

- Galaxy selection biases
- Chromatic effects / "colour gradient" biases
- **Realistic galaxy profiles**
- Star/galaxy separation
- **Uncertainty about the Point Spread Function**
- Detector non-linearities
- **Shape measurement from multiple, shallow exposures**
- Object deblending / field crowding
- Background estimation
- Redshift dependent effects

Credit Barney Rowe

GREAT3

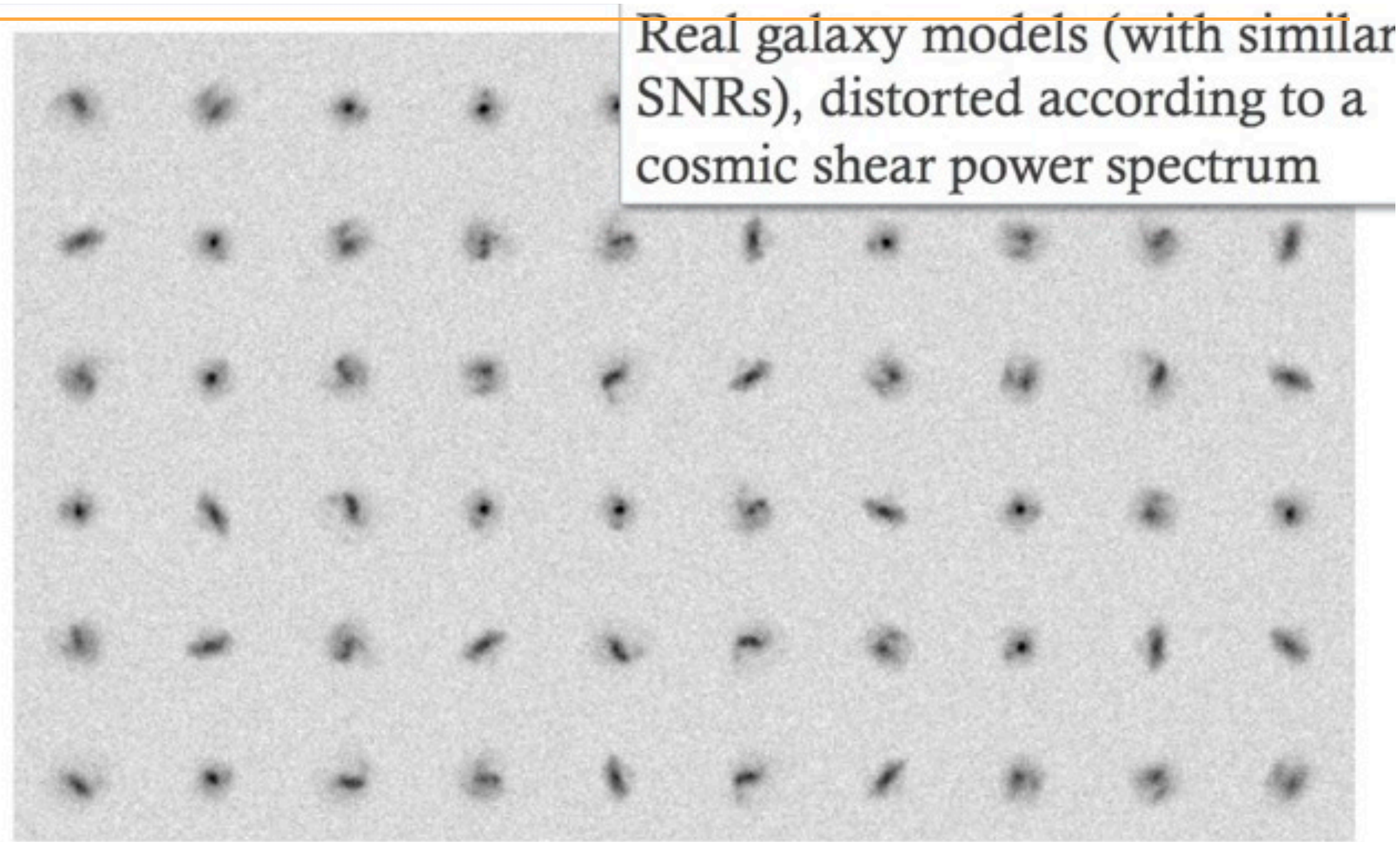

- Galaxy selection biases
- Chromatic effects / “colour gra
- **Realistic galaxy profiles**
- Star/galaxy separation
- **Uncertainty about the Point Spread Function**
- Detector non-linearities
- **Shape measurement from multiple, shallow exposures**
- Object deblending / field crowding
- Background estimation
- Redshift dependent effects

Credit Barney Rowe

GREAT3

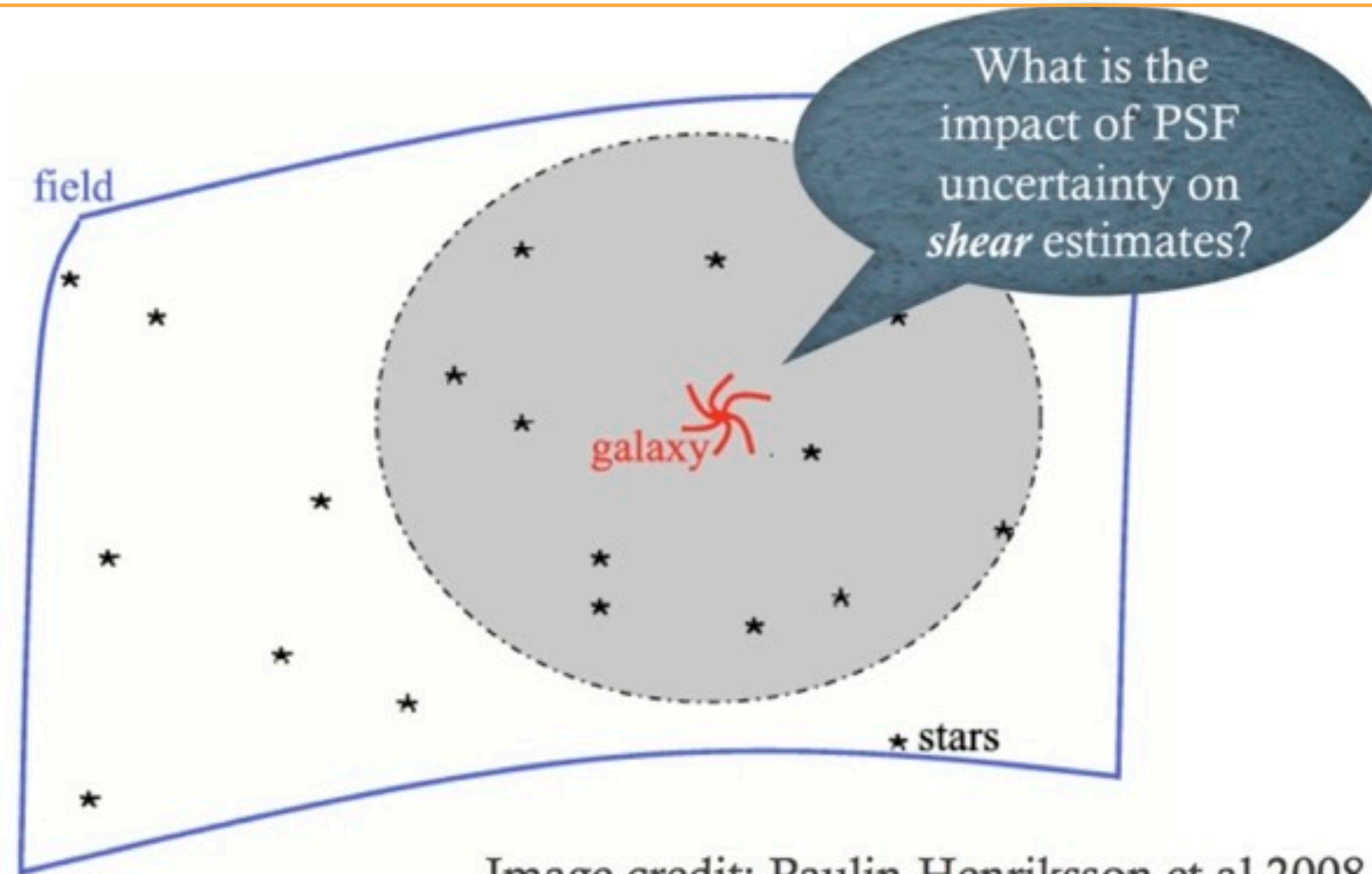

Image credit: Paulin-Henriksson et al 2008

- Galaxy selection biases
- Chromatic effects / "colour gra
- **Realistic galaxy profiles**
- Star/galaxy separation
- **Uncertainty about the Point Spread Function**
- Detector non-linearities
- **Shape measurement from multiple, shallow exposures**
- Object deblending / field crowding
- Background estimation
- Redshift dependent effects

Credit Barney Rowe

GREAT3

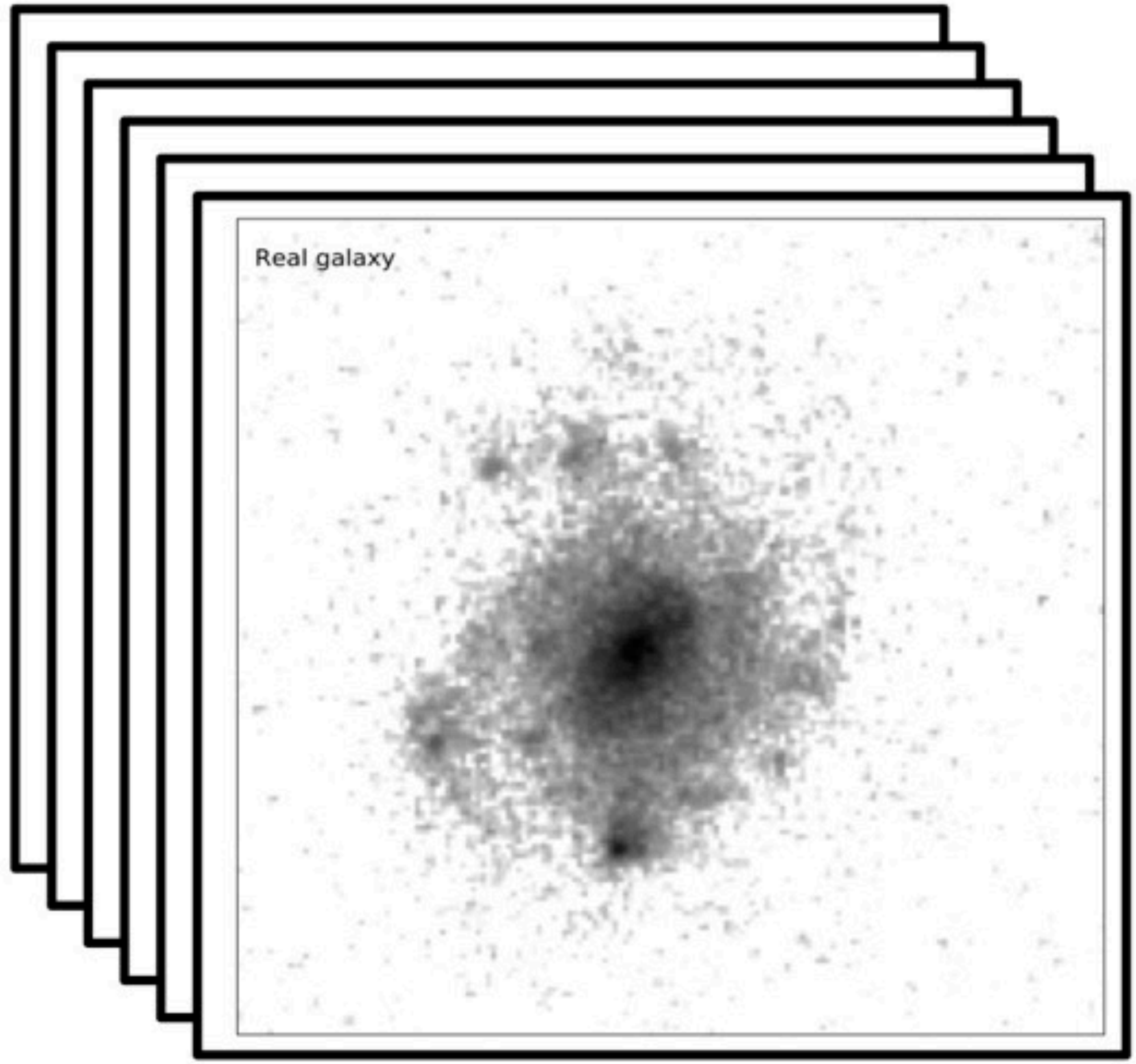

- Galaxy selection biases
- Chromatic effects / "colour gra
- **Realistic galaxy profiles**
- Star/galaxy separation
- **Uncertainty about the Point Spre**
- Detector non-linearities
- **Shape measurement from multip**
- Object deblending / field crowdir.g
- Background estimation
- Redshift dependent effects

Credit Barney Rowe

Important Additions to Previous Challenges

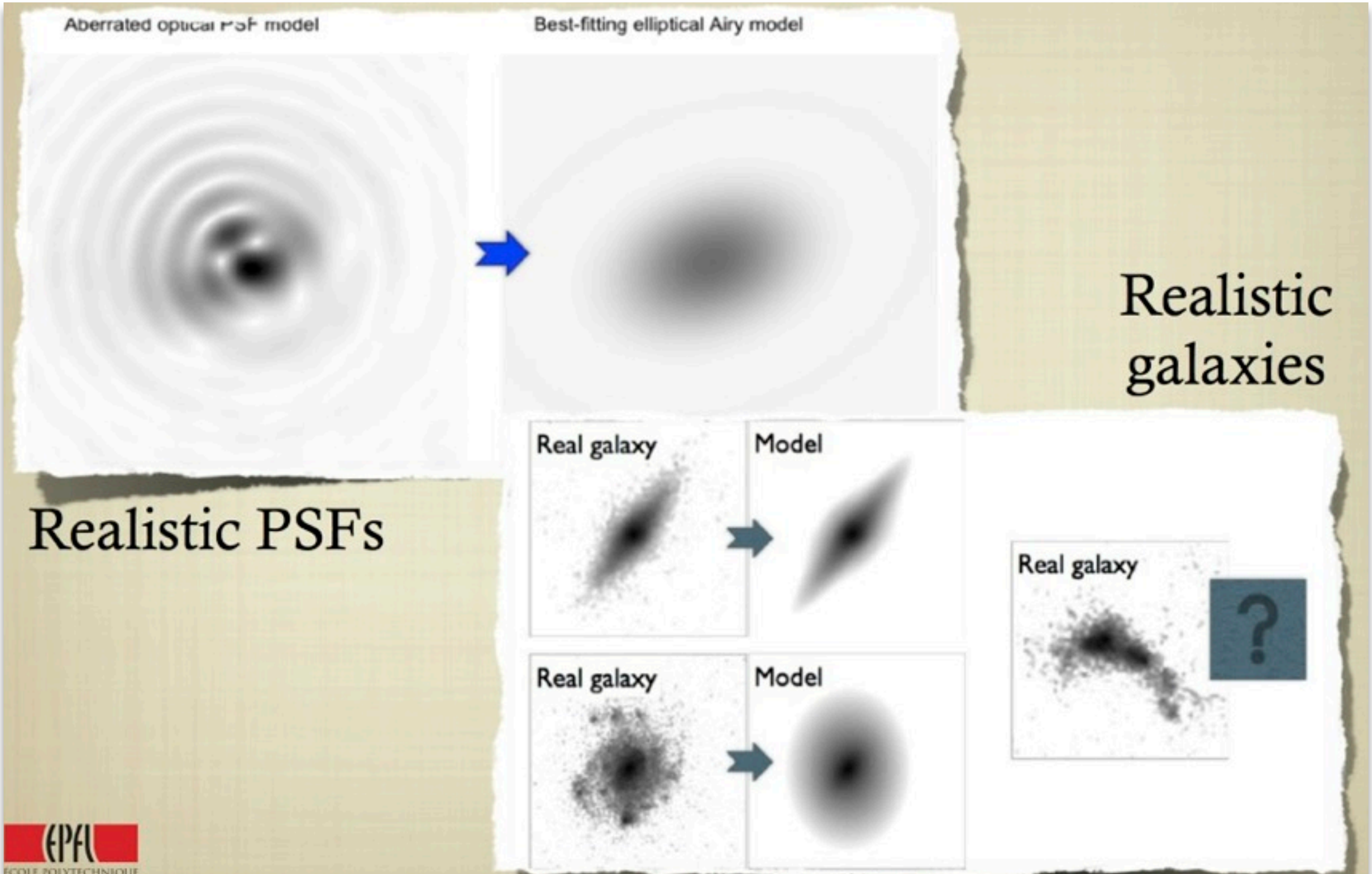

Credit Frederic Courbin

GREAT3

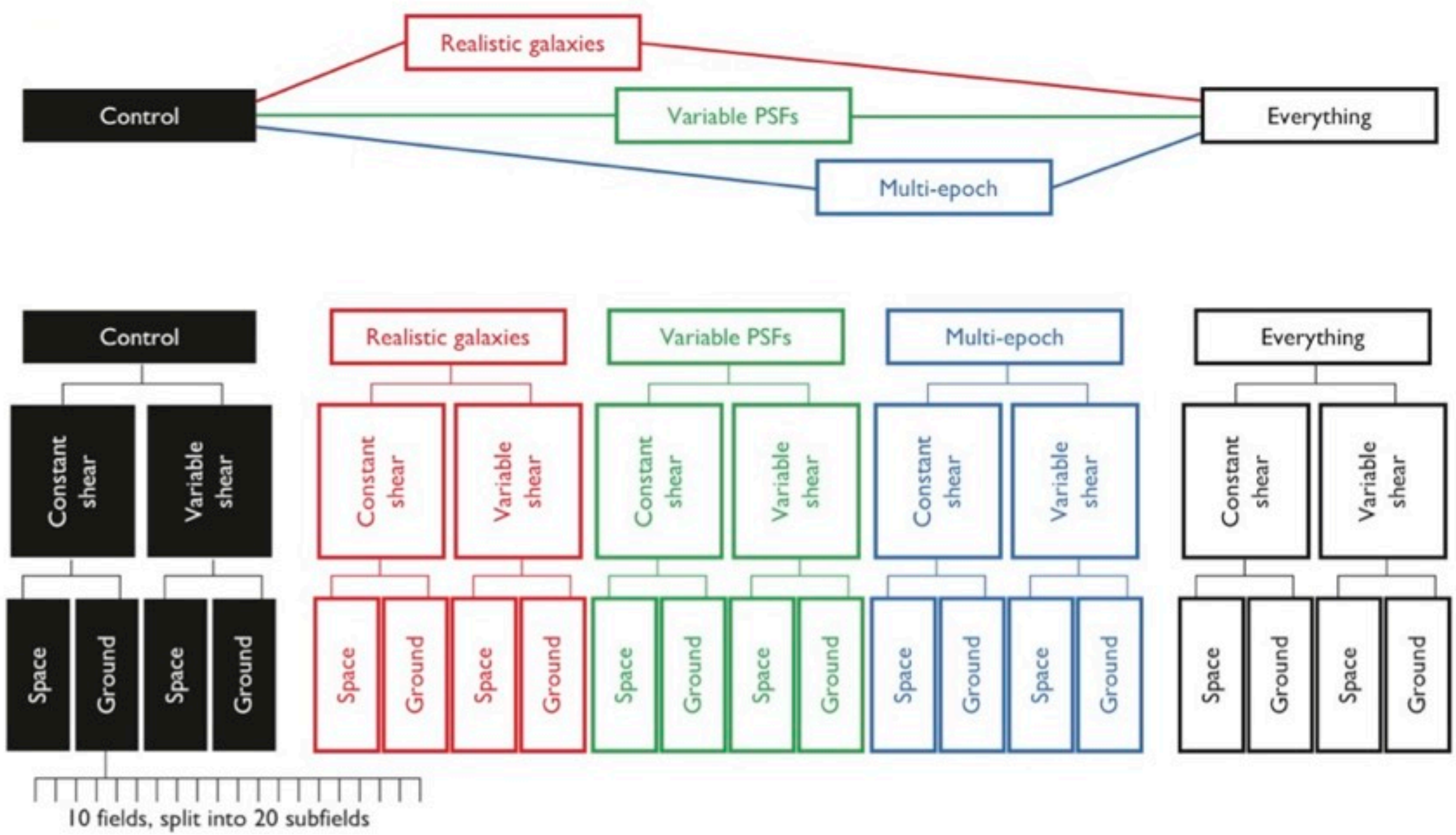

Credit Barney Rowe

GREAT3 Metrics

GREAT3 metrics (scores): $g_i^{obs} - g_i^{true} = m_i g_i^{true} + c_i$

constant shear: $$Q_c = \frac{2000 \times \eta_c}{\sqrt{\sigma^2_{\mathrm{min,c}} + \sum_{i=+,\times} \left(\frac{m_i}{m_{\mathrm{target}}}\right)^2 + \left(\frac{c_i}{c_{\mathrm{target}}}\right)^2}}.$$

Euclid requirements --> $m_{\mathrm{target}} = 2 \times 10^{-3}$ and $c_{\mathrm{target}} = 2 \times 10^{-4}$

variable shear: $$Q_v = \frac{1000 \times \eta_v}{\sigma^2_{\mathrm{min,v}} + \frac{1}{N_{\mathrm{norm}}} \sum_{k=1}^{N_{\mathrm{bins}}} \left| \sum_{j=1}^{N_{\mathrm{fields}}} [M_{E,j}(\theta_k) - M_{E,\mathrm{true},j}(\theta_k)] \right|}$$

Q~1000 when target accuracy is achieved

CEA-EPFL: gfit

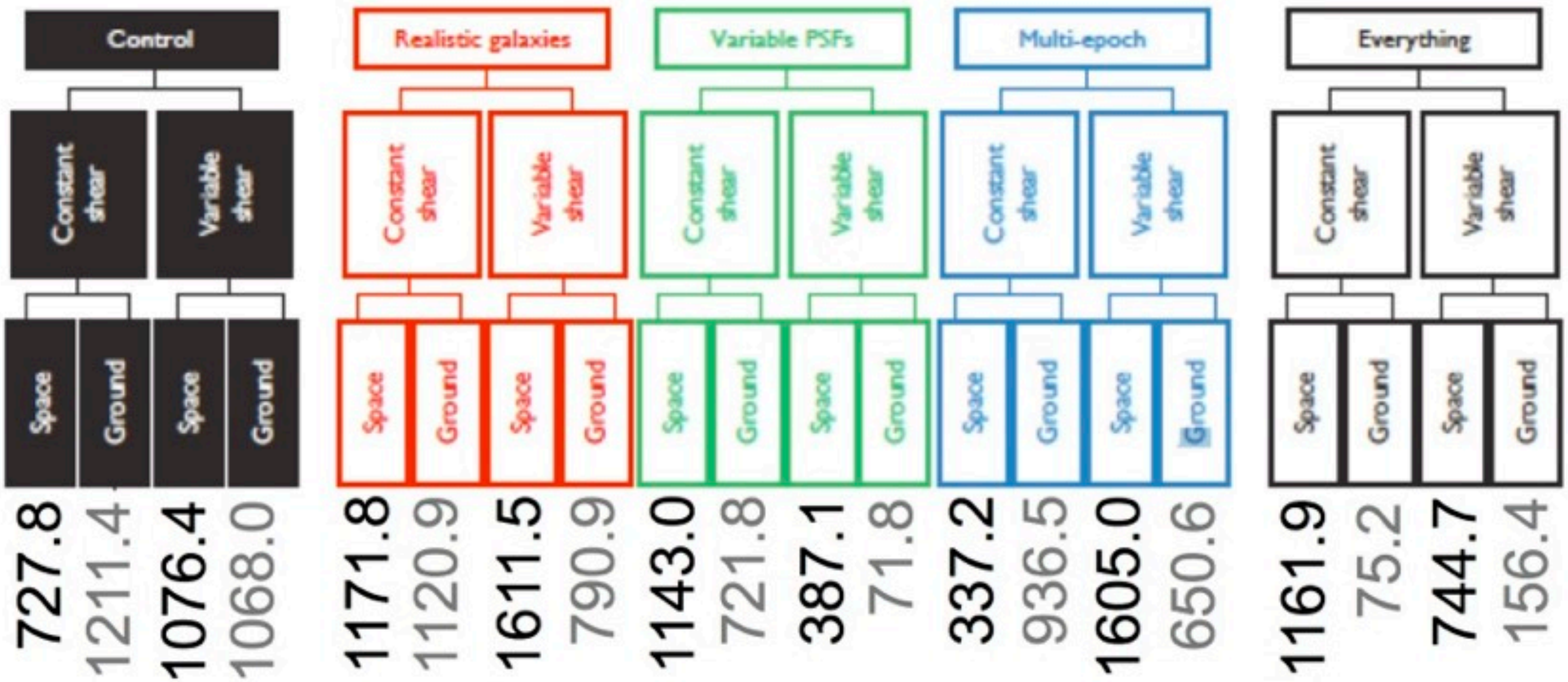

Credit Reiko Nakajima

Great3: 25 Teams

Branch	Winning team	Winning score	# of teams	# of entries
CGC	CEA-EPFL	1211	22	250
CGV	CEA-EPFL	1068	16	160
CSC	Amalgam@IAP	1516	16	110
CSV	Amalgam@IAP	1199	11	96
RGC	Amalgam@IAP	1121	20	195
RGV	CEA-EPFL	791	14	93
RSC	Fourier_Quad	1919	12	92
RSV	MegaLUT	1667	9	83
MGC	sFIT	1017	9	71
MGV	MegaLUT	1131	7	53
MSC	sFIT	841	6	48
MSV	CEA-EPFL	1605	6	45
VGC	sFIT	884	7	60
VGV	Amalgam@IAP	230	6	60
VSC	Amalgam@IAP	1183	4	25
VSV	sFIT	1276	4	17
FGC	sFIT	800	2	11
FGV	sFIT	379	2	17
FSC	sFIT	1184	2	17
FSV	sFIT	856	2	25

Credit Barney Rowe

What has been learned

Rachel Mandelbaum, Barnaby Rowe, et al, "GREAT3 results I: systematic errors in shear estimation and the impact of real galaxy morphology" in preparation, 2014.

- Model-fitting methods now dominate the field in term of performence.

- Calibration of the results using simulation helps.

- Shear systematic errors due to realistic galaxy morphology are typically of order ~ 1 per cent.

- Significant progress has been made in controlling multiplicative biases since GREAT10: the number of methods in GREAT10 with $|\langle m \rangle| < 0.05$, 0.02, and 0.005 is 7, 5, and 2, to be compared with 12, 10, and 6 in GREAT3.

The GREAT3 results provide new reasons to be optimistic about delivering reliably accurate shear estimates for the next survey generation.

Euclid & Weak Lensing

- Part 1: Introduction to Euclid & Weak Lensing
- Part 2: Shear WL Measurements
- Part 3: From Shear to 2D and 3D Maps
- Part 4: Challenges in the WL Community
- **Part 5: WL Inverse Problems and Sparse Solutions**
  - **Point Spread Function superresolution**
  - 2D mass mapping
  - 3D mass mapping

Sparse Recovery & Inverse Problems

$$Y = HX + N$$

$X = \Phi\alpha$, and α is sparse

- Denoising
- Deconvolution
- Component Separation
- Inpainting
- Blind Source Separation
- Minimization algorithms
- Compressed Sensing

$$\min_{\alpha} \|\alpha\|_p^p \quad \text{subject to} \quad \|Y - H\Phi\alpha\|^2 \leq \epsilon$$

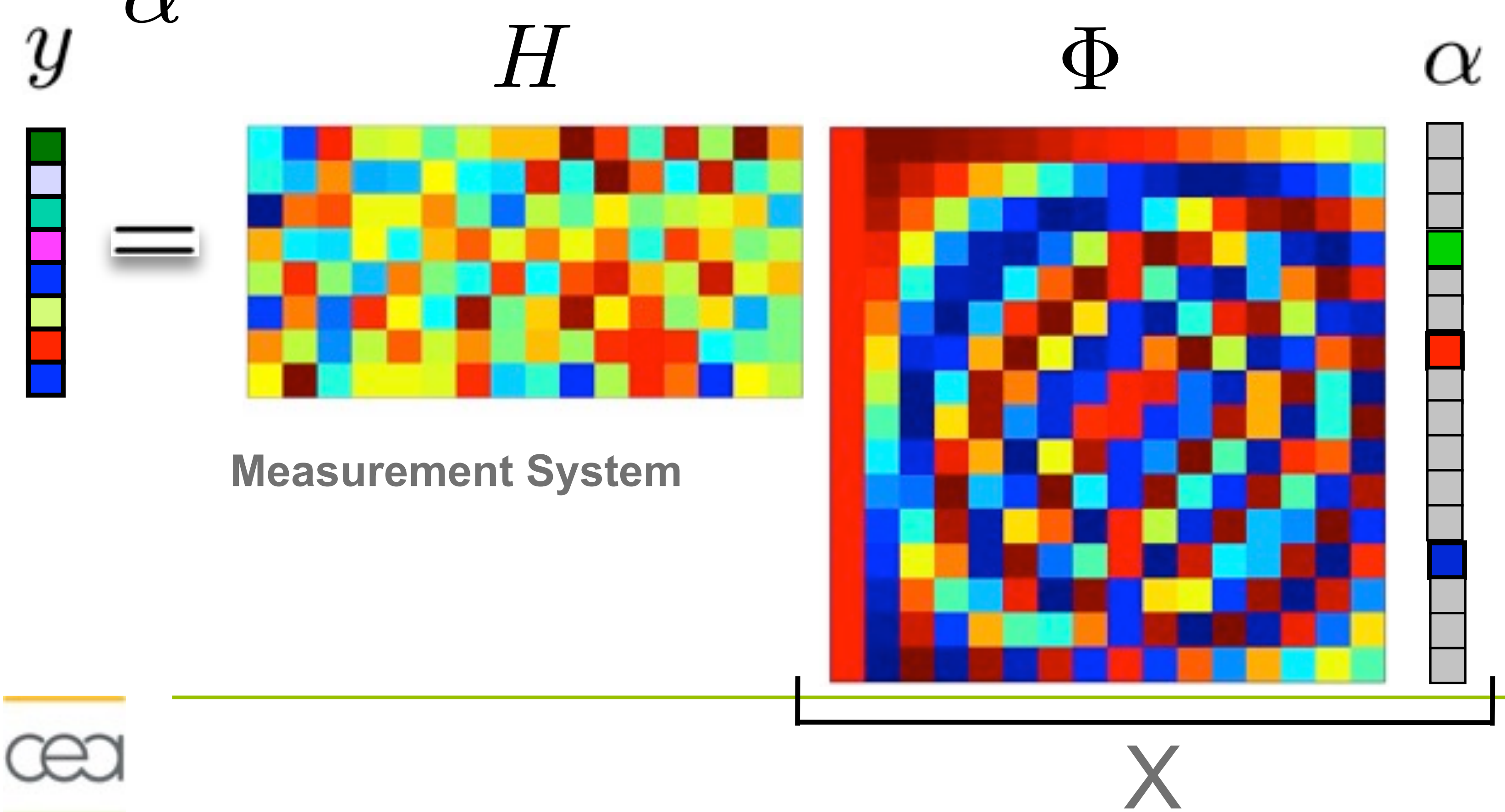

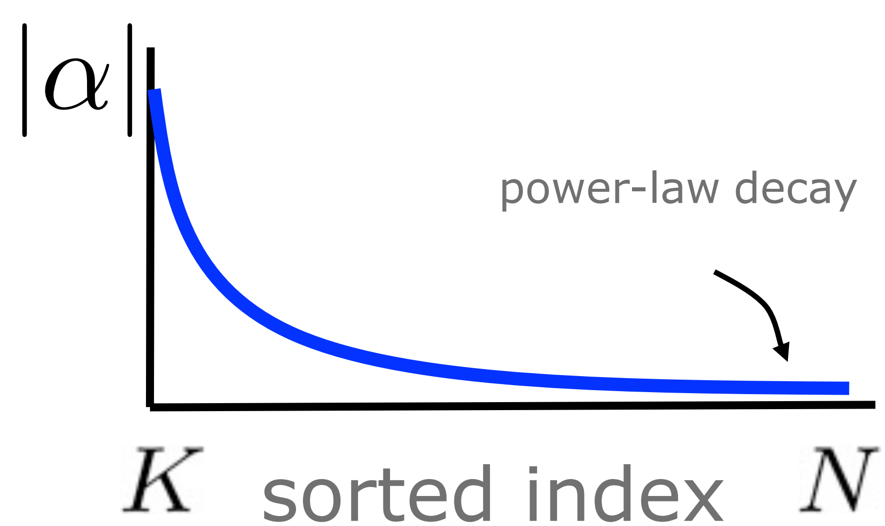

Superresolution

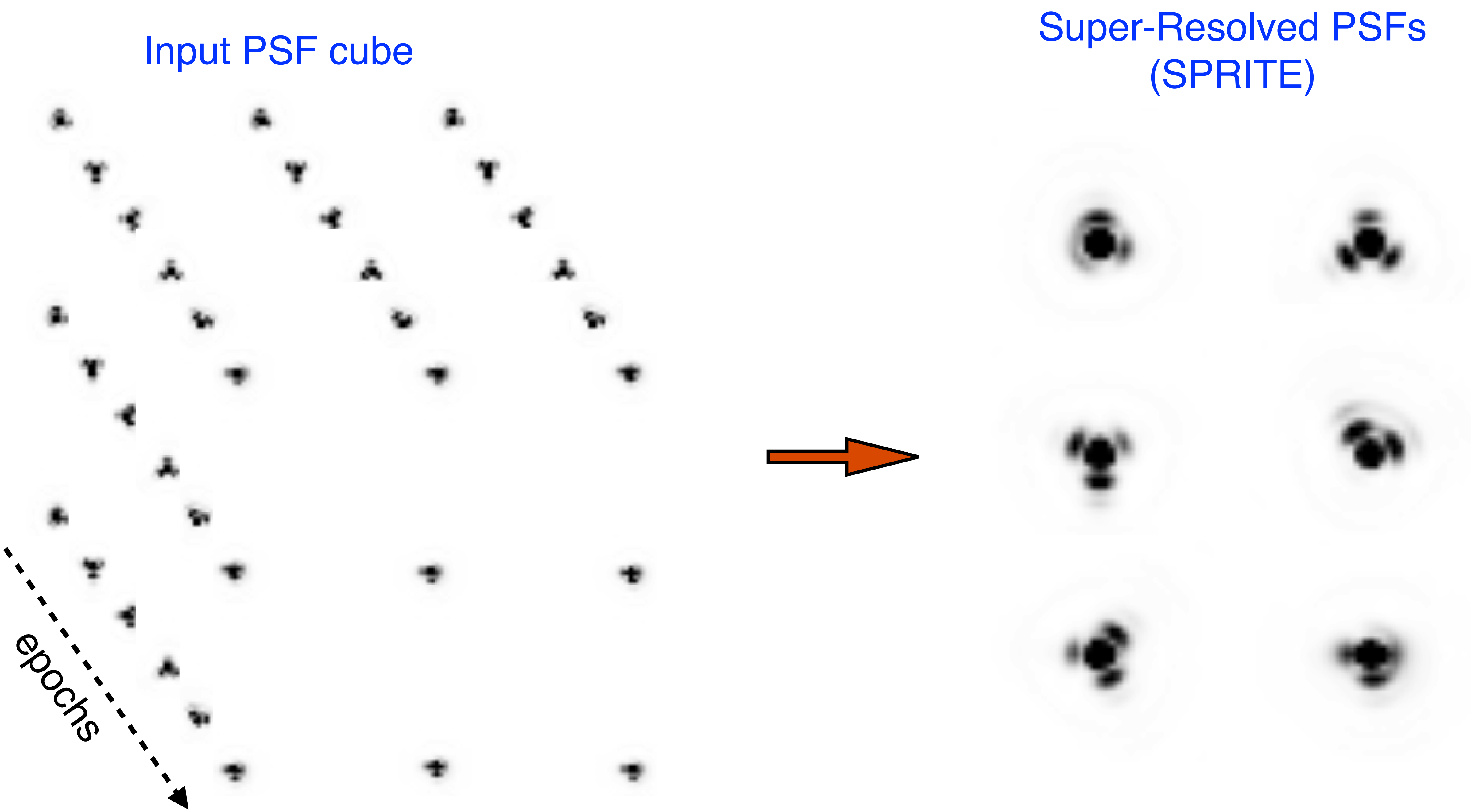

Sparse Regularization

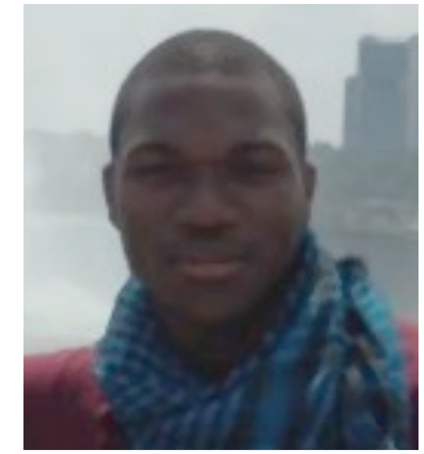

$$\left\{ \begin{array}{l} \min_{\Delta_X} \parallel Y - H(X^{(0)} + \Delta_X) \parallel_2^2 \\ \textbf{+ sparsity constraint} \quad \Delta_X = \Phi\alpha \\ X^{(0)} \text{ calculated with shift-and-add} \\ \quad \text{– Registration based on centroids positions} \end{array} \right.$$

$$\min_{\Delta_X} \parallel Y - H(X^{(0)} + \Delta_X) \parallel_2^2 \quad s.t. \quad \lambda \parallel \Phi^t \Delta_X \parallel_1$$

Experiments

- 150 Zemax PSF at 12 x Euclid Resolution
- For each PSF, 4 randomly shifted and noisy PSF at Euclid resolution

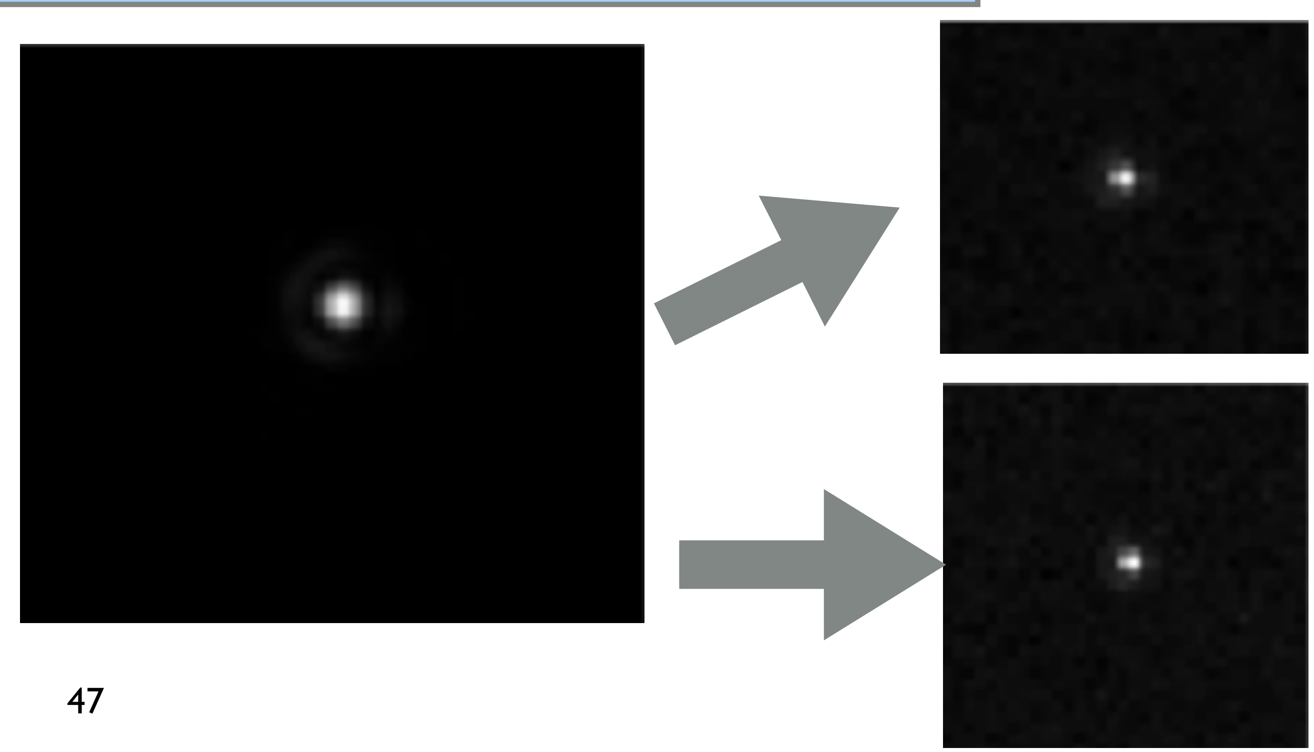

GOAL: PSF modeling at twice Euclid resolution

Numerical Experiment

==> Goal: Reconstruction these PSF at 2 x Euclid Resolution from 4 subsample noisy images.

$$e_1 = \log \frac{1}{n} \sum_{i=1}^{n} \mid (\gamma_1^e)_i - (\gamma_1^t)_i \mid$$

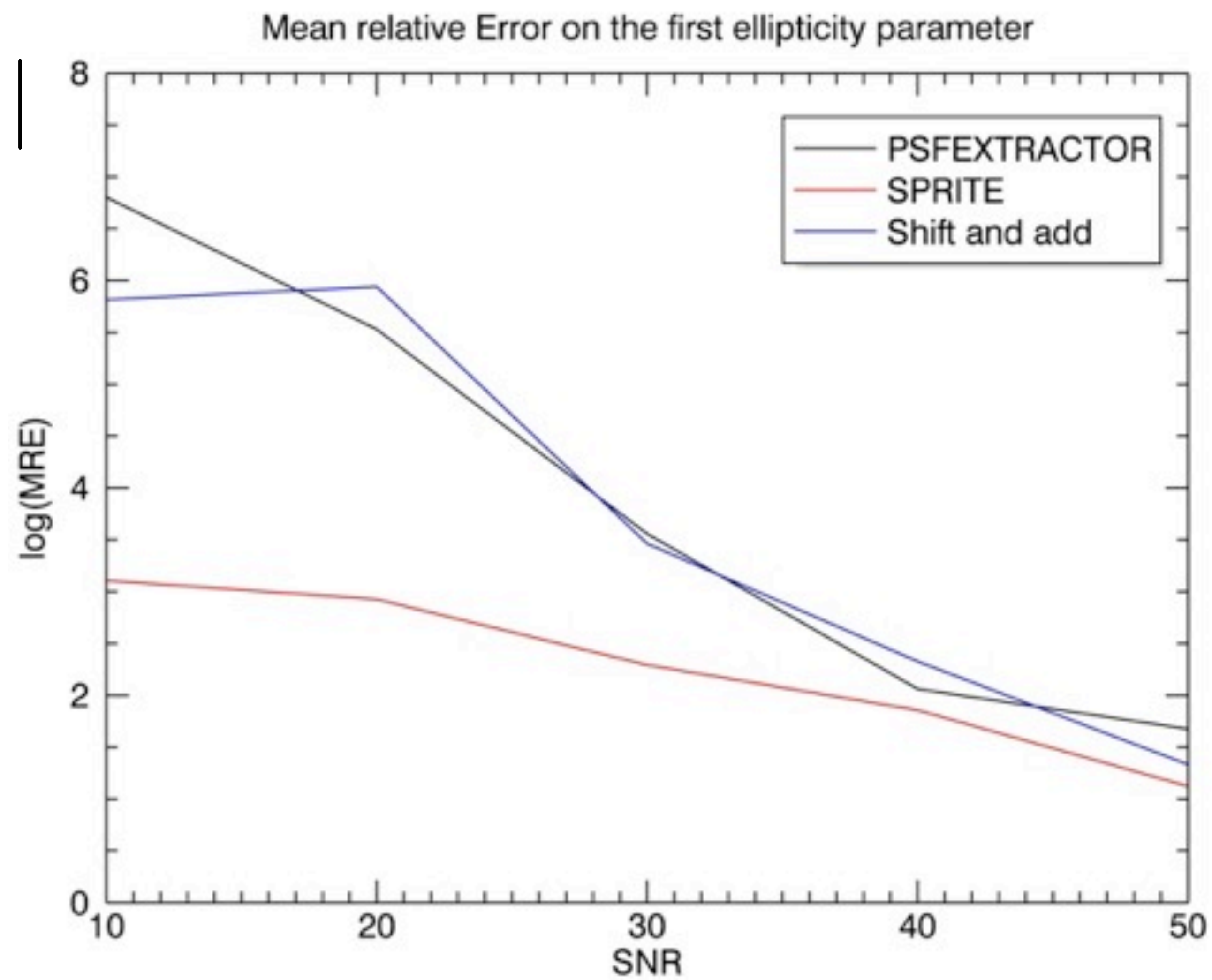

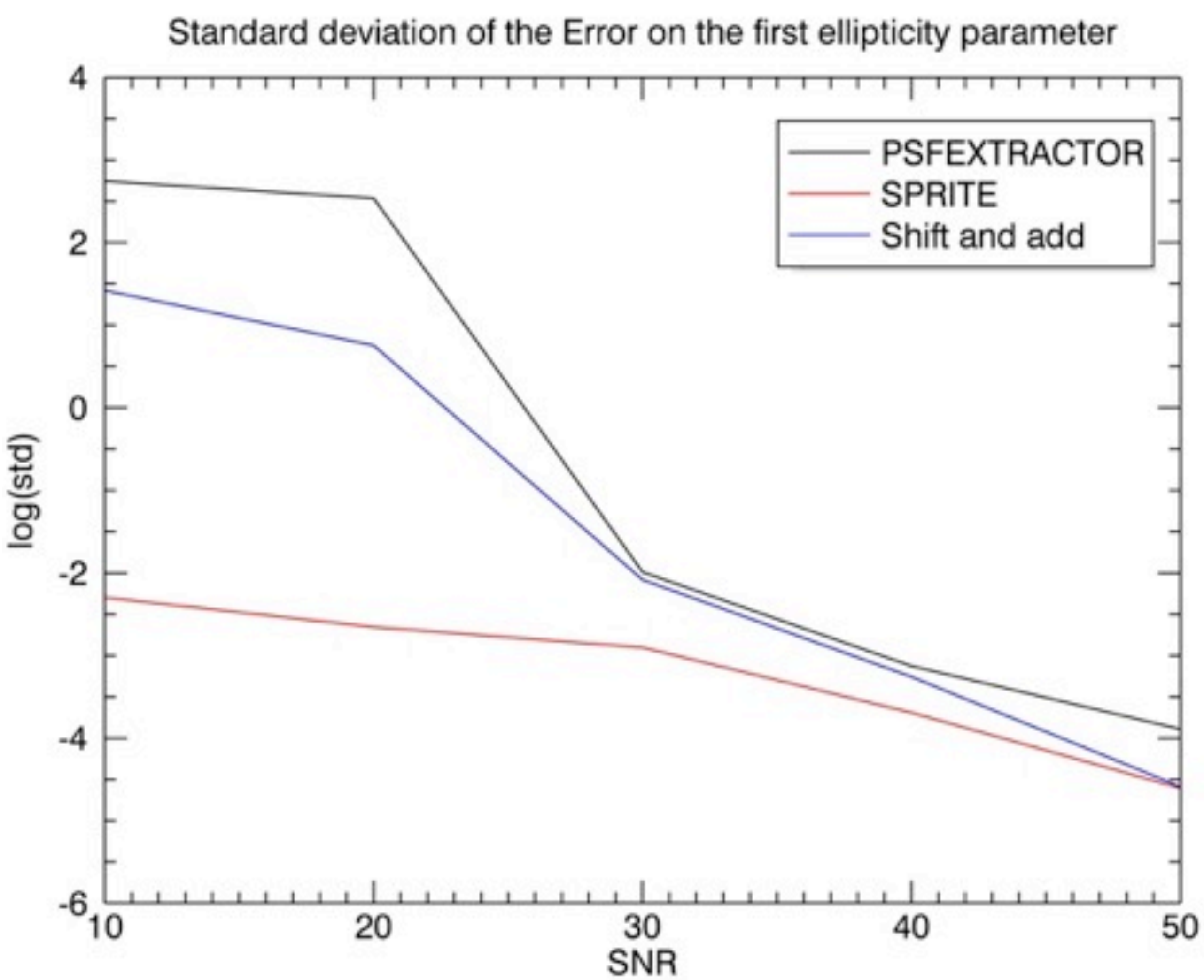

- F.M. Ngolè Mboula, J.-L. Starck, S. Ronayette, K. Okumura, J. Amiaux, "Super-resolution method using sparse regularization for point spread function recovery", A&A, in press.

Numerical Experiment

==> Goal: Reconstruction these PSF at 2 x Euclid Resolution from 4 subsample noisy images.

$$e_2 = \log \frac{1}{n} \sum_{i=1}^{n} | (\gamma_2^e)_i - (\gamma_2^t)_i |$$

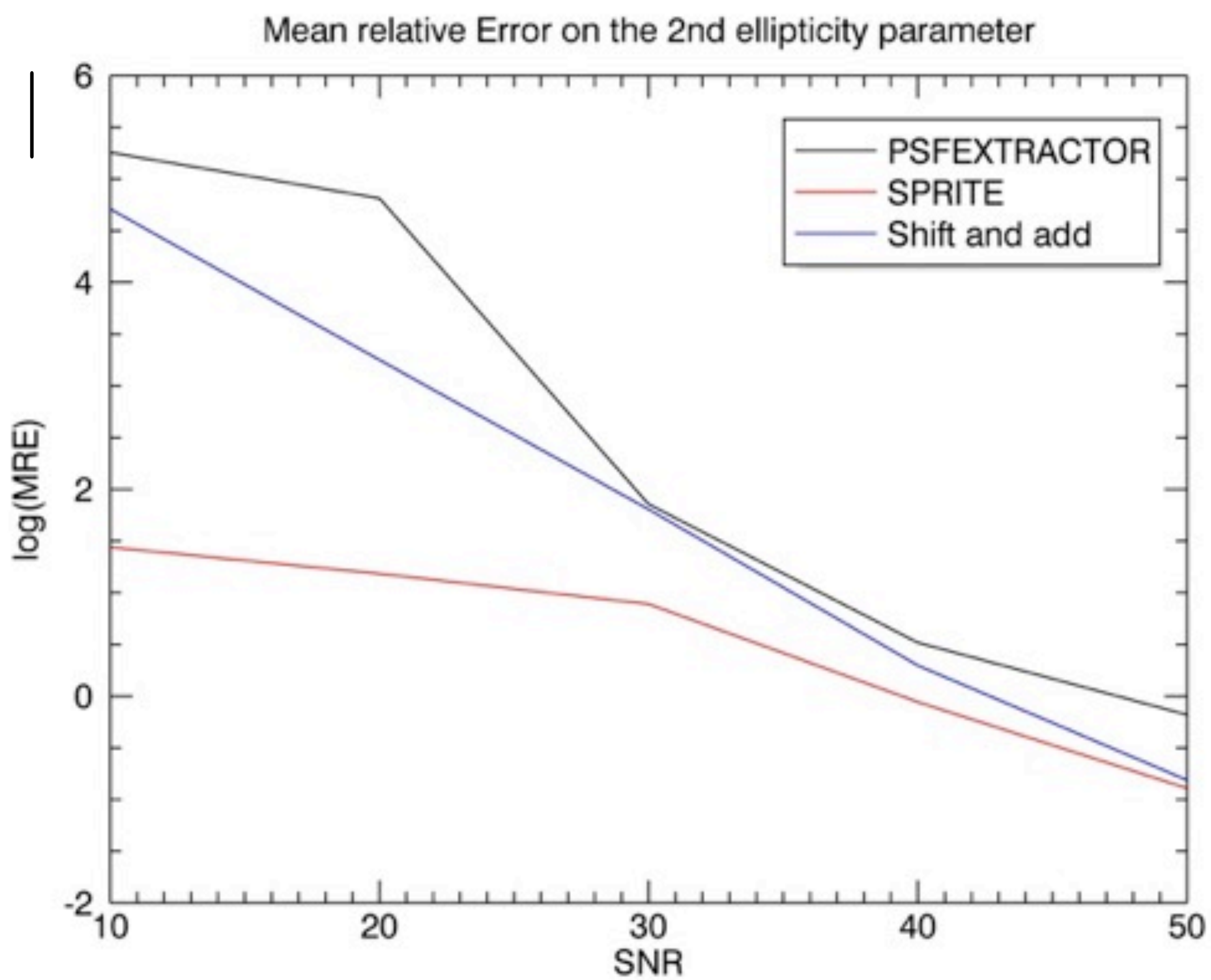

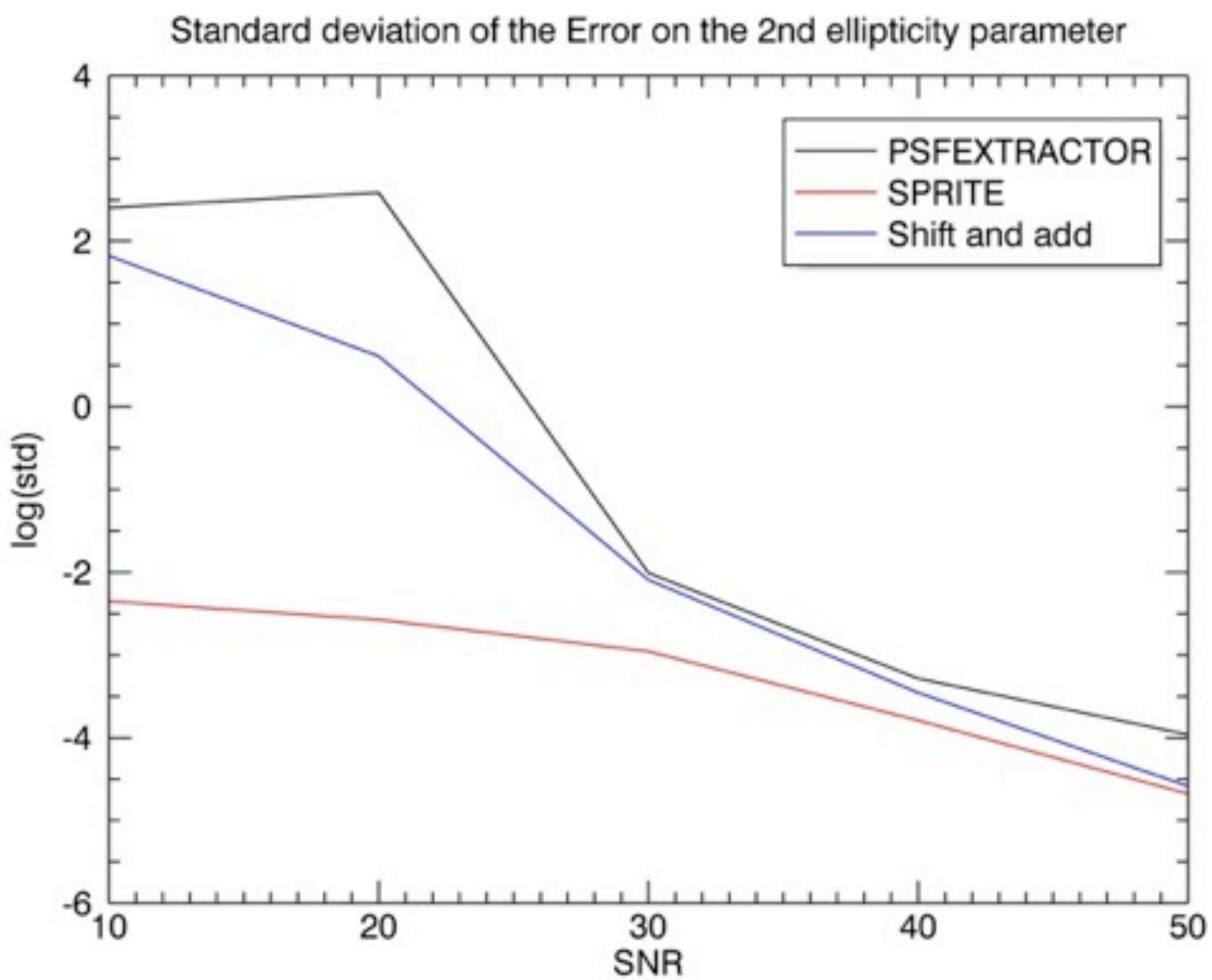

- F.M. Ngolè Mboula, J.-L. Starck, S. Ronayette, K. Okumura, J. Amiaux, "Super-resolution method using sparse regularization for point spread function recovery", A&A, in press.

2D Mass Mapping

* S. Pires, J.-L. Starck, A. Amara, R. Teyssier, A. Refregier and J. Fadili, "FASTLens (FAst STatistics for weak Lensing) : Fast method for Weak Lensing Statistics and map making", Monthly Notices of the Royal Astronomical Society, Volume 395, Issue 3, pp. 1265-1279, 2009.

* S. Pires, J.-L. Starck and A. Refregier, "Light on Dark Matter with Weak Gravitational Lensing", IEEE Signal Processing Magazine, 27, 1, pp 76--85, 2010.

$$\gamma_i \rightarrow \boxed{\min_\kappa \| \Phi^t \kappa \|_{l_0} \text{ subject to } \sum_i \| \gamma_i - M(P_i * \kappa) \|^2_{l_2} \leq \varepsilon} \rightarrow \kappa$$

$$\hat{P}_1(k) = \frac{k_1^2 - k_2^2}{k^2}$$

$$\hat{P}_2(k) = \frac{2k_1 k_2}{k^2}$$

2D Mass Mapping

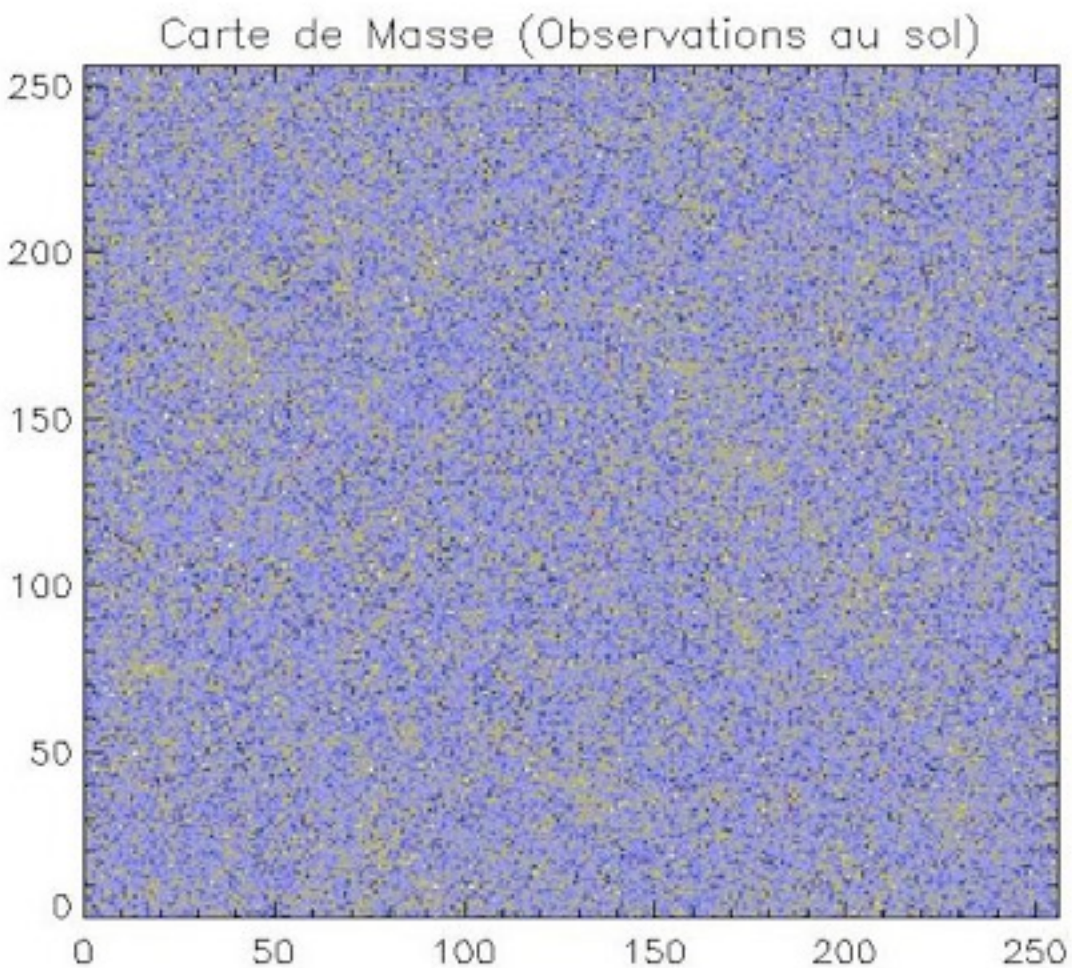

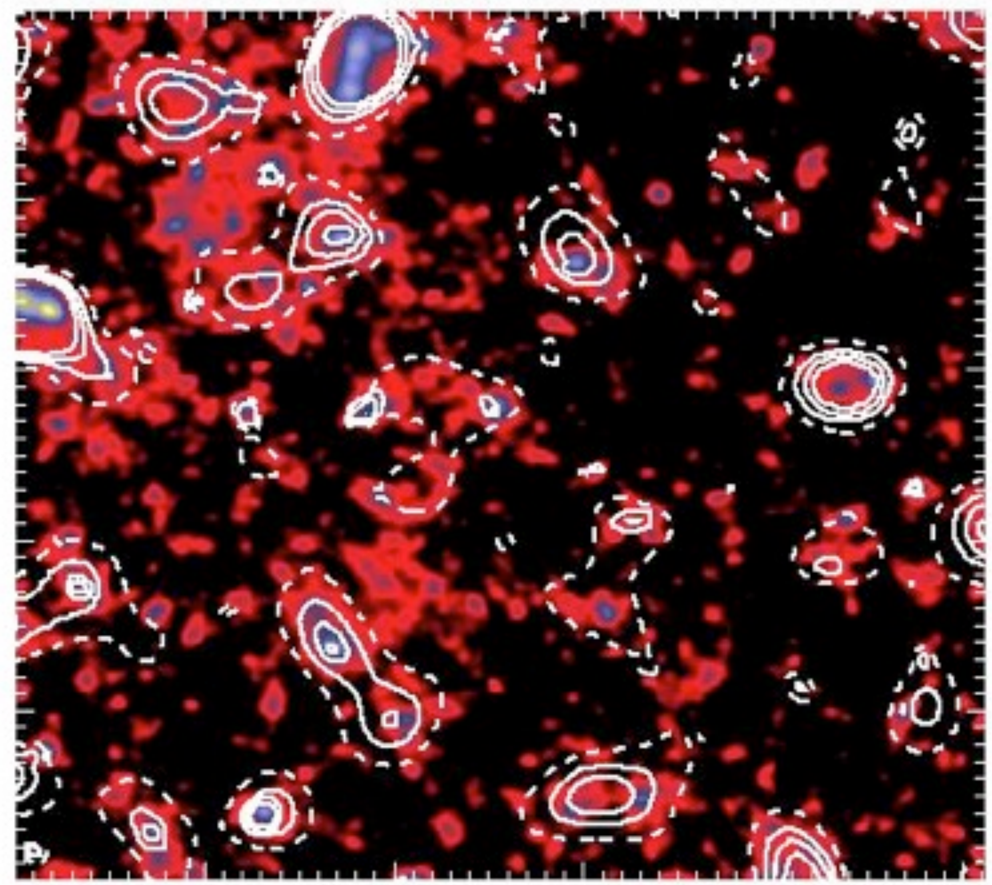

J.-L. Starck, S. Pires and A. Réfrégier, Astronomy and Astrophysics, 451, 3, 2006, pp.1139-1150 , 2006.
S. Pires, J.-L. Starck, and A. Réfrégier, , Light on Dark Matter with Weak Gravitational Lensing, 2010.

2D Mass Mapping

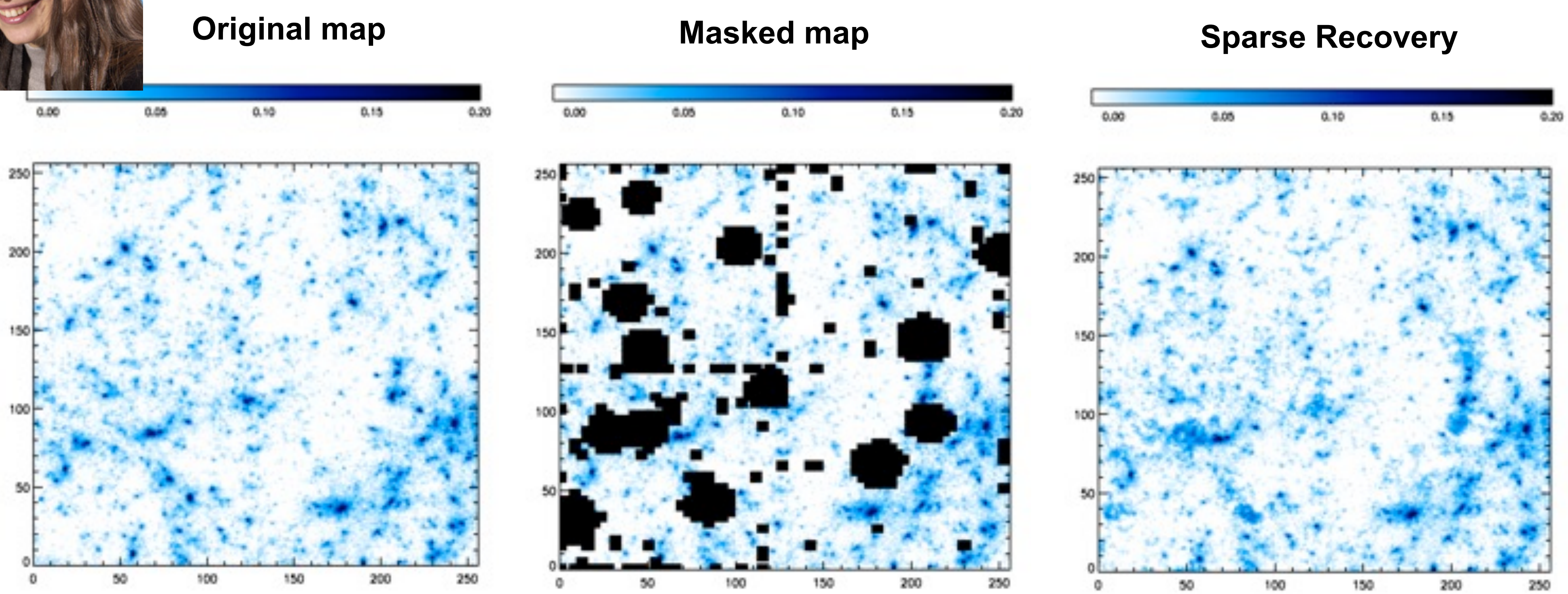

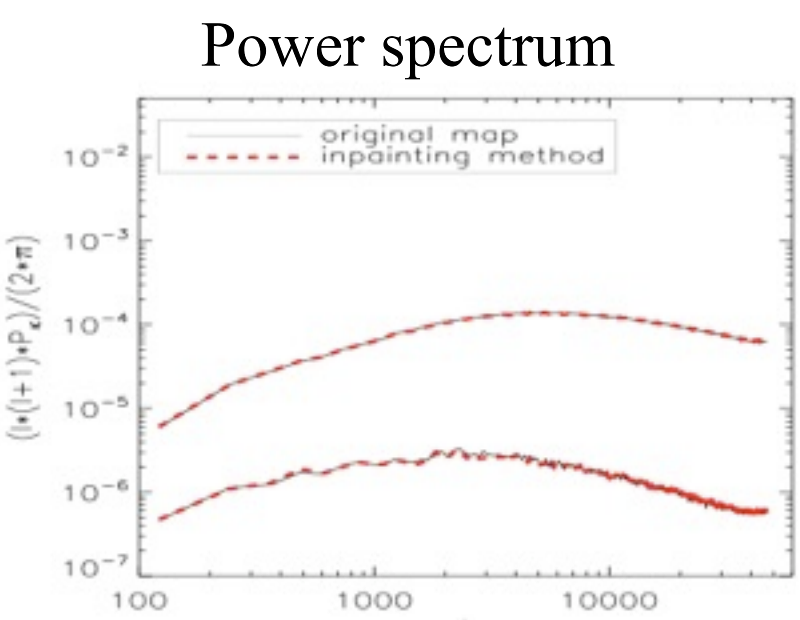

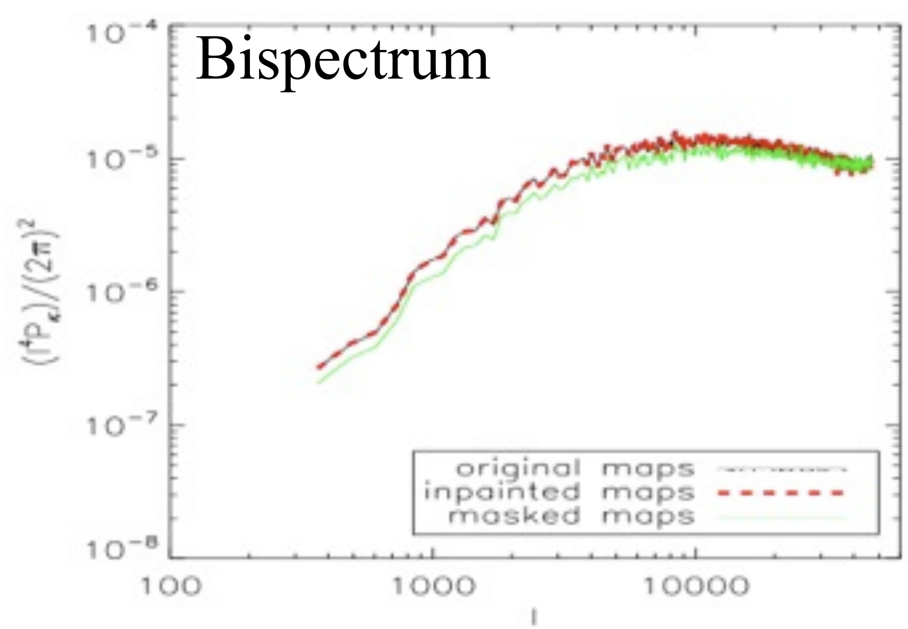

2D Mass Mapping

Original map

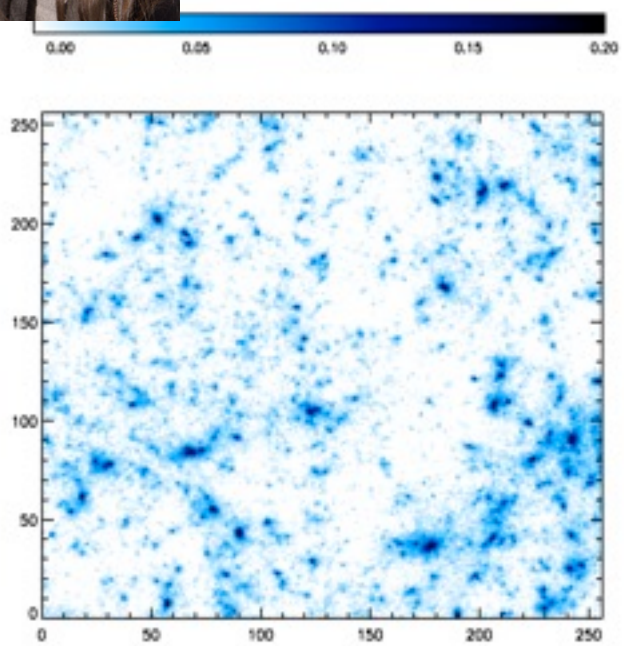

Masked map

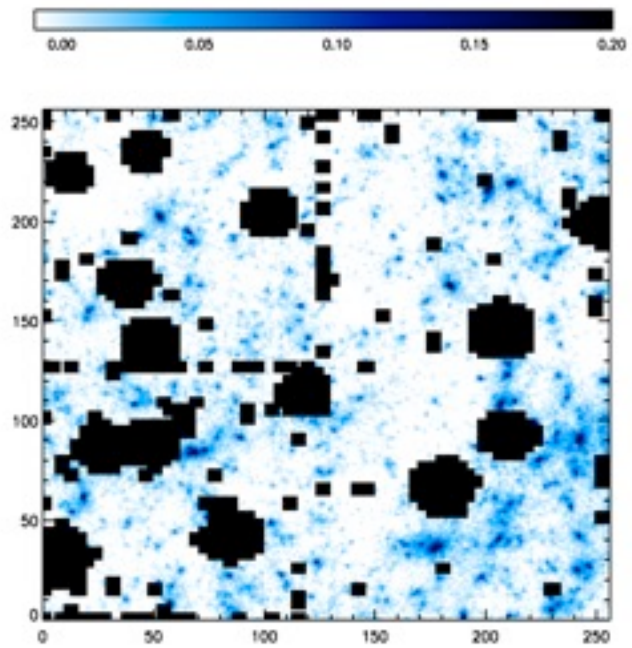

Sparse Recovery

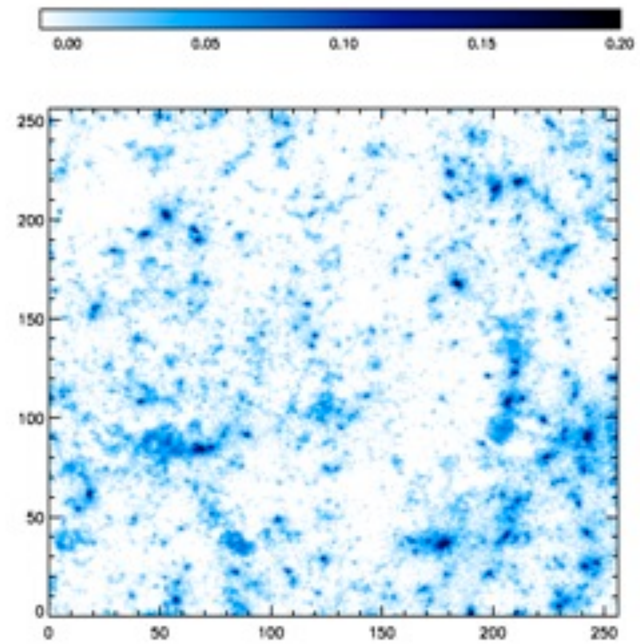

Power spectrum

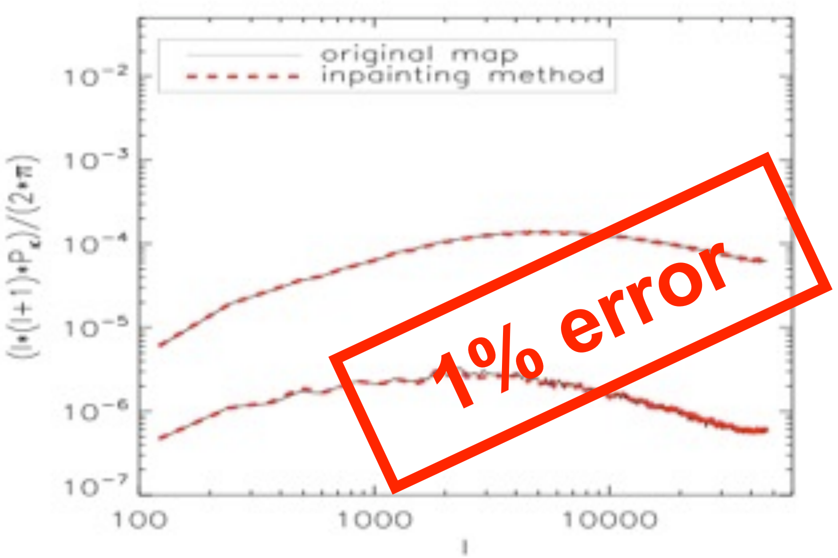

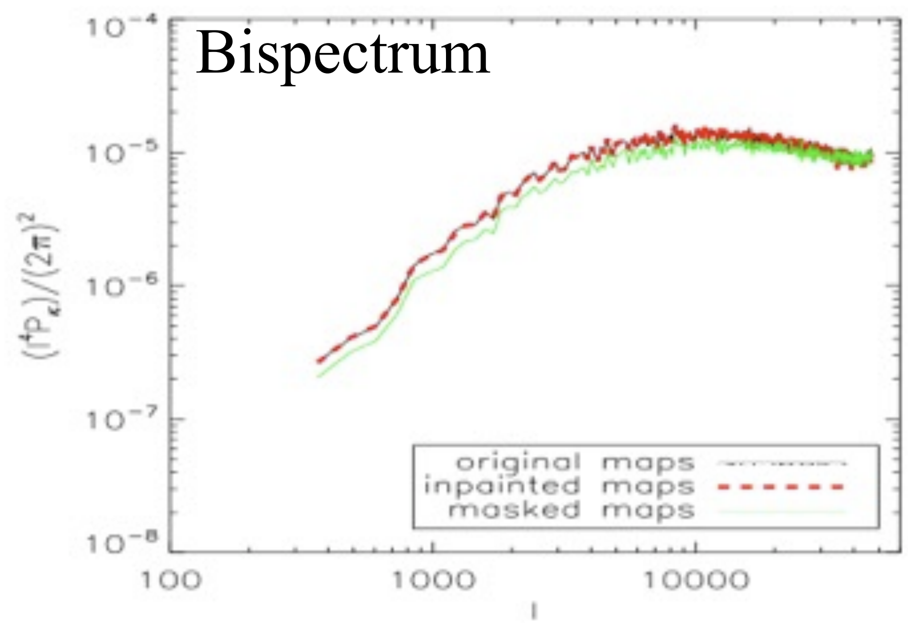

2D Mass Mapping

Original map **Masked map** **Sparse Recovery**

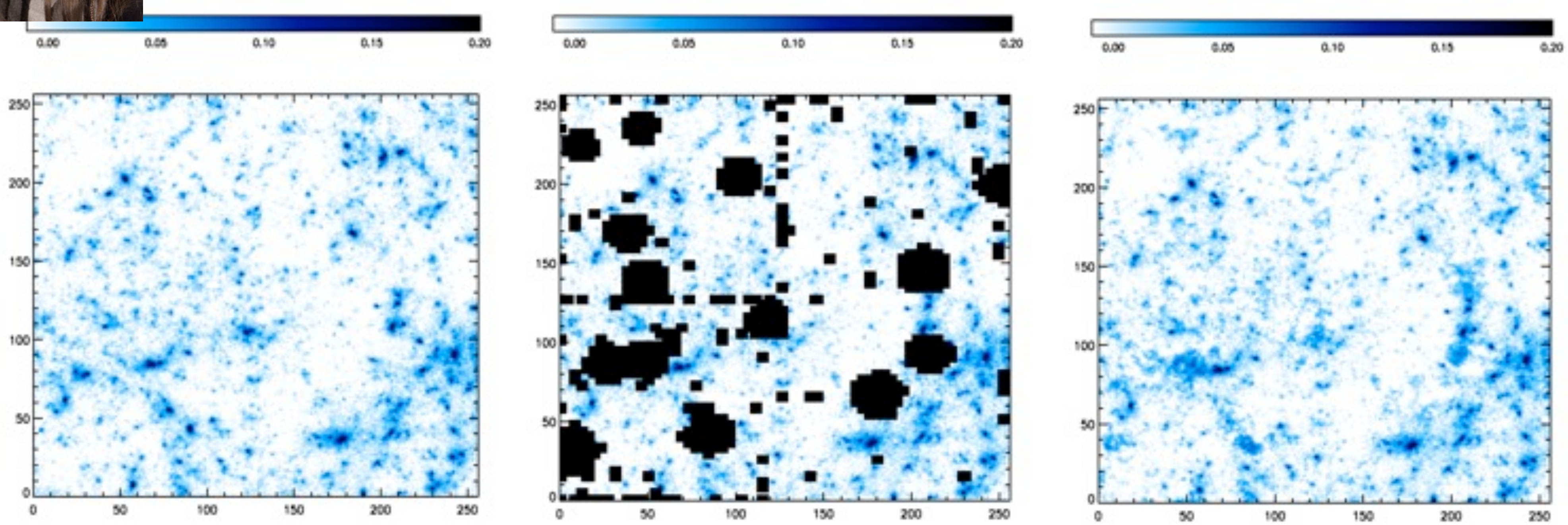

Power spectrum

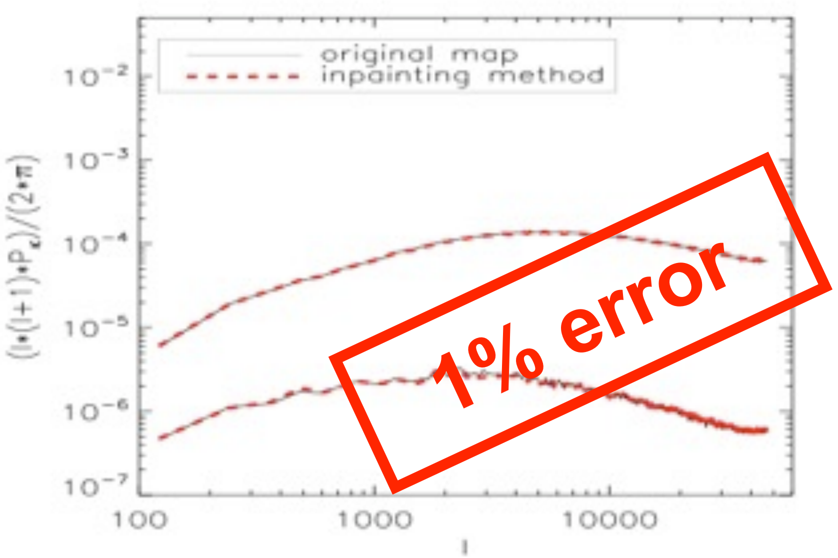

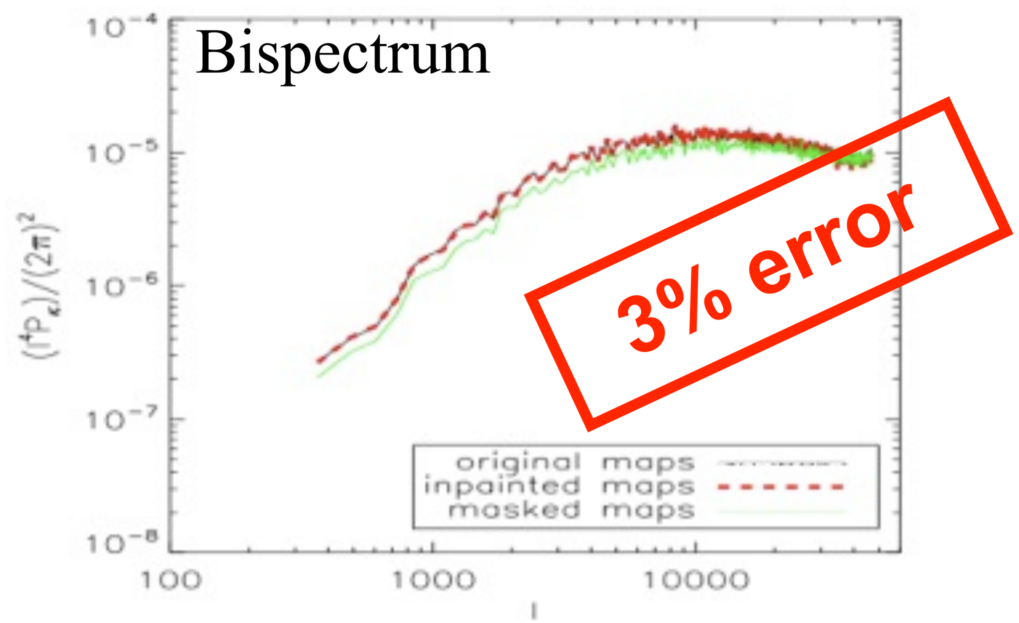

Cosmological Parameters Constraints and High Order Statistics

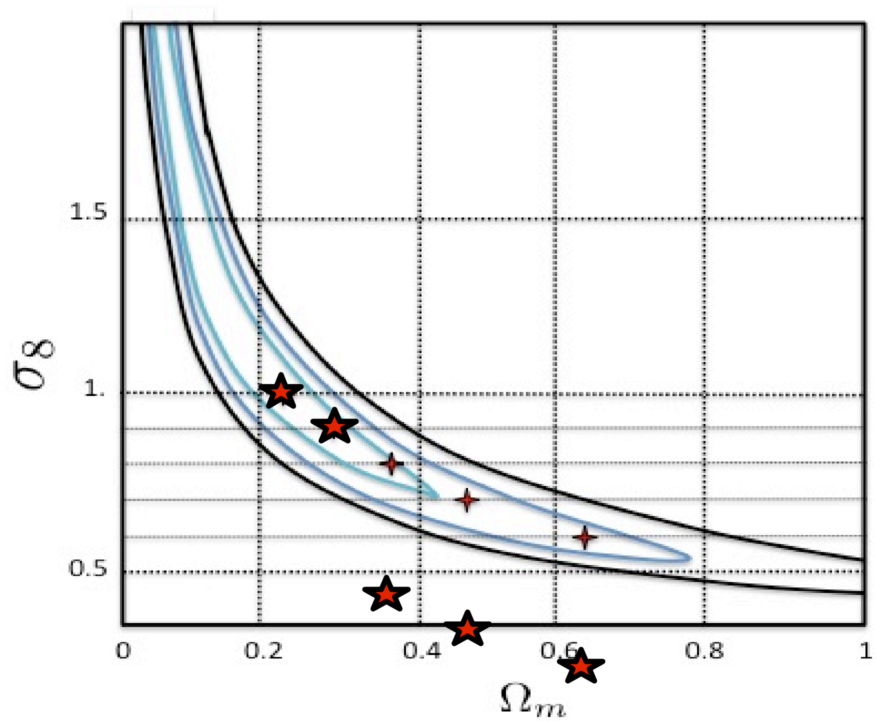

Model1 (σ_8=1, Ω_m=0.23)

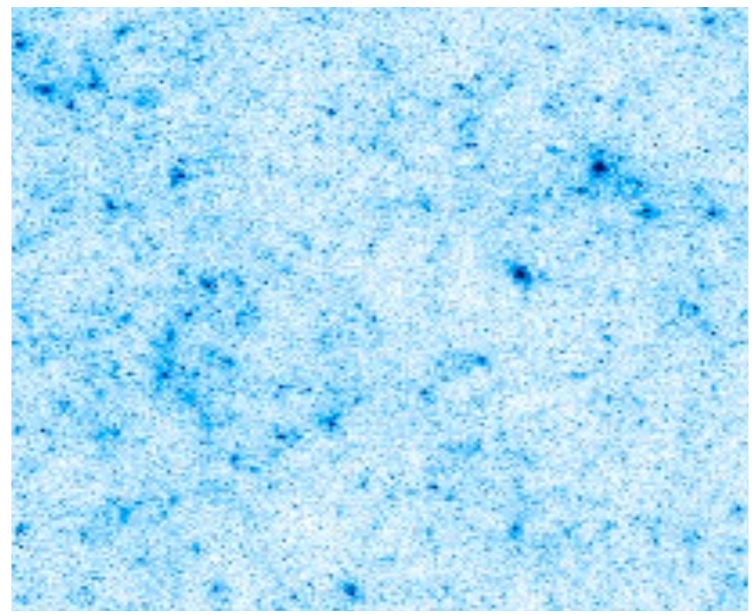

Model2 (σ_8=0.9, Ω_m=0.3)

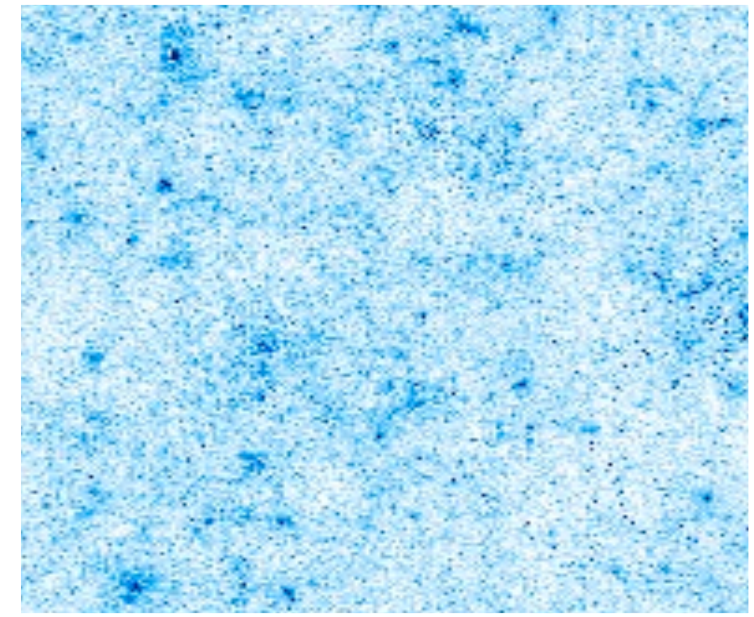

Model3 (σ_8=0.8, Ω_m=0.36)

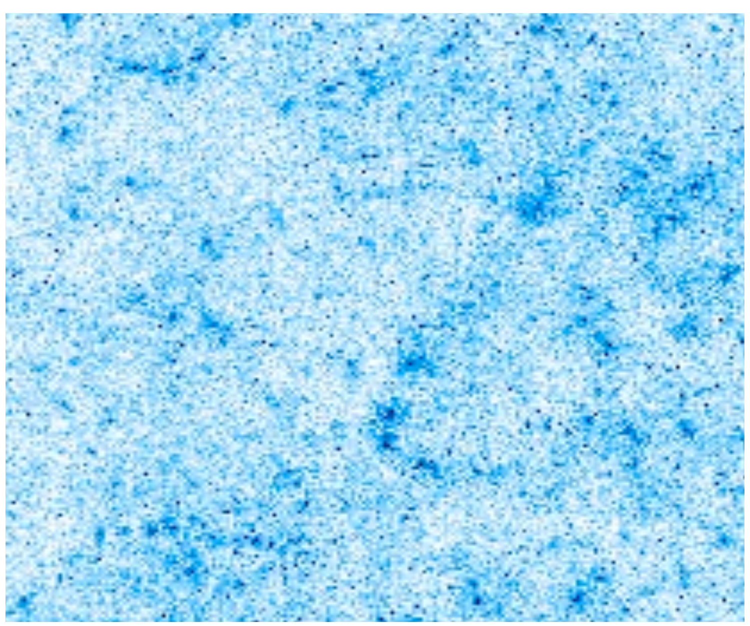

Model4 (σ_8=0.7, Ω_m=0.47)

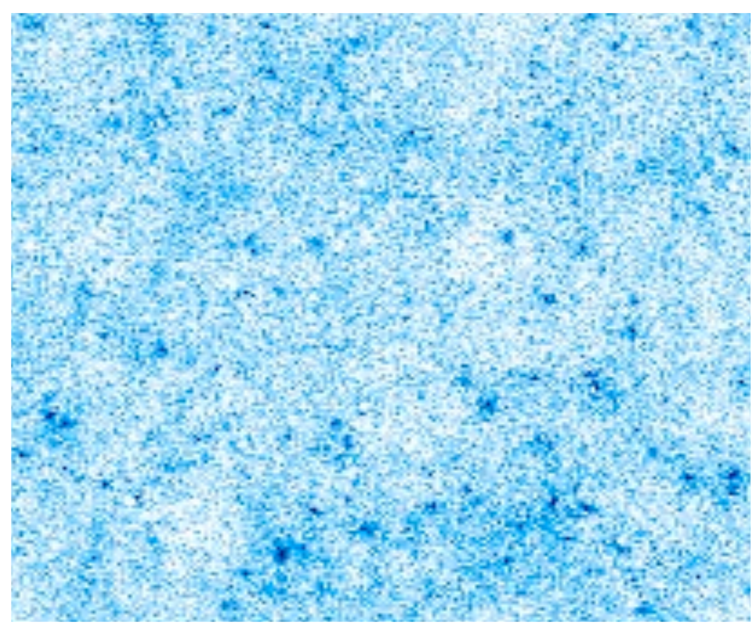

Model5 (σ_8=0.6, Ω_m=0.64)

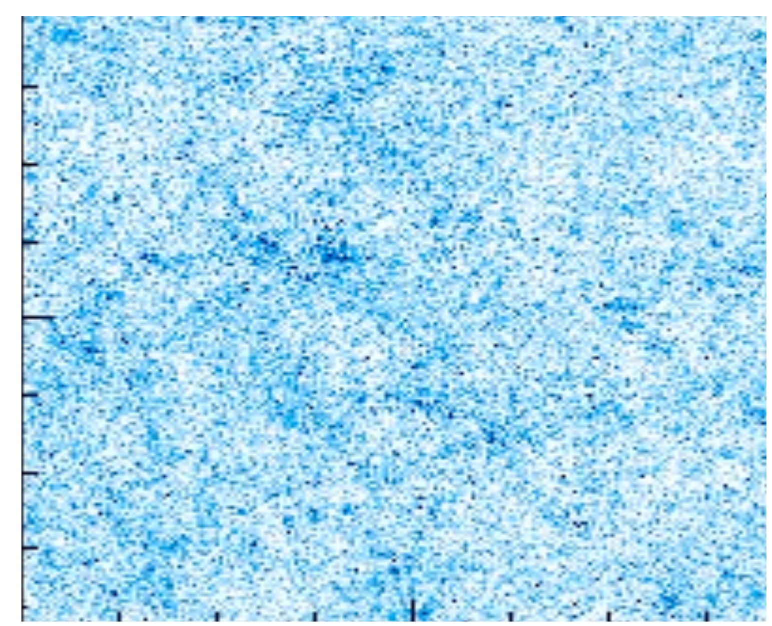

Cosmological Parameters Constraints and High Order Statistics

- Aperture mass map = wavelets, but wavelets calculation is between 10 and 1000 times faster.

- A. Leonard, S. Pires, J.-L. Starck, "Fast Calculation of the Weak Lensing Aperture Mass Statistic", MNRAS, 423, pp 3405-3412, 2012.

- Wavelet Denoising + Wavelet Peak Counting is the most efficient statistical tool to discreminate Cosmological Models.

- S. Pires, J.-L. Starck, A. Amara, A. Refregier, R. Teyssier, "Cosmological models discrimination with Weak Lensing", 505, A&A, pp 969-979, 2009.
- S. Pires, A. Leonard, J.-L. Starck, "Cosmological Parameters Constraint from Weak Lensing Data", MNRAS, 423, pp 983-992, 2012.

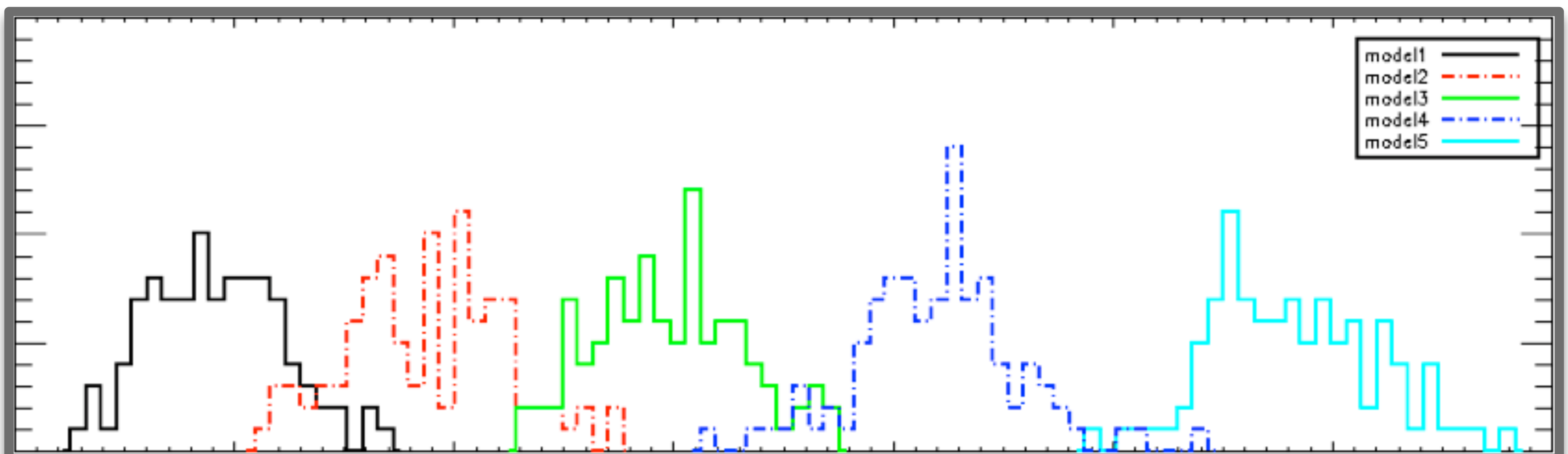

WAVELET PEAK COUNTING ON MRLENS FILTRED MAPS (AT SCALE OF ABOUT 1 ARCMIN)

Cosmological Parameters Constraints and High Order Statistics

- Aperture mass map = wavelets, but wavelets calculation is between 10 and 1000 times faster.

- A. Leonard, S. Pires, J.-L. Starck, "Fast Calculation of the Weak Lensing Aperture Mass Statistic", MNRAS, 423, pp 3405-3412, 2012.

- Wavelet Denoising + Wavelet Peak Counting is the most efficient statistical tool to discreminate Cosmological Models.

- S. Pires, J.-L. Starck, A. Amara, A. Refregier, R. Teyssier, "Cosmological models discrimination with Weak Lensing", 505, A&A, pp 969-979, 2009.
- S. Pires, A. Leonard, J.-L. Starck, "Cosmological Parameters Constraint from Weak Lensing Data", MNRAS, 423, pp 983-992, 2012.

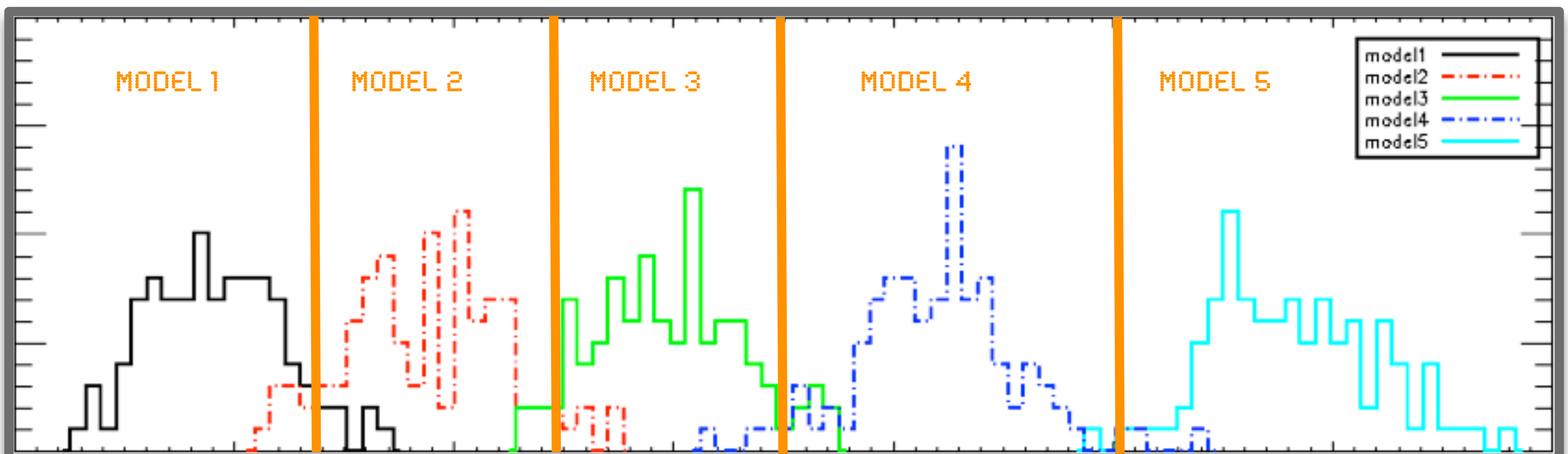

WAVELET PEAK COUNTING ON MRLENS FILTRED MAPS (AT SCALE OF ABOUT 1 ARCMIN)

3D Mass Mapping

$$\gamma(\boldsymbol{\theta}) = \frac{1}{\pi} \int d^2\boldsymbol{\theta}' \mathcal{D}(\boldsymbol{\theta} - \boldsymbol{\theta}')\kappa(\boldsymbol{\theta}')$$

Kappa (or convergence) is a dimensionless surface mass density of the lens

$$\kappa(\boldsymbol{\theta}, w) = \frac{3H_0^2\Omega_M}{2c^2} \int_0^w dw' \frac{f_K(w')f_K(w-w')}{f_K(w)} \frac{\delta[f_K(w')\boldsymbol{\theta}, w']}{a(w')} ,$$

f_K is the angular diameter distance, which is a function of the comoving radial distance r and the curvature K.

$$\boldsymbol{\gamma} = \mathbf{P}_{\gamma\kappa}\boldsymbol{\kappa} + \boldsymbol{n}_\gamma ,$$

$$\kappa = Q\delta + n$$

$$\gamma = \mathbf{R}\delta + n$$

- Galaxies are not intrinsically circular: intrinsic ellipticity ~ 0.2-0.3; gravitational shear ~ 0.02
- Reconstructions require knowledge of distances to galaxies

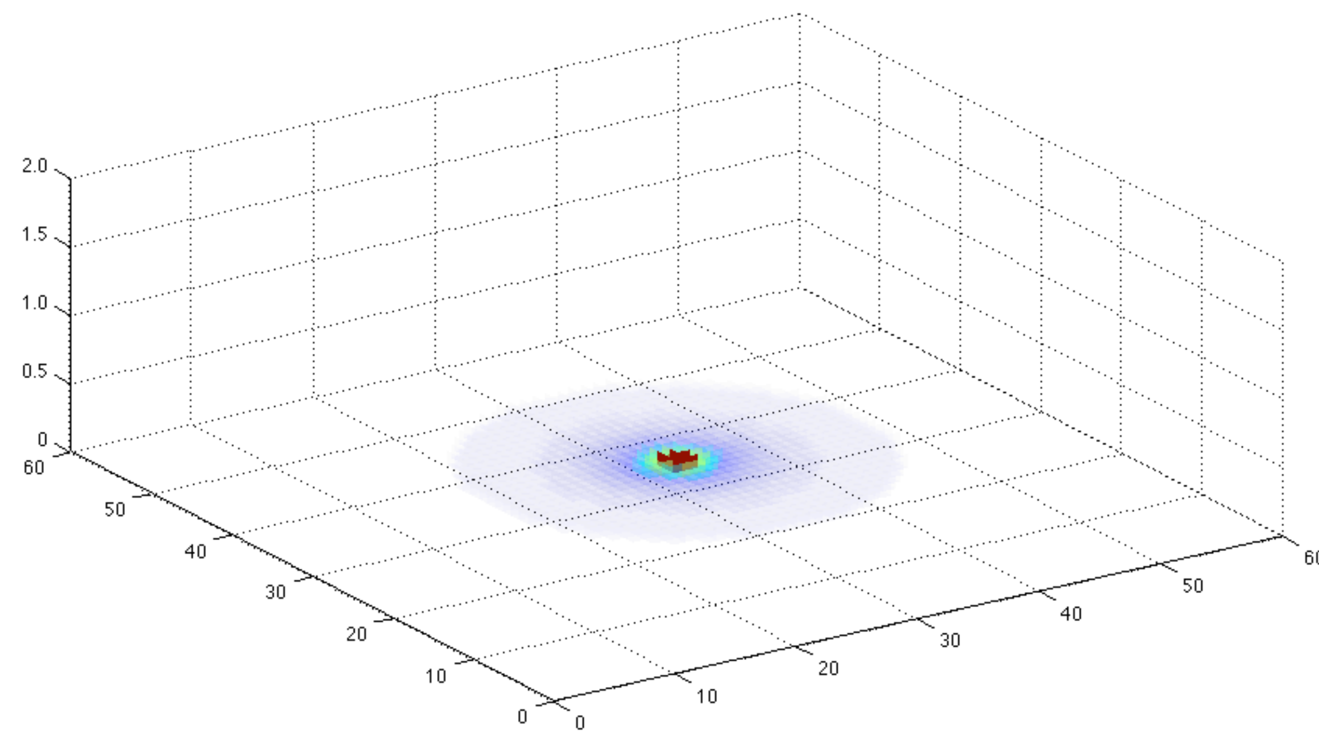

2.0
1.5
1.0
0.5
0
60
50
40
30
20
10
0
0
10
20
30
40
50
60

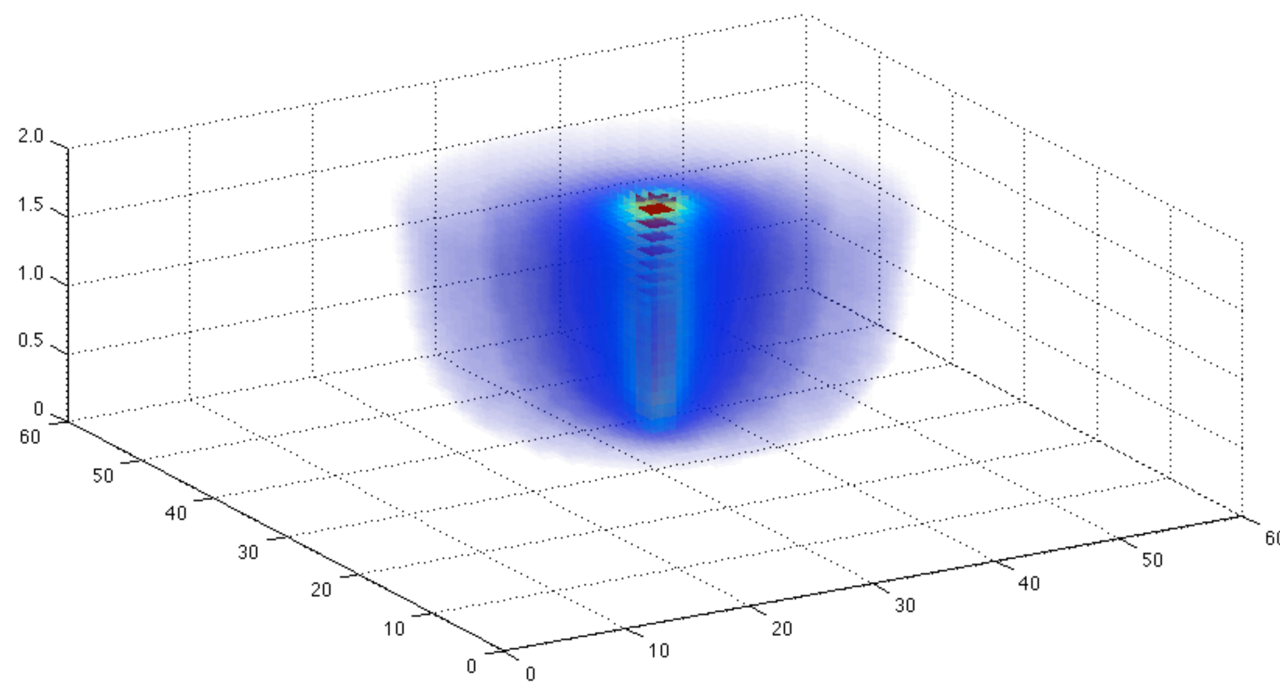
2.0
1.5
1.0
0.5
0
60
50
40
30
20
10
0
0
10
20
30
40
50
60

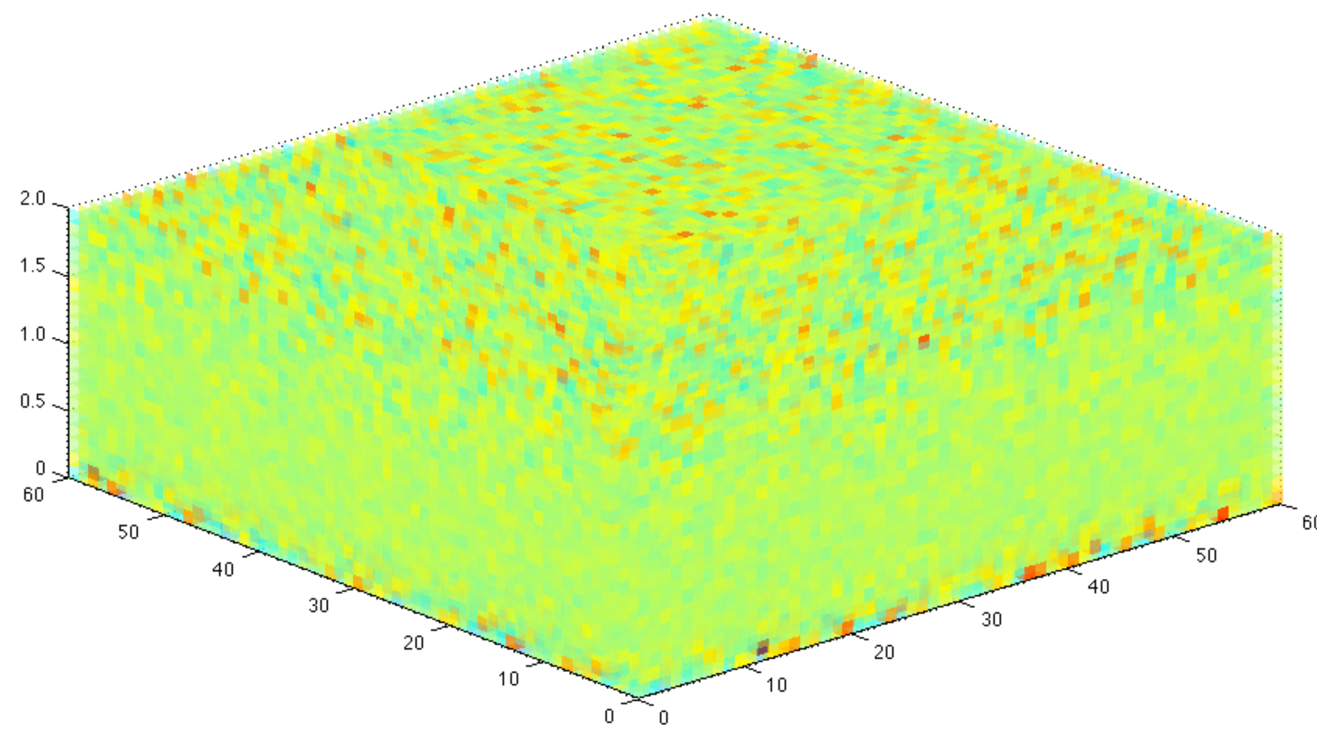
2.0
1.5
1.0
0.5
0
60
50
40
30
20
10
0
0
10
20
30
40
50
60

Linear Methods

- Assume uncorrelated Gaussian noise*
- Linear methods
  - Wiener/inverse variance filter (Simon et al., 2009)
  - $$\hat{s}_{MV} = [\alpha\mathbf{1} + \mathbf{S}\mathbf{R}^{\dagger}\mathbf{\Sigma}^{-1}\mathbf{R}]^{-1}\mathbf{S}\mathbf{R}^{\dagger}\mathbf{\Sigma}^{-1}\boldsymbol{d}\ .$$
  - SVD decomposition & thresholding (VanderPlas et al., 2011)

$$\hat{s}_{IV} = \mathbf{V}\mathbf{\Lambda}^{-1}\mathbf{U}^{\dagger}\mathbf{\Sigma}^{-1/2}\boldsymbol{d}\ ,$$

Reconstruction resolution limited by resolution of data

Linear Methods

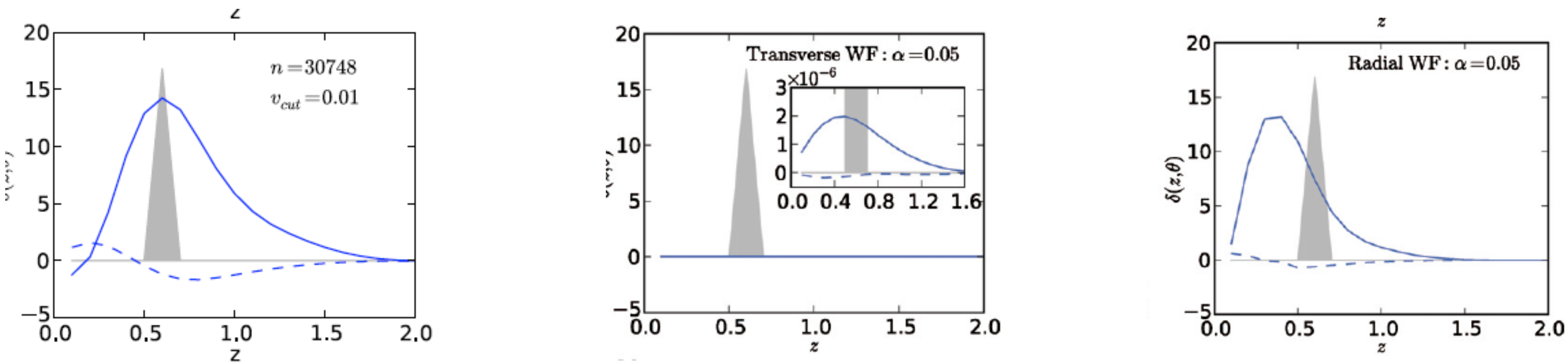

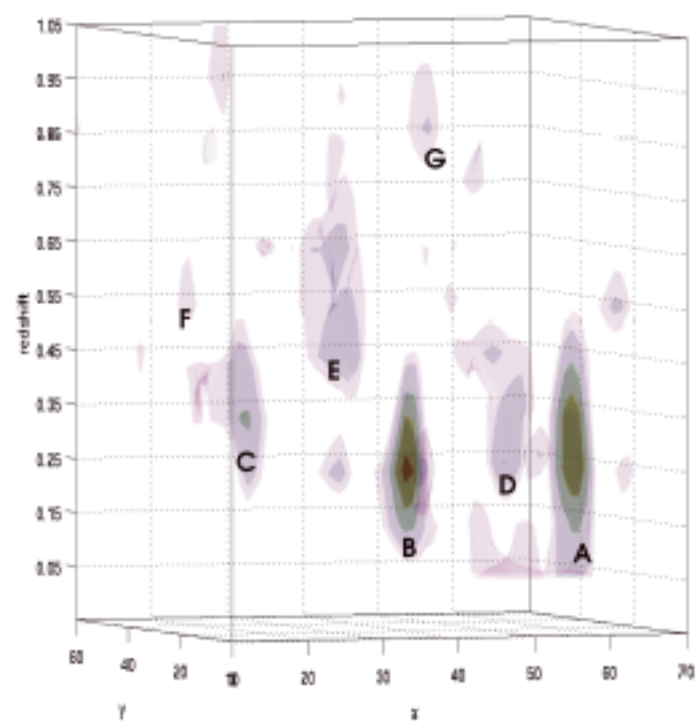

Target Areas for Improvement

- ✧ Redshift bias in location of detected peaks
- ✧ Smearing along the line of sight
- ✧ Damping of the reconstruction
- ✧ Sensitivity at high redshift
- ✧ Improving resolution in reconstructions

Weak Lensing & 3D Matter Distribution

A. Leonard, F.X. Dupe, and J.-L. Starck, "A Compressed Sensing Approach to 3D Weak Lensing", **Astronomy and Astrophysics** , 539, A85, 2012.

A. Leonard, F. Lanusse, J-L. Starck, GLIMPSE: Accurate 3D weak lensing reconstruction usiing sparsity, Astronomy and Astrophysics, A&A, 2014

$$\gamma = P\kappa$$
$$\kappa = Q\delta$$

$$\delta = \Phi\alpha \rightarrow \gamma = PQ\Phi\alpha = R\Phi\alpha$$

$$R = PQ \qquad \alpha$$

γ

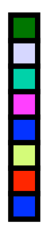

$=$

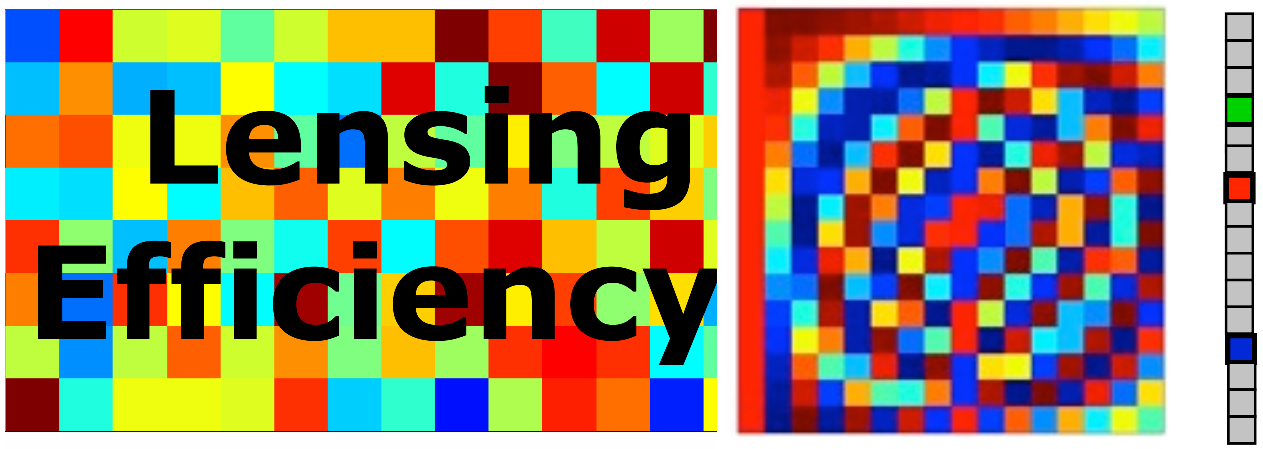

Shear Measurements
M measurements: number of bins in the source plan x number of pixels at for given bin

Density constrast wavelet coefficients

Related to Compressed Sensing theorem
==> Use Sparse recovery and Proximal optimization theory

$$\min_{\alpha} \| \alpha \|_1 \quad s.t. \quad \frac{1}{2} \| \gamma - R\Phi\alpha \|^2_{\Sigma^{-1}} \leq \epsilon$$

$$\delta = \Phi\alpha$$

Φ = 2D Wavelet Transform on each redshift bin

WL 3D Cosmo-Door is now open

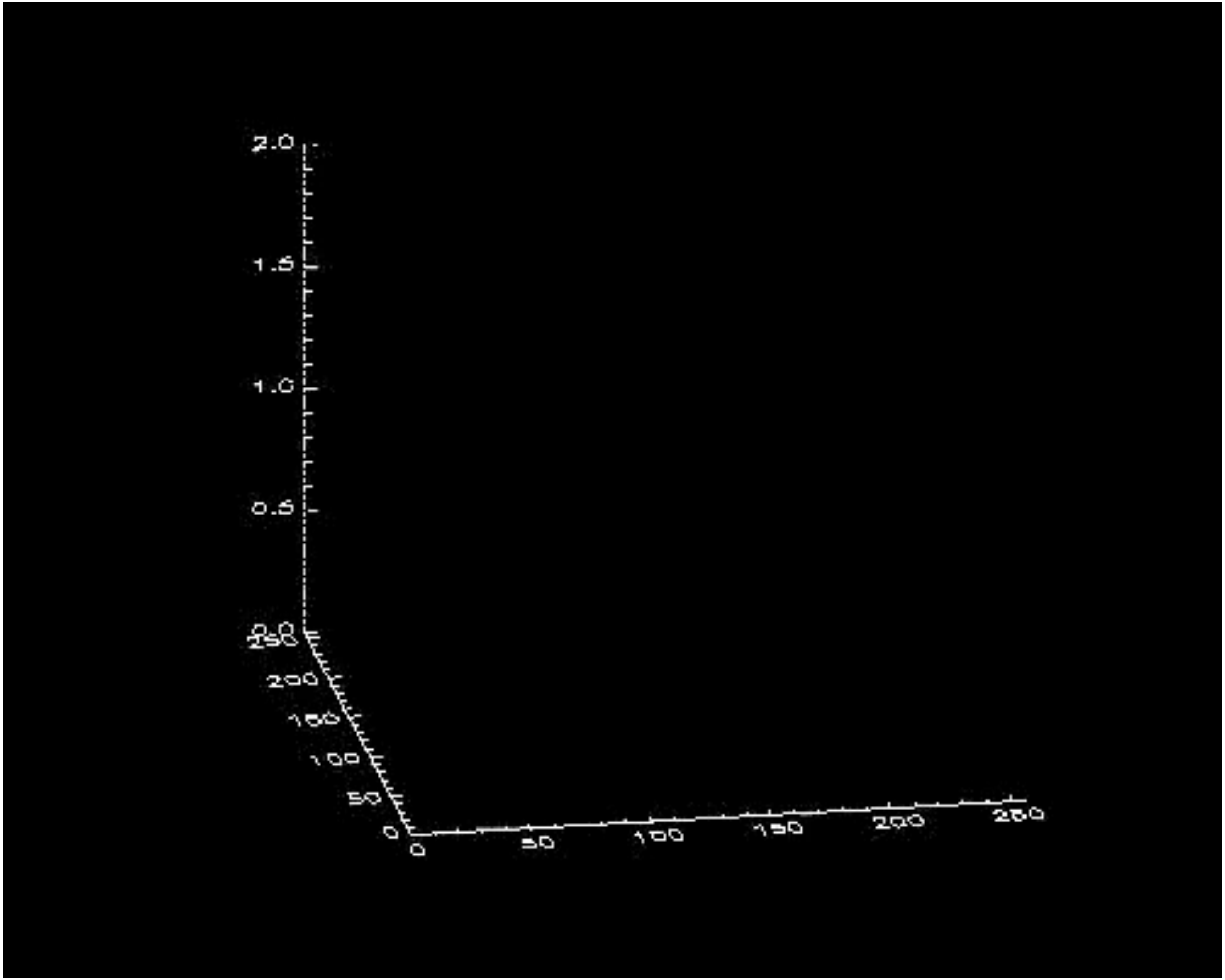

WL 3D Cosmo-Door is now open

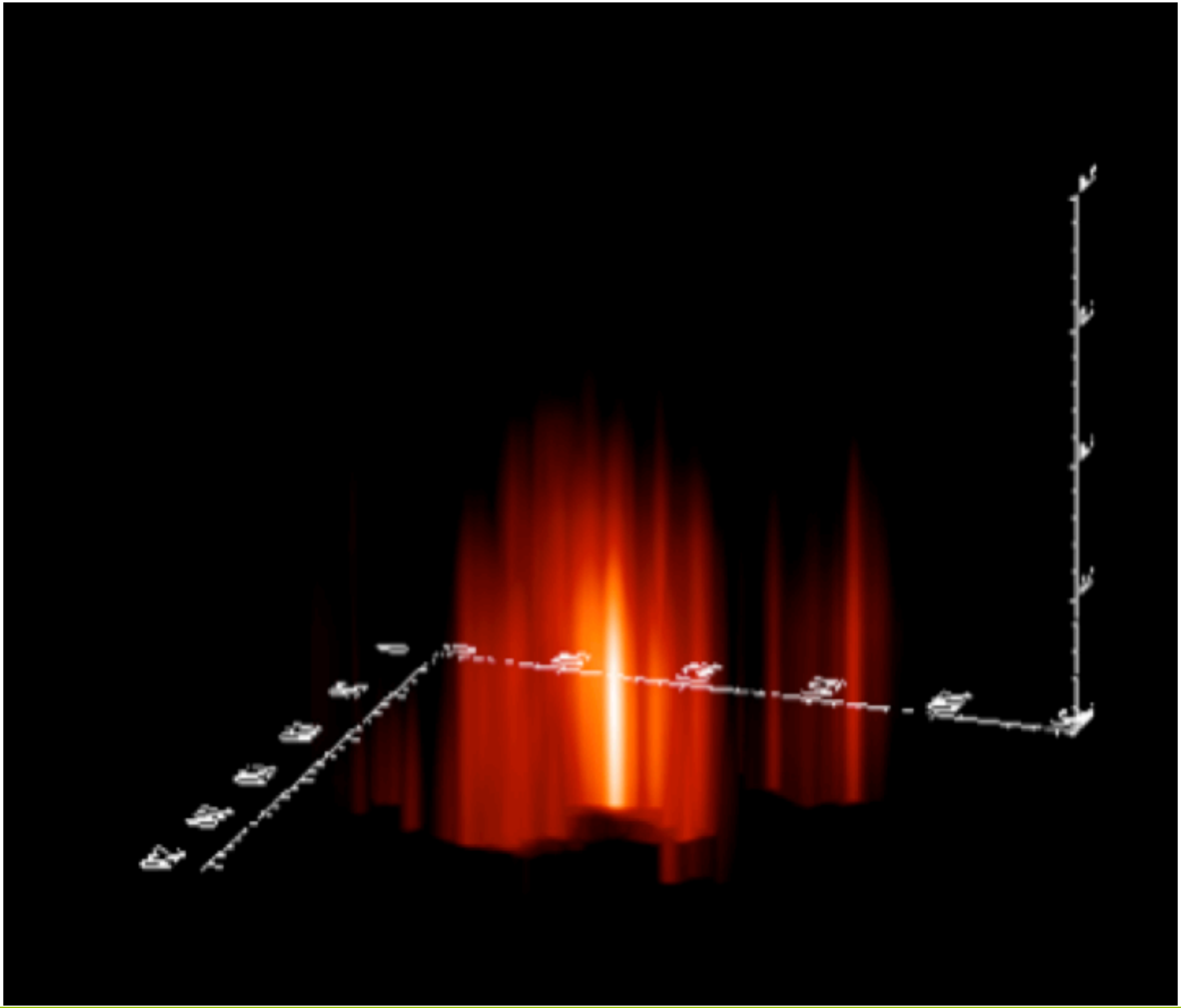

Mass &Redshift Estimation

Single halo simulations

- One NFW profile at the center of a 60x60 arcmin field
- Noise and redshift errors corresponding to an Euclid-like survey
- Mass varying between 3.10^13 and 1.10^15 h−1M⊙ • Redshifts between 0.05 and 1.55

We ran 1000 noise realisations on each of the 96 fields.

$m_{vir} = 8.10^{14} h^{-1} M_{\odot}$

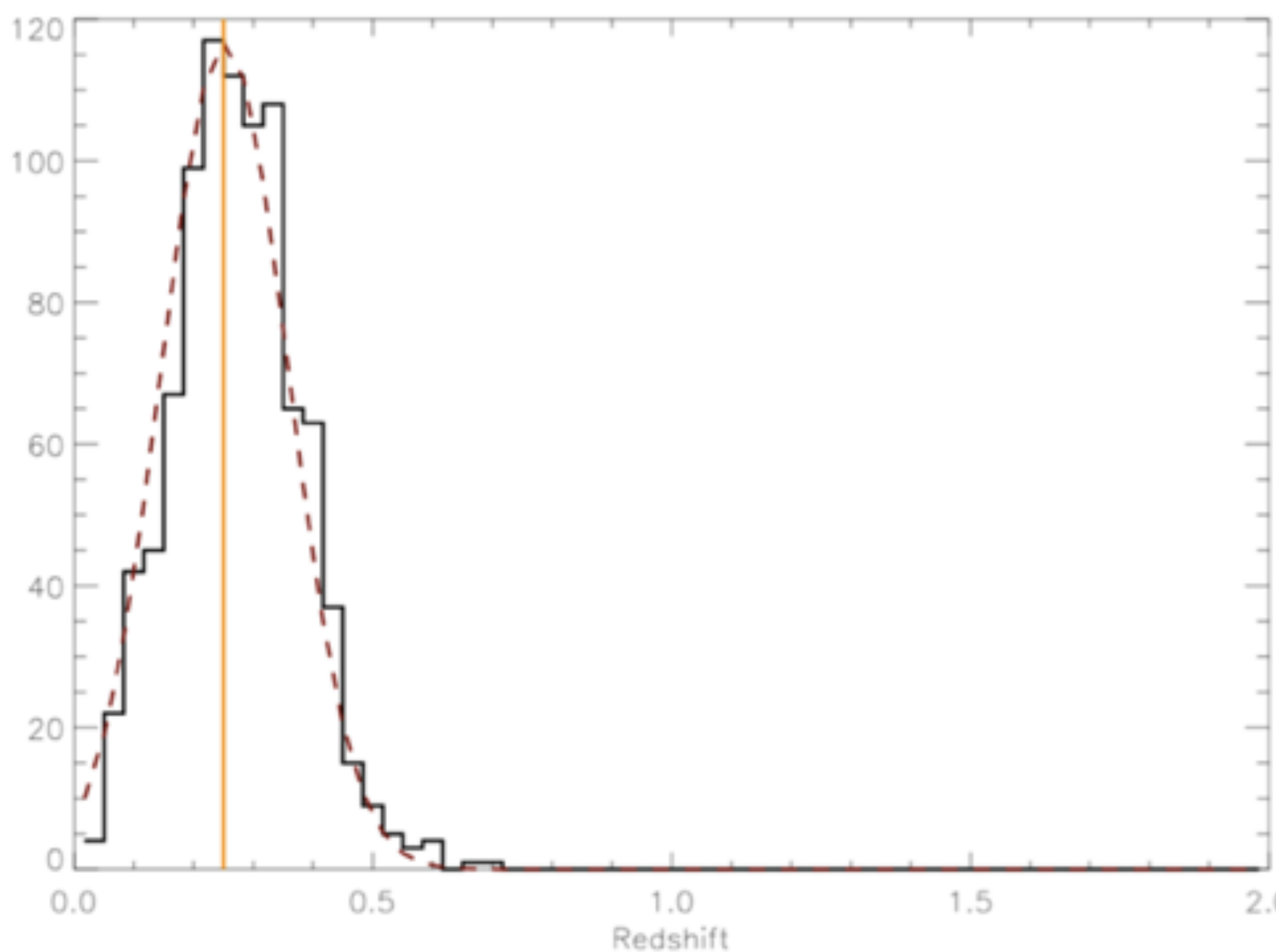

$\sigma_z = 0.1$

$m_{vir} = 4.10^{14} h^{-1} M_{\odot}$

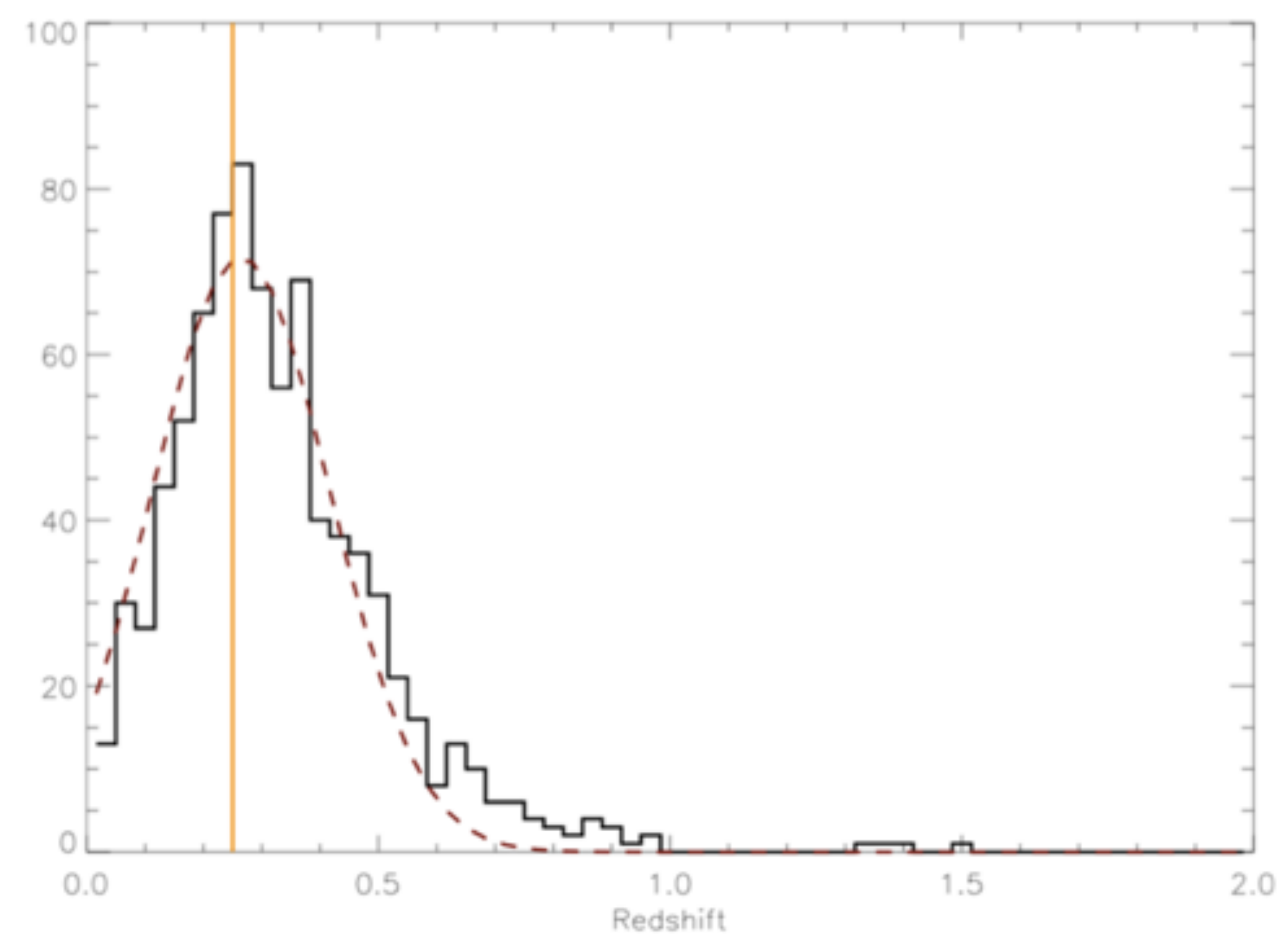

$\sigma_z = 0.15$

Mass &Redshift Estimation

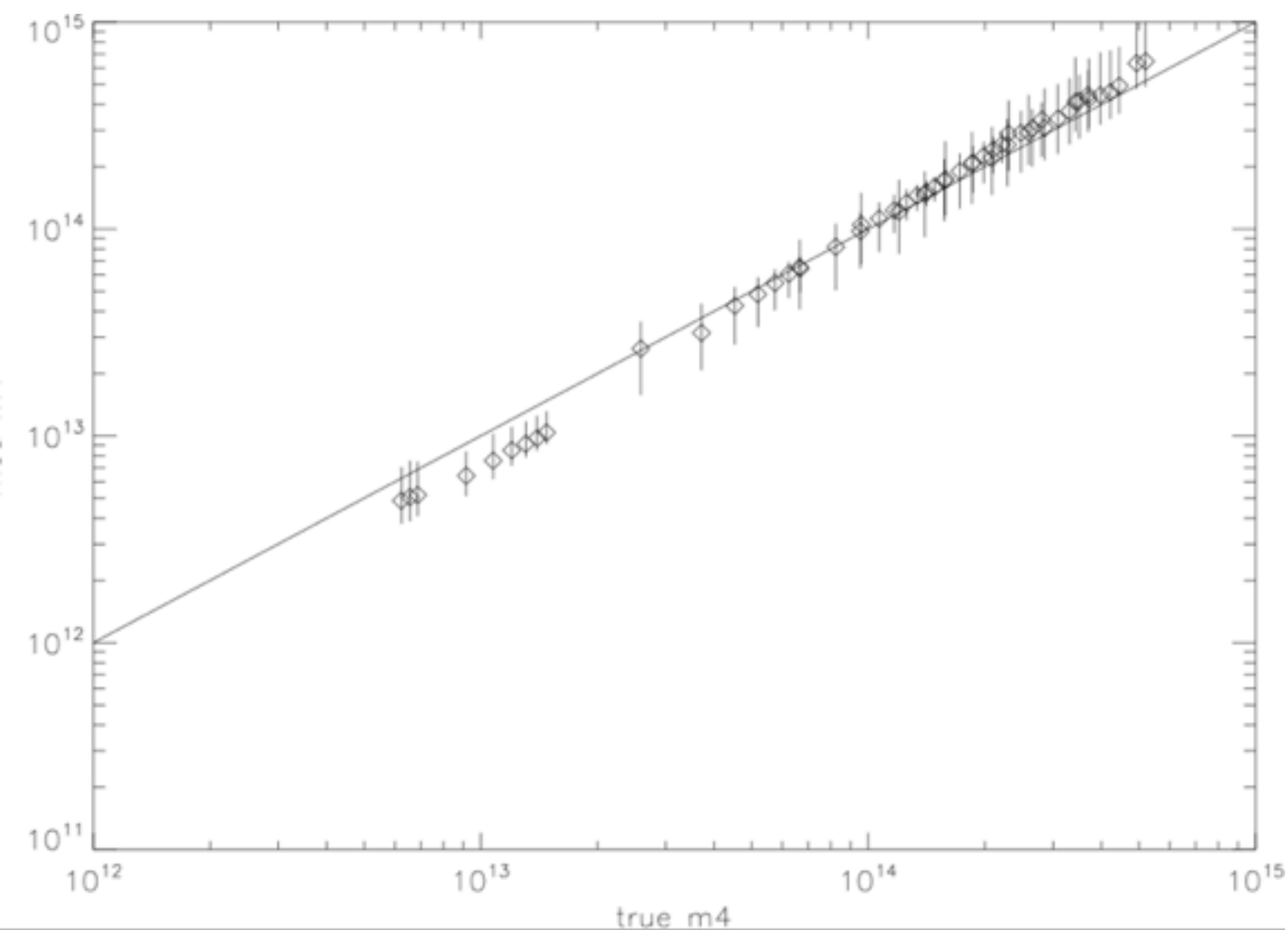

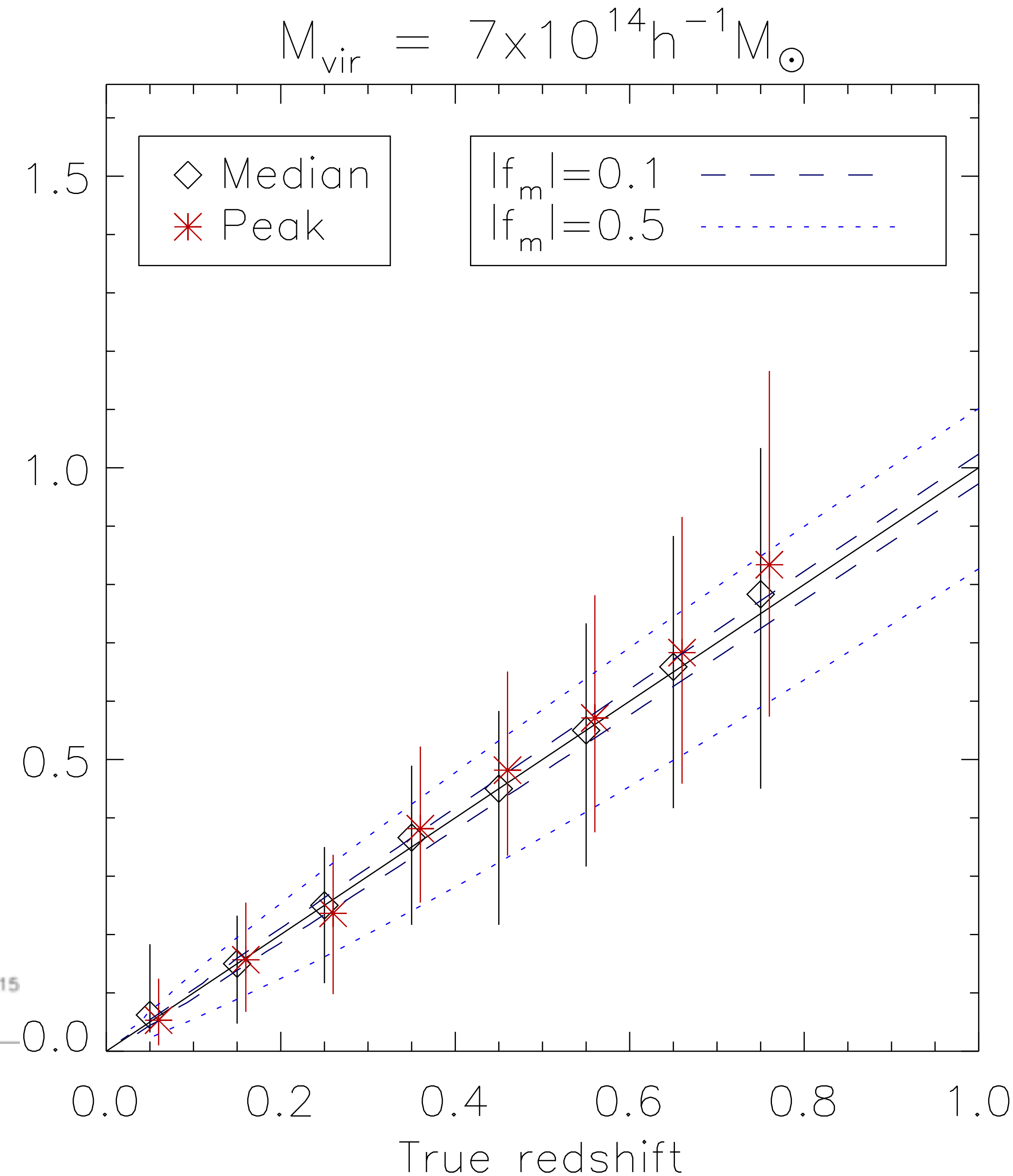

Conclusions

* **Euclid** will provide tight constraints on DE, MG models
- Weak lensing directly measures the mass (as opposed to light).
- But require tight control of systematic
- Algorithms need clearly to be improved in order to meet Euclid scientific requirements.

* **Great3 Challenge** shows significant progress, especially on the multiplicative bias

* 3D lensing is a very noisy, ill-posed inverse problem
Linear methods use weak priors, and suffer from several drawbacks:

- Redshift bias
- Smearing
- Damping
- Resolution limited by data

Sparse Recovery approach allows us to improve on all four points

* Recent developments in applied mathematics (sparsity concept, compressed sensing, proximal optimization theory, optimal transport etc) may be extremely useful to optimize Euclid Science.